THE
PHYSICAL REVIEW

A Journal of Experimental and Theoretical Physics Established by E. L. Nichols in 1893

VOL. 55, NO. 7 APRIL 1, 1939 SECOND SERIES

Radiations from Radioactive Substances: Au^{198}, Eu^{152}, Ag^{106}, Cu^{64} and N^{13}

J. REGINALD RICHARDSON*
Department of Physics, University of Michigan,† Ann Arbor, Michigan

(Received February 10, 1939)

By the use of a twelve-inch hydrogen-filled cloud chamber situated in a magnetic field, investigation has been made of the gamma-radiation from Au^{198} and Eu^{152}. Observations on the 2.7-day period of Au^{198} indicate three lines with energies 70 kv, 280 kv and 440 kv, and relative intensities 0.15, 1.0 and 1.2. The beta-spectrum has an inspection upper limit of 0.83 Mev and the distribution shows that the 440-kv gamma-radiation is internally converted with a coefficient of 0.1. Thus the 70-kv radiation is probably entirely K radiation emitted after internal conversion. The Eu^{152} gamma-distribution shows three main groups of 40 kv, 0.3 Mev and 0.9 Mev. The 40-kv radiation is ascribed to the K radiation of Sm emitted as a consequence of the orbital electron capture process in Eu^{152}. Evidence is also found for the K-electron capture process in the eight-day isomer of Ag^{106}. In fact the electron spectrum probably consists of secondary electrons from the gamma-radiation following the capture process. The distribution of electrons ejected from a lead radiator by a thin source of N^{13} is compared with that from a Cu^{64} source under the same geometrical conditions. The data seem to indicate the presence of a gamma-ray of 280 kv from N^{13} with the relative probability of roughly 0.4 quantum per positron. The necessity of employing radiators of different materials for the complete investigation of a gamma-ray spectrum is emphasized.

THE sources investigated in these experiments[1] were prepared by neutron or deuteron bombardment in the Michigan cyclotron. The radiations were examined principally by means of a cloud chamber. The chamber was twelve inches in diameter, and was situated in a magnetic field uniform to ± 0.5 percent throughout the volume of the chamber. The current through the coils producing the magnetic field was maintained constant and continuous in time. The chamber was filled with hydrogen at atmospheric pressure, and a mixture of ethyl alcohol and water was used as the condensible vapor. Illumination was obtained from three 110-volt, 500-watt lamps flashed on 200 volts dc. The control circuit was of the vacuum tube type described elsewhere.[2]

In the measurements on gamma-radiation, a beam of gamma-rays was formed by a lead collimator so that the source could not "see" the bottom or top of the chamber, but only the radiator. Different materials were used as radiators; the one called the "carbon" radiator was formed from paper dipped in paraffin.

Au^{198}

The source was formed by slow neutron bombardment of gold[3] and the 2.7-day activity was investigated. The beta-rays were first examined by hanging a piece of gold foil directly in the chamber. The momentum distribution of the

* National Research Fellow.
† Now at the University of Illinois.
[1] Some of these results have been reported previously, J. R. Richardson, Phys. Rev. **53**, 942 (1938).
[2] J. R. Richardson, Rev. Sci. Inst. **9**, 152 (1938).
[3] E. McMillan, M. Kamen and S. Ruben, Phys. Rev. **52**, 375 (1937).

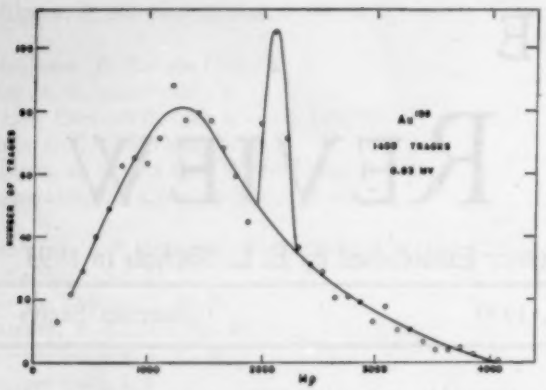

FIG. 1. The momentum distribution of the electrons from Au^{198}. The inspection upper limit is at 0.83 Mev. The internal conversion of the 440-kv gamma-ray is indicated with coefficient 0.1.

electrons obtained is shown in Fig. 1. The general shape of the distribution is similar to that usually obtained from an electron emitter of high atomic number with the exception, however, of the large number of electrons at 2100 $H\rho$. The obvious conclusion, of course, is that these are internal conversion electrons from a gamma-ray transition. This is born out when the gamma-radiation is examined. The internal conversion coefficient is then about 0.1 since there are 140 tracks in the line and 1400 in the whole distribution. The inspection upper limit of the beta-ray spectrum is 0.83 Mev.

The gamma-radiation from this source was examined with a lead radiator of surface density 20 mg/cm². The resulting distribution of the electrons ejected from this radiator is shown in Fig. 2. Two well-defined groups are indicated by the distribution. Considering the more energetic group we see that it must be produced by a gamma-ray of about 400 kv. Using a combination of theoretical and experimental results on the relative probabilities of the different processes we can calculate the shape and relative number of the distributions of electrons due to the Compton effect, the photoelectric effect in the K shell of lead, and the photoelectric effect in the L shell, named in the order of increasing energy. The curves in Fig. 2 have been drawn in accordance with these calculations. It must be emphasized that the data do not determine the relative size or shape of the curves. They are drawn for two reasons, first to determine if the data are consistent, second to separate out the distribution due to the K shell photoelectrons, from which the best determination of the energy can be made.

The energy is determined from the peak of the distribution of the K shell photoelectrons. This eliminates the broadening effect of the probable error of track measurement from the energy determination. Some account must be taken of the slowing down of the photoelectrons in the radiator. This can be estimated from the data of White and Millington[4] on the loss of momentum of electrons while traversing matter. For example, from their results, the loss of momentum $\Delta(H\rho)$ for the positron annihilation radiation photoelectrons (2610 $H\rho$) would be estimated as 70 $H\rho$ whereas the maximum of the K electrons experimentally occurs at 2520 $H\rho$, or a loss of 90 $H\rho$—a satisfactory check considering the errors involved.

Thus in the case of the more energetic line of gold, the maximum of the K electrons is at 2200 $H\rho$ so $\Delta(H\rho)$ is 100 $H\rho$, and the energy of the group from a very thin radiator would correspond to 2300 $H\rho$, or 348 kv. Taking account of the binding energy of the K shell of lead we see that the energy of the gamma-radiation must be 435 kv.

In the lower energy group one can ignore the contribution of the Compton effect in deter-

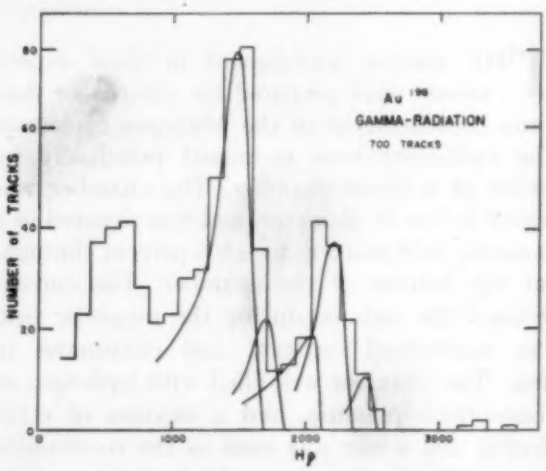

FIG. 2. The photoelectrons ejected from a lead radiator by the gamma-radiation of Au^{198}. Two gamma-ray lines are deduced at 280 kv and 440 kv and relative intensities 1.0 and 1.2. The low energy group of electrons is produced by 70-kv radiation with relative probability 0.15.

[4] P. White and G. Millington, Proc. Roy. Soc. **A120**, 701 (1928).

mining the K-electron distribution because of its much smaller probability relative to the photoelectric effect. The peak of the latter appears to be at 1470 $H\rho$. This corresponds to a gamma-ray energy of 280 kv.

The relative intensity of the two gamma-ray lines is also of interest. This can be obtained from a consideration of the relative probability of the photoelectric effect at the two energies compared with the experimental data. The result obtained is that there are 0.8 quantum of 280-kv radiation for every quantum of 440-kv radiation. This ratio is uncertain by about 30 percent.

Since internal conversion is observed only for the 440-kv line (as far as the sensitivity of the cloud chamber is concerned), and the coefficient is 0.1, it is logical to presume that the 440-kv radiation is quadrupole while the 280-kv radiation is dipole in character. There is some evidence from pictures taken with a carbon radiator for a weak line corresponding in energy to the sum of the energies of the two strong lines. The group of low energy electrons in Fig. 2 (relative probability 0.1) is undoubtedly produced by K radiation from the gold (more exactly Hg^{198}) emitted as a consequence of the internal conversion process. These x-rays would have an energy of about 70 kv and would eject photoelectrons of about 55 kv from the L shell of lead. This corresponds well with the electrons observed, both in energy and relative intensity.

The drawing of a level scheme for any β-radioactive nucleus is probably premature until more certain knowledge is obtained of the shape of a simple beta-spectrum for a given atomic number and spin change. If the beta-spectrum in the case of gold is simple, one must assume that the excited Hg^{198} nucleus subsides to the ground state in two steps—by emission of dipole radiation of 280 kv and by emission of 430-kv quadrupole radiation, or possibly in one step by the emission of a 0.7-Mev quantum.

Eu^{152}

The europium source was in the form of europium oxide which had been purified by Dr. D. W. Stewart. It was exposed to slow neutrons and the gamma-radiation associated with the 9.2-hour activity of Eu^{152} was investigated.

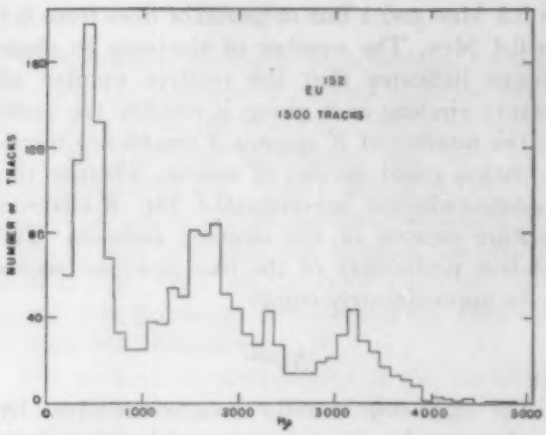

FIG. 3. Electrons ejected from a lead radiator by the gamma-radiation of Eu^{152}. The slow electrons correspond to an energy of 25 kv to be added to the binding energy of the electrons. Most of them originate in the L shell of lead, as is shown by comparison with a Cd radiator. The electrons above 2500 $H\rho$ are principally produced by the Compton process.

The momentum distribution of the electrons ejected from a lead radiator is shown in Fig. 3. The gamma-radiation is quite evidently complex, but the most interesting feature is the large number of low energy electrons. This group has an energy of about 25 kv and must obviously be composed of photoelectrons, so the question arises as to which shell in the lead atom is their origin. This can be ascertained by observing the electrons ejected from a cadmium radiator, since the binding energy of an electron in the K shell of cadmium is of the same order of magnitude as the binding for the L shell of lead. Observations on the cadmium radiator indicated the group as even more prominent and of a similar energy. Thus one may say that the energy of the radiation ejecting this group of electrons must be about 40 kv. This radiation is probably to be assigned as K radiation of Sm emitted after the capture of an orbital electron by Eu^{152}. Thus this isotope of europium has the possibility of either emitting an electron and decaying to Gd^{152} or capturing a K electron and forming Sm^{152}. The electron distribution has been investigated by Dr. Stewart.

The gamma-radiation itself is obviously complex, and it seems that one must wait for stronger sources and the use of thinner radiators before completely resolving the spectrum. It seems apparent, however, that there is one line

at 0.8 Mev and a line or group of lines from 0.3 to 0.4 Mev. The number of electrons in these groups indicates that the relative number of quanta ejecting each group is roughly the same as the number of K quanta. Coincidence measurements could decide, of course, whether the gamma-radiation accompanied the K-electron capture process or the electron emission. The relative probability of the two processes seems to be approximately equal.

Ag^{106}

The eight-day activity induced in silver by fast neutron bombardment was assigned to Ag^{106} by Pool, Cork and Thornton[5] as isomeric with the 24.5-minute positron activity. Pool[6] later postulated the process of K-electron capture in the eight-day isomer to account for the abnormally large gamma to beta ratio that it exhibits. The results discussed here were presented previously before the American Physical Society.[7]

The electron spectrum of Ag^{106} was investigated by placing an activated silver foil of thickness 0.0025 cm in the cloud chamber. The momentum distribution appears as in Fig. 4. The striking feature of the distribution is the fact that forty-five percent of the tracks are in a small band of energies below 17 kv, while the remainder ranges up to 800 kv. Some of the low energy electrons were measured by means of their range in the gas of the chamber, after calibration of the method had been made. Pool did not observe these electrons because he had an aluminum window between the source and the chamber.

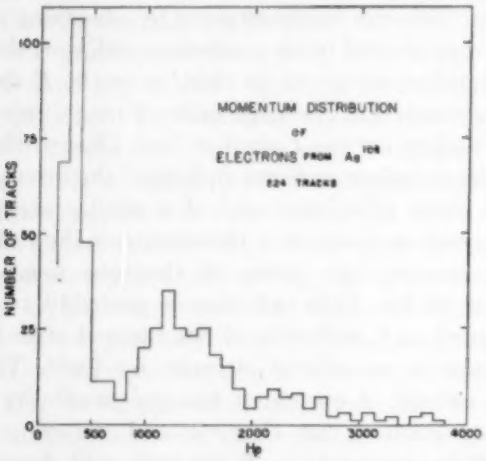

FIG. 4. The momentum distribution of the electrons from the eight-day isomer of Ag^{106}. The low energy group (17 kv) probably consists of Auger and photoelectrons from the K radiation of palladium. The other electrons are probably also secondary in nature.

It seems very unlikely that electrons of such low energy could arise from an ordinary beta-transition. The most probable explanation seems to be that the low energy group consists of Auger electrons and photoelectrons associated with the K-electron capture process in Ag^{106}. The process, of course, should be accompanied by emission of the K radiation of palladium. The writer was unable definitely to detect this radiation, however, while using a copper radiator in the cloud chamber. Other workers[8, 9] have also searched for this radiation with negative results. However, the gamma-ray activity is so intense that the method illustrated by Fig. 4 is undoubtedly much more sensitive.

From the known thickness of the foil (0.002 cm) the fluorescent yield (0.75), the absorption coefficient of Pd K radiation in silver (150 cm^{-1}), and the range of the electrons (0.6 mg/cm^2), one can determine the number of slow electrons observed per disintegration. Then taking account of the relative number of slow and fast electrons observed, one finds that there are roughly 50 transitions leading to the low energy group for every transition producing a higher energy electron.

Feather[9] estimates that there are four gamma-rays per disintegration, and in this connection it is interesting to ascertain whether or not it is necessary to assume that the higher energy electrons observed form an ordinary beta-spectrum.

If μ is the absorption coefficient of a gamma-ray, and t is the thickness of a foil throughout which the radioactive atoms are uniformly spread (e.g. by neutron activation), then the fraction of the gamma-quanta ejecting an electron from one side of the foil is given approxi-

[5] M. L. Pool, J. M. Cork and R. L. Thornton, Phys. Rev. **52**, 380 (1937).
[6] M. L. Pool, Phys. Rev. **53**, 116 (1938); M. L. Pool and E. C. Campbell, Phys. Rev. **53**, 272 (1938).
[7] J. R. Richardson, Phys. Rev. **55**, 236 (1939).
[8] L. W. Alvarez, Phys. Rev. **54**, 486 (1938).
[9] N. Feather and J. Dunworth, Proc. Roy. Soc. **A168**, 566 (1938).

mately by the expression

$$n = \{\mu t/2\}\{\ln (1/\mu t) + 0.92\}.$$

This is strictly valid only for small values of μt and spherical symmetry of the gamma-ray electron interaction; but it is approximately applicable here.

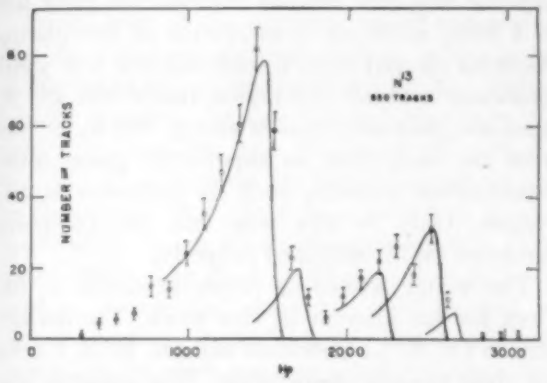

FIG. 5. The electrons ejected from a lead radiator by the radiation from a thin source of N^{13} arranged so that most of the positrons are annihilated behind the lead collimating shield. The energy of the gamma-ray is 280±30 kv.

For 350-kv radiation in the foil used, one finds that $n = 0.016$. This means that one would expect 1.6 percent of the gamma-quanta to eject an electron from one side of the foil. The corresponding number for a gamma-ray of 800 kv is 0.7 percent. Thus the number of electrons observed in the main part of the distribution can be easily accounted for by the ordinary processes of gamma-ray degradation. In addition, the calculations of Dancoff and Morrison[10] have made it clear that the internal conversion process would play an important role at the low energies, particularly for quadrupole and higher multipole transitions.

Sources of Ag^{106} have not yet been available which were sufficiently strong to make possible an accurate investigation of the gamma-ray spectrum. However, preliminary results with a lead radiator (200 tracks) indicate that the spectrum is certainly complex, with lines at least at 0.3 Mev, 0.5 Mev and 0.9 Mev. It is readily seen that this complex gamma-radiation could account for the "beta"-spectrum observed in Fig. 4.

[10] S. M. Dancoff and P. Morrison, Phys. Rev. **55**, 122 (1939).

N^{13} AND Cu^{64}

Evidence has previously been reported[11] which indicates the presence of gamma-radiation from N^{13} in addition to the positron annihilation radiation. An additional experiment has been performed by arranging a thin source of N^{13} so that most of the positrons were annihilated behind the lead collimating shield, but keeping the source itself in full "view" of the cloud chamber. The source was produced by bombarding charcoal with six-Mev deuterons.

The momentum distribution of the electrons ejected from a lead radiator is shown in Fig. 5. Again the components drawn in as smooth curves are determined from the theoretical ratios rather than the experimental points. Statistical probable errors are indicated by the vertical lines. The annihilation radiation, of course, is still present but the slower group of electrons is much more predominant than in Fig. 1 of reference 11, which shows the distribution obtained when all the positrons are stopped near the source. In order to examine the possibility that this group of electrons was due to some unrecognized scattering process, a source of Cu^{64} of equivalent strength was produced by deuteron bombardment of copper. The distribution obtained under the same geometrical conditions as in the case of N^{13} is shown in Fig. 6. No evidence of the low energy group is to be seen.

Assuming that this presents evidence for the existence of gamma-radiation from N^{13}, we may

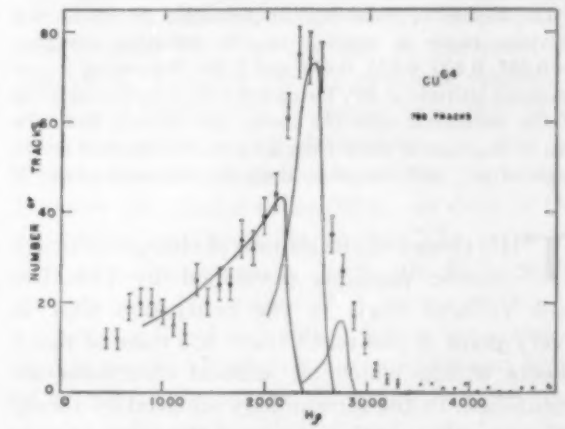

FIG. 6. The electron distribution obtained under the same geometrical conditions as in Fig. 5, but with an equivalent source of Cu^{64}.

[11] J. R. Richardson, Phys. Rev. **53**, 610 (1938).

inquire as to its energy. The radiation, of course, may consist of several lines, but if it is embodied in a single line we see from the data of Fig. 5 that the energy is about 280 kv. This is obtained from the maximum of the K-photoelectron distribution by using the method explained in the case of Au^{198}. The relative intensity of the gamma-ray must be determined from the data obtained with all the positrons of the source stopped in its immediate neighborhood. The result is found that there is 0.21 quantum of 0.3-Mev radiation for every quantum of annihilation radiation. In other words, there is 0.4 quantum of 0.3-Mev radiation for every positron emitted. This intensity estimate is uncertain by a factor of two. The result given previously was in error.

It is interesting to observe that in the case of Cu^{64} there is indication of a high energy tail to the annihilation radiation, as was found previously in the case of a carbon radiator.[12] This may mean the presence of some gamma-radiation from this source.

[12] J. R. Richardson, Phys. Rev. **53**, 124 (1938).

Conclusion

It seems evident that for a complete investigation of a gamma-ray spectrum, it is necessary to employ radiators of various materials. A carbon radiator will give reliable information from 0.5 to 4 Mev, while an investigation of the photoelectrons ejected from a lead radiator will yield information about the region below 500 kv. If there are photoelectrons of energy 100 kv or less from the lead, then an experiment using some intermediate radiator such as cadmium is advisable. Only in this way can the complete spectrum be investigated properly.

The writer wishes to thank Professor J. M. Cork for his interest in this work. Thanks are due to Dr. R. L. Thornton and Dr. B. R. Curtis for their friendly cooperation. This research was supported by the Horace H. Rackham Trust Fund.

APRIL 1, 1939 PHYSICAL REVIEW VOLUME 55

The Penumbra at Geomagnetic Latitude 20° and the Energy Spectrum of Primary Cosmic Radiation

R. Albagli Hutner
Massachusetts Institute of Technology, Cambridge, Massachusetts

(Received December 17, 1938)

The method of obtaining the penumbra presented in a previous paper is applied to the following energies: $r=0.385$, 0.400, 0.425, 0.450 and 0.500 Störmer at a geomagnetic latitude of 20°. Two graphs showing the variation of the penumbra with the energy are derived from the (γ_1, η) diagrams of these energies: one at a constant zenith angle of 60°, and the other along the east-west plane. If the number of primaries is assumed to vary inversely as the 2.8 power of their energy, the contribution of the penumbra to the directional intensity at a zenith angle of 60° is calculated, and is shown to be far from negligible. The calculated intensities are quite sensitive to the energy distribution used, and this suggests a possible method for determining the energy spectrum of primary cosmic rays.

THE theory of the motion of charged primary cosmic particles developed by Lemaître and Vallarta leads to the conclusion that at every point of the earth there is a cone of many sheets within which all allowed directions are contained. In the terminology adopted by them,[1] the penumbra is the region of the allowed cone situated between the main cone and the Störmer cone, more precisely between the main cone and the simple shadow cone of Schremp.[2] In a previous paper[3] a description of methods for the determination of the penumbra was given, together with a brief summary of its structure. It was there pointed out that a complete analysis of this region, at least at one latitude, is imperative before definite theoretical conclusions, suit-

[1] G. Lemaître and M. S. Vallarta, Phys. Rev. **49**, 719 (1936).

[2] E. J. Schremp, Phys. Rev. **54**, 158 (1938).

[3] R. Albagli Hutner, Phys. Rev. **55**, 15 (1939).

able for an experimental verification, could be given. In this paper it is proposed to present such an analysis for the geomagnetic latitude 20°. Similar results may be presented later for other latitudes where the penumbra is still important.

I. Further Development of the Theory

In the part of the previous paper[3] concerning Fig. 8, it was pointed out that all orbits eventually going to (or coming from) infinity had to bounce between the two vertical envelopes F_0' and F_1' (Lemaître and Vallarta's F_0 and F_1, Fig. 1).[1] This leads to the fact first pointed out by Schremp,[4] that there is a value[5] of x, and therefore r, above which the penumbra is completely dark. The data as obtained directly from Bush's Differential Analyzer[6] are plotted in Fig. 4 (previous paper[3]), upper diagram. However when the work was continued in the summer and fall of 1938 it was found that a lower limit than that of the F_0 cut-off can be assigned for certain values of γ_1. In the method for generating re-entrant orbits[4] (third program[3]), starting points were taken along the equator at definite

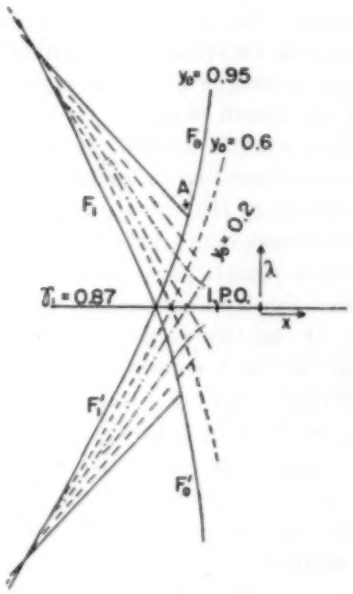

Fig. 1. The loci $dx/d\sigma=0$ of the re-entrant orbits through three values of y_0 for $\gamma_1=0.87$. The solid lines are, within the error of the Differential Analyzer, those for the asymptotic orbits. I. P. O. is the point of intersection of the inner periodic orbit and the equator.

[4] E. J. Schremp, Phys. Rev. **54**, 153 (1938).
[5] For the necessary definitions see reference 1.
[6] V. Bush, J. Frank. Inst. **212**, 447 (1931).

Table I. *Positions of A corresponding to each* γ_1.

γ_1	x	r(Störmers)
0.82	−0.070	0.568
0.85	−0.095	0.535
0.87	−0.118	0.511
0.89	−0.125	0.496
0.93	−0.143	0.466
0.97	−0.170	0.435

intervals between the outer and inner periodic orbits for each γ_1. The set of curves corresponding to each initial point is indicated by a value[3] of y_0; Fig. 7 of the previous paper[3] shows an example for $y_0=0.1$ and $\gamma_1=0.97$. The dots marked on these orbits, at the turning points on the left (not at the bottom), indicate the points at which $\dot{x}=0$ ($\dot{x}=dx/d\sigma$). A line connecting the successive points where $\dot{x}=0$ would intersect the two vertical dashed lines (the envelopes for the asymptotic orbits). Those orbits touching the line $\dot{x}=0$ in the part contained between the envelopes of the asymptotic orbits will go directly to infinity, while all other orbits will have at least one more re-entrant section.

The superposition of the different sets of curves for a given γ_1 but successive y_0's shows an orderly arrangement for the corresponding $\dot{x}=0$ curves, as indicated in Fig. 1 for $\gamma_1=0.87$ and for just three y_0's (to avoid confusion). The symmetry of the solutions about the equator permits the same set of lines to be drawn on each side of the $\lambda=0$ line, as shown. A study of Fig. 1 yields the fact that all re-entrant orbits must cross the envelopes of the asymptotic orbits (solid lines) to the left of the point A. Therefore, although the F_0 envelope reaches a value of x (and hence r) greater than that of A, it is the latter which determines the energy[7] above which the penumbra is dark for a given γ_1. Likewise all greater values of γ_1 are dark in the penumbra for the value of r at the point A. The quantitative data from the Differential Analyzer for the values of A corresponding to each γ_1 are listed in Table I, where the position of A is given in both Störmer units (r) and units of x. Fig. 2 shows the deviation between the results (solid line) published previously (referred to as the F_0 cut-off) and those (dashed line)

[7] For a table of equivalences between Störmer units and energy in ev see G. Lemaître and M. S. Vallarta, Phys. Rev. **43**, 90 (1933).

contained in Table I. For γ_1 equal to about 0.93 and above, the two curves coincide. An example of the use of the dashed curve appears in Fig. 5, line AB.

II. Analysis of Further Results Obtained from the Differential Analyzer

A description of the third program used on the Differential Analyzer, as well as a table designating all the curves obtained, appeared in a previous paper.[3] These data were used as the bases of the attempt to complete the diagrams

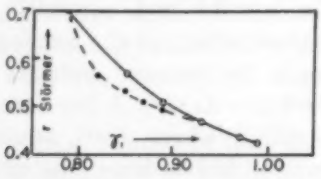

Fig. 2. All values of (γ_1, r) above the dashed line have the penumbra completely dark. The solid line was determined from the F_0 cut-offs; the dashed line is a result of all the diagrams like that of Fig. 1.

of the penumbra for all pertinent energies at one latitude, i.e., for the range $0.376 < r < 0.700$ störmer at geomagnetic latitude 20°. In practice, energies above $r = 0.500$ Störmer contribute very little so that the final selection of values of r were: 0.385, 0.400, 0.425, 0.450 and 0.500 Störmer.

Description of the fourth program

As the η diagrams for these values were drawn it became evident that more data were needed, and the Differential Analyzer was resorted to once again in the spring of 1938. Since a more definite and limited goal was then in view, a new approach (the fourth program) was decided upon, in which runs were started at the particular (r, λ) desired and for such values of η as were needed to complete the η diagrams derived from the trajectories obtained in the third program. As a check on the results deduced from the third program, the runs of the fourth program were made to overlap those of the third program, with a resulting discrepancy that proved larger than was expected. It had always been known that the ends of long trajectories were not to be trusted, and one of the excellent features of the third program was the fact that all runs were cut approximately in half by starting at the equator. But even with this advantage some of the results deduced from the third program were shown to be definitely wrong. This depended on the fact that the points (r, λ) through which the orbits were desired came at the ends of the runs of the third program and very often at curved portions of the trajectories, where the slope (and hence the angle η) changes very rapidly. (See Fig. 10 of previous paper.[3]) Thus, because of the cumulative error, orbits were made to reach points in the immediate vicinity of the bounce which they would not have attained had the path been traced correctly. On the other hand the runs of the fourth program were made to start at the desired point and slope, and hence were known to go through that point, but, at the same time, the total trajectories were usually longer.

A study of the two sets of curves and several test runs led the writer to believe that most of the error is introduced whenever there is a long drive in any one direction for either x or λ and considerably amplified when this is followed by a sharp turn. In this case the error would not depend merely on the total arc length traversed but rather on the particular twists of each orbit. It was thought that a rough calibration of some sort between the two programs could be obtained by running a complete set of curves, by the method of the fourth program, for the η diagram of $\gamma_1 = 0.91$, $r = 0.425$, $\lambda = 20°$, and comparing it with the corresponding η diagram as derived from the curves of the third program. This and other direct comparisons between trajectories of the third and fourth programs were the bases for the successive approximations which brought the curves of the two programs into agreement and led to the final results presented here. In the case of high values of η (positive or negative) the curves of the fourth program were relied on entirely, which was perfectly valid, for the majority of such cases were short runs. For the entire η diagrams of $r = 0.385$ and 0.400, the third program orbits were not to be trusted since the orbits were in the immediate vicinity of a bounce when passing through these points; the results were based wholly on the fourth program.

Results

Figures 3 to 5, inclusive, give the final appearance of the penumbra for the energies desig-

nated, in the form of (γ_1, η) diagrams rather than in the cone projection of Lemaître and Vallarta.* The reason for the use of the (γ_1, η) diagram is that the cone projection distorts the results to the disadvantage of the regions close to the horizon, whereas the former gives the same weight to all angles. Areas of "light" are shaded by lines NW to SE, closely spaced; while those of "darkness" are NE to SW, widely spaced. Blank spaces between the strips have bands of narrow to infinitesimal width; any long blank columns indicate lack of sufficient data. The exact limits of the regions bordered by dashed lines are uncertain, but there is evidence for the shape of each such region. The point marked "zenith" is the horizontal projection of the zenith direction. The type of orbit in the conformal, meridian plane (x, λ) giving rise to each patch is shown. The curve marked $z=60°$ is the projection of the locus of points at an angle of 60° with the zenith direction at the given point (r, λ); this zenith angle, rather than the one for $z=45°$, is chosen because the contribution of the penumbra is greater. The values of θ corresponding to the values of some of the γ_1's are marked at the bottom of each diagram. Note that the diagram for $r=0.425$ Störmer published previously[3] has been not only completed but also improved. All diagrams in this paper are for positive particles in the Northern Hemisphere.

* See reference 3 for examples of each for the same (r, λ).

Deductions

From the relation:

$$\cos z = \cos\theta \cos\eta,$$

where z is the zenith angle, the values of θ and η corresponding to a constant zenith angle can be calculated; the γ_1 belonging to each θ for a given (r, λ) can be determined; and finally the curves of constant z drawn on the (γ_1, η) diagrams, as shown on Figs. 3 to 5 for $z=60°$. In order to see the variation of the penumbra with the energy, r, the changes along the curve of constant zenith angle may be plotted as in Fig. 6 for $z=60°$. There is the choice of plotting either η or θ against r. Both were tried and the (η, r) graph found to be more convenient; however

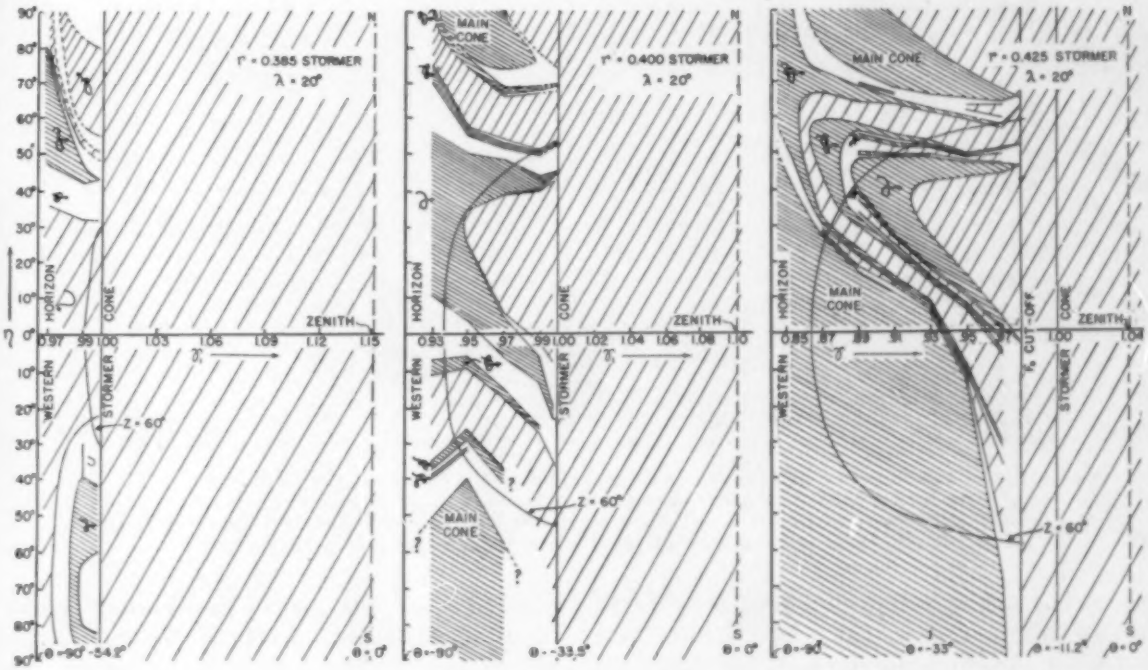

FIG. 3. General appearance of the penumbra for various values of r at $\lambda=20°$. Positive particles; Northern Hemisphere. For $r=0.385$ Störmer (0.881×10^{10} ev for electrons) the eastern horizon appears at $\gamma_1=1.33$; for $r=0.400$ Störmer (0.954×10^{10} ev) it begins at $\gamma_1=1.29$; and for $r=0.425$ (1.07×10^{10} ev) it begins at $\gamma_1=1.24$. In all cases the region from the Störmer cone line to the eastern horizon are "dark."

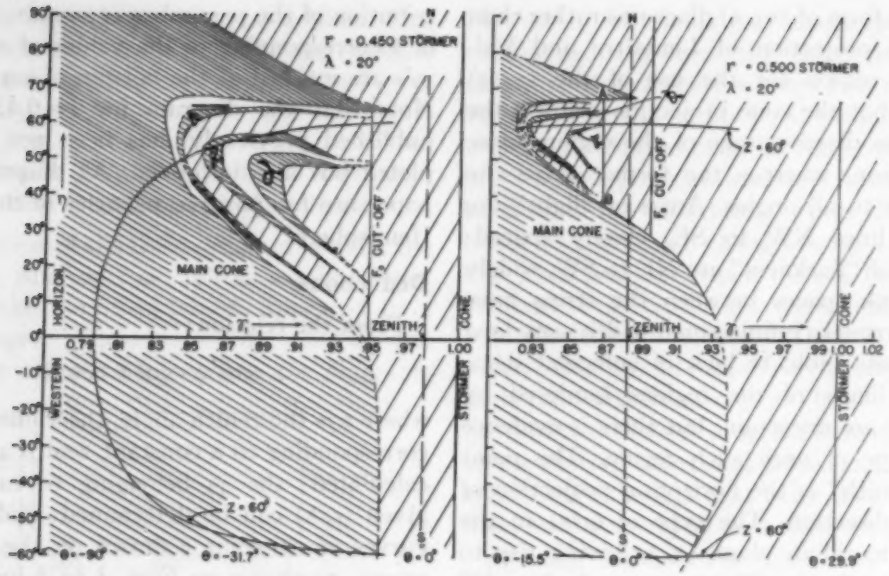

FIG. 4.

FIG. 5.

FIG. 4. General appearance of the penumbra for $r=0.450$ Störmer (1.20×10^{10} ev for electrons). On the right, the eastern horizon appears at $\gamma_1=1.19$, all of the region from the Störmer cone line to the eastern horizon being dark. The diagram continues in essentially the same way from $-60°$ to $-90°$ in η. Positive particles; Northern Hemisphere.

FIG. 5. General appearance of the penumbra for $r=0.500$ Störmer (1.49×10^{10} ev for electrons). On the left, the western horizon appears at $\gamma_1=0.648$, with complete light except for Schremp's simple shadow cone; on the right, the eastern horizon appears at $\gamma_1=1.12$. The line AB is determined by the dashed line in Fig. 2. The diagram continues in essentially the same way to $\eta=-90°$. Positive particles; Northern Hemisphere.

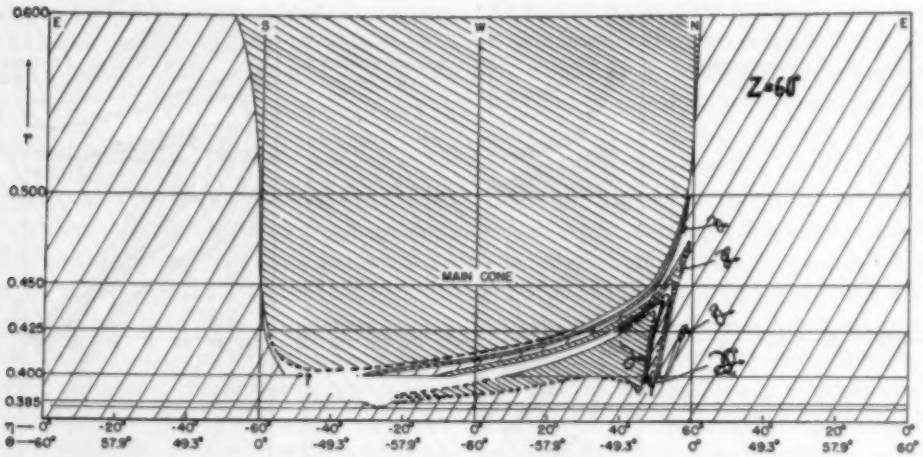

FIG. 6. The effect of r, in Störmers, on the areas of light and dark along the constant zenith angle of 60°. The heavy, black band above the right-hand question mark is a region of light, the type of orbit being indicated by the lower right-hand figure. The letters at the top of the diagram represent the East, North, West and South directions. Positive particles; Northern Hemisphere.

the corresponding values of θ are given in the bottom line of Fig. 6. The East, North, West and South directions are marked. The data from the (γ_1, η) diagrams (Figs. 3 to 5) are represented by horizontal, heavy lines at the marked values of r in Störmers. Sections of "light" are cross-hatched from NW to SE and closely spaced; those of "darkness" are from NE to SW and widely spaced. The narrow blank regions contain strips of small to infinitesimal widths; the blank space around each question mark is due to insufficient data. By studying the diagrams

of the successive γ's (Figs. 3 to 5) quite thoroughly, some conjectures have been hazarded as to how the strips of "light" and "dark" may be extrapolated, and in all cases have been bordered with dashed lines. The values of γ for which these particular strips terminate are not at all certain but there is evidence that the general shapes of the regions are as indicated.

In Fig. 7 the effect of the energy on the "light" and "dark" regions along the East-West plane is shown by plotting γ against the zenith angle along the East-West plane. The markings have the same significance as in the previous diagram.

To obtain cosmic-ray intensities, diagrams like those of Figs. 6 and 7 are especially convenient for determining the limits of integration for the distribution function depending on γ.[8] Fig. 6 makes it clear that for any intensity distribution which emphasizes the lower energies, the penumbra will make important contributions.

To illustrate this, the number of rays per second, $n=\int F(E)dE$, was calculated for the three energy distributions:

$$F_1(E)=B/E^{2.5}, \quad F_2(E)=K/E, \quad F_3(E)=D/e^{E}.$$

The first is made plausible by Nordheim's[9] paper, where he discusses the results and suggestions of many other workers; the others were conveniently chosen to show how sensitive the resultant intensity may be to the energy distribution function used. In all cases n, in arbitrary units, (Fig. 8) is plotted against the azimuthal angle, α, along the curve $z=60°$ from a direction due North to one due West. The relation between the azimuthal angle, α, counted clockwise from the North, the zenith angle, z, and the angle θ, already introduced before is:

$$\sin\theta=\sin z\sin\alpha.$$

This zenith angle and range of azimuths were chosen because a study of Fig. 6 indicates that these directions are the most promising for striking contributions by the penumbra. All of the humps are due entirely to the irregularities of the penumbra; without it the curve in each case would rise very gradually from N to W, without any maxima or minima. Fig. 8 shows that the presence and size of these humps is indeed sensitive to the energy distribution function.

It should be pointed out that the possibility of the presence of humps in curves of this sort was qualitatively predicted by Schremp several years ago and first published[4] in 1938.

The curves of Fig. 8 are valid for positive particles in the Northern Hemisphere. For negative particles in the Northern Hemisphere each (γ_1, η) diagram is to be rotated about the N-S line, so that what appears on the West for posi-

[8] For electrons at high energies: $E=Mer^2/R^2=0.095\gamma^2$; where M is the magnetic moment in e.m.u., e is the electronic charge in e.s.u., R is the radius of the earth in cm, E is the energy in ergs and γ is in Störmers.

[9] L. W. Nordheim, Phys. Rev. **53**, 694 (1938).

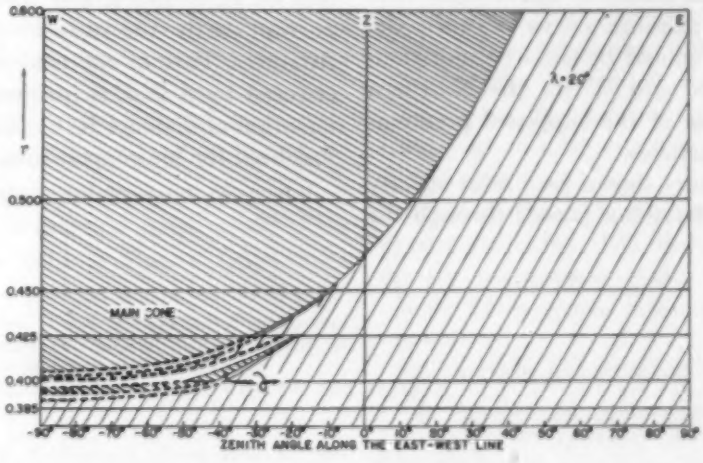

FIG. 7. The energies, γ, are in Störmers. The W, Z and E at the top of the diagram indicate the West, zenith and East directions, respectively. Positive particles; Northern Hemisphere.

tive particles is now on the East for negative ones. The study of Fig. 6 shows that there is no contribution to the penumbra in the N to W section by the negative particles. The effect of their main cones is a rapidly decreasing contribution from N to W, which would just barely wipe out the first small hump of the $B/E^{2.8}$ distribution, if there were an equal number of positive and negative particles; but would serve to increase the difference between the large hump and the rest of the curve toward the West.

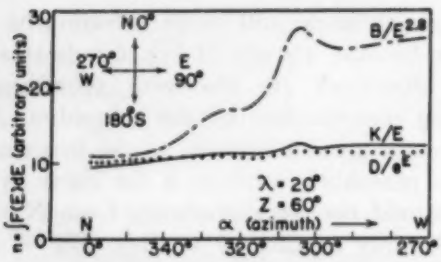

FIG. 8. The azimuthal effect resulting from the three energy distribution functions indicated, with the energy limits obtained directly from Fig. 6. The integrations were made over all energies, including those which are too high to be affected by the earth's magnetic field. Positive particles; Northern Hemisphere. For a mixture of positives and negatives see text.

For the values of the azimuth from 0° to 90°, i.e., from N to E, the curves of Fig. 8 hold for the negative particles, and the positive particles would contribute by their main cones only, in the way mentioned in the previous paragraph for negative particles. Thus if suitable counter experiments could be made, it would seem that the number *versus* azimuth curve between the N and E directions should be less irregular than that between the N and W (in the Northern Hemisphere) because of the supposed predominance of positive particles.

Of course the results shown here refer strictly to primaries which have not passed through the atmosphere. As for the secondaries, it is possible that the soft cosmic rays do not show up these irregularities, since, if they are produced to a large extent by cascade showers, any original directional effect might well be hidden by the time that the rays reach low altitudes. On the other hand the more penetrating secondaries would seem to be more promising, especially at altitudes higher than sea level, as already emphasized by Rossi.[10] He points out that the East-West asymmetry is greater if the particles of least energy are filtered out. At Asmara, Eritrea ($\lambda = 11.5°$, altitude 2730 m) a ratio of 1.32 ± 0.03 at $z = 45°$ was found with a lead screen of 8 cm between counters, while without the screen this dropped to 1.19 ± 0.02.

It should be pointed out that although the penumbra for this latitude has been fairly well outlined, no definite decisions on that for other latitudes can be reached. By referring to Fig. 5 of the previous paper,[3] it is seen that latitudes from 25° to 40° may well prove interesting because of the range of energies involved.

ACKNOWLEDGMENTS

The author takes pleasure in acknowledging a grant by the American Association for the Advancement of Science, which has made possible the carrying out of this research. The constant interest and encouragement of Professor M. S. Vallarta is highly appreciated; as well as the cooperation of Professor S. H. Caldwell, Mr. C. E. Shannon and their assistants in connection with the use of Bush's Differential Analyzer. Part of the cost of its operation was covered by a W.P.A. project under the administration of Colonel R. C. Eddy, to whom we are indebted for his cooperation.

[10] B. Rossi, International Conference on Physics **1**, 237 (1934).

On Asymptotic Orbits of Primary Cosmic Rays

ALFREDO BAÑOS, JR.*
Massachusetts Institute of Technology, Cambridge, Massachusetts
(Received September 17, 1938)

I

IN a recent paper by Lemaître and Vallarta,[1] to which reference should be made for a complete statement of the problem treated here and of their methods of attack, results were presented from the analysis of some three hundred trajectories, asymptotic to a known family of unstable periodic orbits, as obtained by means of Bush's Differential Analyzer.[2] These results were submitted then with reservations pending a critical examination of the precision associated with machine trajectories. In a later article,[3] Lemaître and Vallarta presented a full discussion of their method for the determination of asymptotic trajectories by means of the differential analyzer together with a brief outline of the method of calculation of asymptotic trajectories which they developed, using a generalized method of numerical integration, to afford a comparison between machine trajectories and computed trajectories.

To ascertain the magnitude of possible systematic errors in the mechanical determination of asymptotic trajectories Lemaître and Vallarta computed, for $\gamma_1=0.93$, the complete inner family of asymptotic orbits, which they represented by means of two trigonometric series in the total phase $(\omega\sigma+\varphi)$ whose amplitudes, as functions of the independent variable σ, they determined by numerical integration.[4] The purpose of the present note is to compare the results of a calculation of an asymptotic family of orbits, carried out under more adverse conditions than in Lemaître and Vallarta's case, with those obtained with the help of Bush's Differential Analyzer, thereby affording a more searching critical examination of the precision of their analysis.

II

The computation of a family of asymptotic orbits of $\gamma_1=0.85$ essentially falls into three parts: the calculation, by means of Lemaître's method,[5] of the periodic orbit to which the required family of orbits is asymptotic; the determination, by applying the method of characteristic exponents of Poincaré,[6] of an asymptotic expansion representing the desired family of orbits in the close neighborhood of the periodic orbit; and finally, the numerical integration of the whole family of asymptotic orbits, by means of the methods developed recently by Lemaître and Vallarta and extended by the author in an effort to carry out the numerical integration by bisecting the interval of integration, as far away from the periodic orbit as seemed practicable. The details of these computations are summarized in a paper to be published elsewhere.[7]

The complete results of these computations are represented graphically in Fig. 1 which shows the outer, unstable, symmetric periodic orbit for $\gamma_1=0.85$ and 24 computed orbits, evenly spaced, belonging to the asymptotic family. The numbers designating each orbit represent, in units of $\pi/12$ radians, the values of φ in the total phase $(\omega\sigma+\varphi)$ which appear in the trigonometric series employed to compute the coordinates of individual orbits.

Figure 2 shows the simplest doubly asymptotic symmetric orbit (full line), the self-reversing, doubly asymptotic orbits (dot-dash) and the system of envelopes labeled in accordance with

---

* Fellow of the John Simon Guggenheim Memorial Foundation, now Director of the Institute of Physics of the National University of Mexico, Mexico City.

[1] G. Lemaître and M. S. Vallarta, Phys. Rev. **49**, 720 (1936).

[2] V. Bush, J. Frank. Inst. **212**, 447 (1931).

[3] G. Lemaître and M. S. Vallarta, Phys. Rev. **50**, 500 (1936).

[4] G. Lemaître and M. S. Vallarta, Ann. de la Soc. Sci. de Bruxelles **A56**, 102–130 (1936).

[5] G. Lemaître, Ann. de la Soc. Sci. de Bruxelles **A54**, 162 (1935).

[6] H. Poincaré, *Les Méthodes Nouvelles de la Mécanique Céleste* (Gauthier-Villars, Paris, 1892), Vol. I, Ch. IV; and reference 3.

[7] Alfredo Baños, Jr., "On Asymptotic Orbits in the Theory of Primary Cosmic Radiation," forthcoming paper in the Journal of Mathematics and Physics.

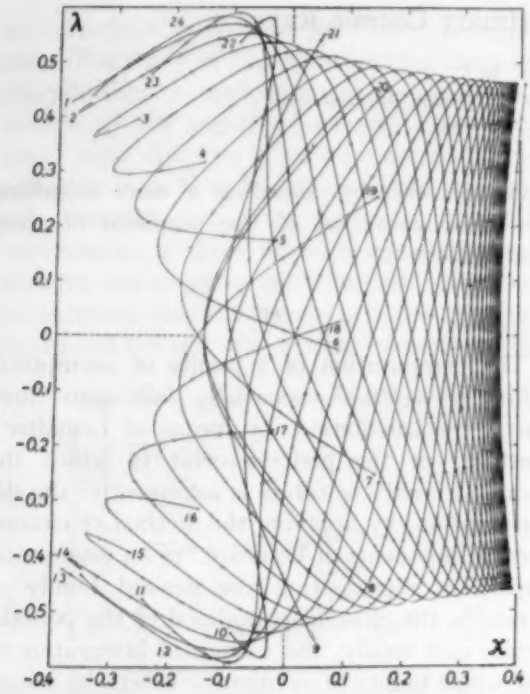

FIG. 1. Calculated family of asymptotic orbits for $\gamma_1 = 0.85$.

the nomenclature adopted by Lemaître and Vallarta.[8] The existence of the simplest, symmetric, doubly asymptotic orbit, known as the *Queen* orbit, which lies in Fig. 1 in the close neighborhood of the orbit $\varphi = 8$ and its symmetric companion $\varphi = 20$, may be predicted from general considerations on the theory of orbits. These considerations, applied to the problem at hand, indicate that, except for a denumerable set of measure zero, which in this case includes the *Queen* orbit and the self-reversing, doubly asymptotic orbits, all orbits belonging to a given asymptotic family eventually cross the periodic orbit and go to infinity.[9]

Figure 3 gives the curves showing the variation, as functions of the latitude λ, of the angles η and η_1, corresponding to those sections of asymptotic orbits which intersect the line $\theta = 0$ coming, respectively, from the envelopes E_0 and E_1 (Fig. 2). As shown in Fig. 3, the curves corresponding to η and η_1 are actually sections of a single smooth curve meeting at the point of maximum latitude $\lambda = 29° 4'$ for which $\eta = \eta_1 = 35°$. The $\eta - \lambda$ diagram of Fig. 3 is estimated to be correct to the nearest 5 minutes; thus, the variation of the zenith angle in the meridian plane, as function of latitude, constitutes a suitable basis of comparison, for this particular value of γ_1, with the values of η, η_1 obtained by means of the differential analyzer. To facilitate this comparison corresponding values of η, η_1 have been tabulated, as read off the curve in Fig. 3, at properly chosen values of λ, in the columns labeled *A* of Table I. These values are to be compared with the corresponding entries given in columns *B*, *C* and *D*, as obtained by means of the differential analyzer.

III

1. An outstanding result of these computations is the proof of the existence of the symmetric, doubly asymptotic *Queen* orbit, now unequivocally established to the extent to which numerical computations, correct to four decimals, constitute sufficient evidence.

2. The complete family of asymptotic orbits for $\gamma_1 = 0.85$, as drawn from the results of the

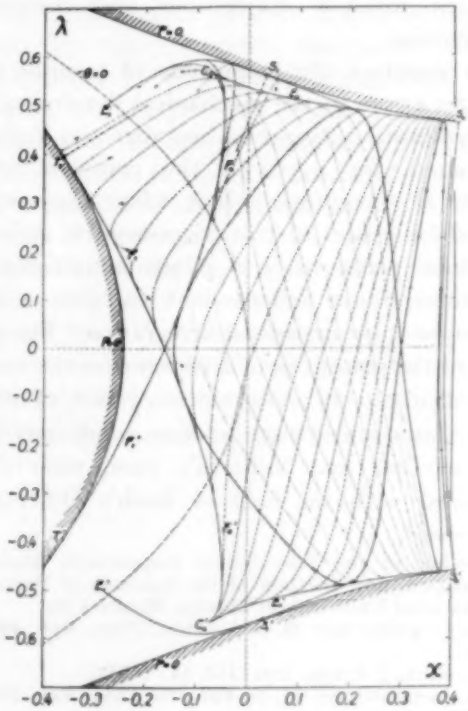

FIG. 2. The "Queen" orbit, the self-reversing doubly asymptotic orbits, and the system of envelopes for $\gamma_1 = 0.85$.

[8] G. Lemaître and M. S. Vallarta, Phys. Rev. **49**, 722–5 (1936).
[9] E. J. Schremp, Phys. Rev. **54**, 153–157 (1938).

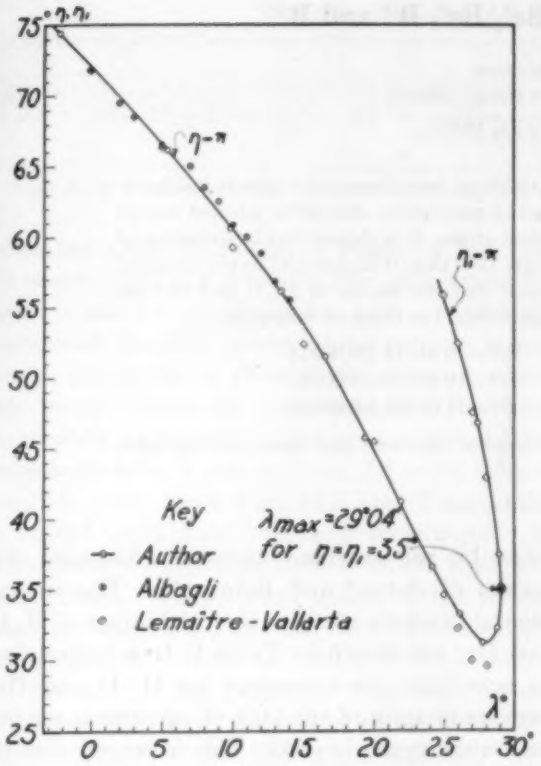

FIG. 3. The zenith angle in the meridian plane as function of latitude for $\gamma_1 = 0.85$.

numerical integration, permits a closer and more critical examination of the precision of the asymptotic trajectories obtained by means of the differential analyzer than had been possible heretofore. By comparing, at a given latitude, the zenith angles in the meridian plane for trajectories drawn by means of the differential analyzer with the corresponding zenith angles for the computed trajectories, it is concluded that the differential analyzer yields for short runs, not exceeding 3 to 4 units of σ, trajectories whose inclinations in the conformal map are correct to better than 1°; and for longer runs, in excess of 10 units of σ, the error may increase to approximately 7°.

3. It is concluded, from these considerations, that the precision of asymptotic trajectories obtained by means of the differential analyzer is ample for all practical purposes connected with the theory of the main cone of allowed directions and allied topics such as the theory of the latitude and azimuthal effects of cosmic radiation.

ACKNOWLEDGMENTS

Grateful appreciation is here extended to Professor M. S. Vallarta for his constant encouragement and able counsel throughout these investigations. For financial assistance, which afforded the necessary leisure to engage in the prosecution of these studies, the writer is happy to acknowledge his debt to the John Simon Guggenheim Memorial Foundation, for a fellowship extending over a period of 28 months; to the National University of Mexico and the Mexican Ministry of Education, for granting leave of absence and financial assistance, and to the Massachusetts Institute of Technology, for two full-tuition scholarships.

TABLE I. *Comparison of values of η and η_1 along line $\theta = 0$ for $\gamma_1 = 0.85$*

λ	η−π	η	η	η	η₁	η₁	η₁−π
0°	72°04′	71°50′	71°48′	74°20′			
2°	69°56′	69°30′					
3°	68°51′	68°30′					
5°	66°35′	66°30′	65°19′	71°30′			
7°	64°12′	65° 0′					
8°	63° 0′	63°30′					
9°	61°35′	62°30′					
10°	60°32′	60°50′	59°18′	67°30′			
11°	59°17′	60° 0′					
12°	58° 0′	58°50′					
13°	56°40′	56°50′					
14°	55°16′	55°30′					
15°	53°48′		52°25′	60°50′			
20°	44°50′		45°30′	50°40′			
25°	35°02′		34°33′	35°40′	57° 0′	55°52′	55°45′
26°	33°25′		32°12′	33°30′	53° 0′	52°26′	52°20′
27°	32° 0′		29°58′	31°20′	48°20′	47°33′	48°35′
28°	31°10′		29°31′	29°50′	43°30′	42°58′	43°50′
29°	33°40′		——	31°40′	33°30′	34°23′	36°40′
Note:	*A*	*B*	*C*	*D*	*D*	*C*	*A*

Note *A*: Author's values read off the $\eta - \lambda$ curve, Fig. 3.
Note *B*: Values obtained by R. Albagli Hutner (Ph.D. thesis, M.I.T., December, 1937; see also Phys. Rev. **55**, 15 (1939)).
Note *C*: Lemaître-Vallarta's critical angles for fundamental points as published in Phys. Rev. **50**, 496 (1936), Table IV.
Note *D*: Lemaître-Vallarta's values read off the corresponding curve for $\gamma_1 = 0.85$ in the $\eta - \lambda$ diagram, published in Phys. Rev. **49**, 725 (1936), Fig. 5.

The Masses of Li^6, Li^7, Be^8, Be^9, B^{10} and B^{11}

SAMUEL K. ALLISON
University of Chicago, Chicago, Illinois

(Received January 23, 1939)

The energy values of the two modes of disintegration of beryllium under proton bombardment, determined by electrostatic analysis, are used in connection with other selected energy release values to set up masses for some of the lightest atoms. It is shown that introduction of the revised electronic charge makes negligible changes (less than 0.07 percent) in the accepted range-energy curve for alpha-particles. It is assumed that the masses of H, D and He^4 are 1.00813 ± 0.00002, 2.01473 ± 0.00002 and 4.00386 ± 0.00006. The deduced masses are:

$Li^6 = 6.01670\pm0.00012$ $\quad$ $Be^9 = 9.01474\pm0.00014$
$Li^7 = 7.01799\pm0.00011$ $\quad$ $B^{10} = 10.01579\pm0.00022$
$Be^8 = 8.00753\pm0.00013$ $\quad$ $B^{11} = 11.01244\pm0.00019$.

These masses are compared with several observed nuclear reactions and mass-spectrographic doublets.

INTRODUCTION

THE precise determinations of the energy released in the two modes of disintegration of beryllium under proton bombardment reported from this laboratory[1, 2] are used in the present paper, in connection with other selected energy data, to construct a revised set of masses for six of the lightest atoms. Masses computed mainly from disintegration data have been previously presented by other authors,[3–6] and it is well known that the masses proposed by Oliphant, Kempton and Rutherford disclosed a rather large error in the mass of helium in use at that time, based on results with the mass spectrograph.

THE MASSES OF H, D AND He^4

In setting up the revised masses, we shall use the values of the masses of hydrogen, deuterium and helium obtained by Bainbridge, and by Bainbridge and Jordan with the mass spectrograph.[7] Our confidence in the mass-spectrographic values for these light atoms seems justified by the excellent agreement between the results of Aston[8] and Bainbridge. The fundamental brackets used for the calculation of H, D and He^4 are shown in Table I. It is instructive to note that the agreement on H, D and He^4 persists in spite of the lack of agreement on the methane-oxygen bracket. This is largely due to the fact that only fractions of the methane-oxygen bracket enter into the computed atomic weights of these lightest atoms. The equations used are given in Table II. In the calculation of the atomic weights of atomic species nearer oxygen, the discrepancy between the two methane-oxygen brackets will appear more and more prominently, and is a large factor in the difference between the weights of C^{12} and B^{10} computed by the two observers.

RE-INVESTIGATION OF THE ALPHA-PARTICLE RANGE CURVE

In order to set up a mass scale, we need to supplement our present results, obtained from the electrostatic analyzer, with other data

TABLE I. *Brackets used in the determination of* H, D *and* He^4 *with the mass spectrograph. Numerical values in thousandths of a mass unit.*

BRACKET	BAINBRIDGE	ASTON
$[H_2 - D]$	1.53 ± 0.04	1.52 ± 0.04
$[D_3 - \frac{1}{2}C^{12}]$	42.19 ± 0.05	42.36 ± 0.18
$[C^{13}H_4 - O^{16}]$	36.49 ± 0.08	36.01 ± 0.24
$[D_2 - He^4]$	25.61 ± 0.04	25.51 ± 0.08

[1] S. K. Allison, Lester S. Skaggs and Nicholas M. Smith, Jr., Phys. Rev. **54**, 171 (1938).
[2] S. K. Allison, E. R. Graves, L. S. Skaggs and N. M. Smith, Jr., Phys. Rev. **55**, 107 (1939).
[3] M. L. E. Oliphant, A. E. Kempton and Lord Rutherford, Proc. Roy. Soc. **150**, 241 (1935).
[4] H. A. Bethe, Phys. Rev. **47**, 633 (1935).
[5] T. W. Bonner and W. M. Brubaker, Phys. Rev. **50**, 308 (1936).
[6] M. S. Livingston and H. A. Bethe, Rev. Mod. Phys. **9**, 245 (1937).
[7] This work is summarized by M. S. Livingston and H. A. Bethe, reference 6.
[8] F. W. Aston, Proc. Roy. Soc. London **A163**, 391 (1937); and Nature **138**, 1094 (1936); **139**, 922 (1937).

TABLE II. *Calculation of* H, D *and* He^4 *from the values of Table I.*

	BAINBRIDGE*	ASTON
$\frac{1}{16}O^{16}+\frac{3}{8}[H_2-D]+\frac{1}{4}[D_2-\frac{1}{2}C^{12}]+\frac{1}{12}[C^{12}H_4-O^{16}]=H$	1.00813±0.00002	1.00812±0.00004
$\frac{1}{8}O^{16}-\frac{1}{4}[H_2-D]+\frac{1}{4}[D_2-\frac{1}{2}C^{12}]+\frac{1}{4}[C^{12}H_4-O^{16}]=D$	2.01473±0.00006	2.01471±0.00007
$2\{D-\frac{1}{2}[D_2-He^4]\}=He^4$	4.00386±0.00006	4.00391±0.00016

* See also K. T. Bainbridge, Phys. Rev. **53**, 922(A) (1938).

obtained from the ranges of produced particles. It seems that the most reliable supplementary data to use is that obtained in cases in which the produced particle is an alpha-particle whose range lies within or close to the region in which the range curve for alpha-particles has been accurately calibrated by magnetic analysis. This region extends in energy from 5.3 to 10.5 Mev, and in range from 4 to 11.5 cm of air under standard conditions. We have recalculated the energies of the alpha-particles from Po, RaC′ and ThC′ (long), using recent values of the fundamental constants. The value of $H\rho$ for the RaC′ alpha-particle is taken as 3.99280×10^5, according to Rosenblum and Dupouy.[9] This value agrees with that of Briggs[10] and was accepted by Rutherford, Wynn-Williams, Lewis and Bowden,[11] who used 3.9930×10^5. The $H\rho$ values for Po and ThC′ (long) particles may then be obtained from the table on page 634 of the paper of Rutherford, *et al.* by multiplying 3.99280×10^5 by the appropriate v/v_0 listed under "new magnet." Table III gives some of the fundamental and derived constants used in the computation of the velocity and energy of the alpha-particle. The following equations are used for the computation of the velocity and energy from the $H\rho$ value:

$$v=c\left[\frac{2e}{mc^2}H\rho-\frac{1}{2}\left(\frac{2e}{mc^2}H\rho\right)^3\cdots\right],$$

$$E=mc^2\left[\frac{1}{2}\left(\frac{v}{c}\right)^2+\frac{3}{8}\left(\frac{v}{c}\right)^4\cdots\right]\text{ in ergs.}$$

The results of the computation, and comparison with previously used values, are shown in Table IV. The mean and extrapolated ranges are from Duncanson[12] and the "previous values" of the velocities are likewise taken from his paper. The "previous values" of the energies are taken from Rutherford, Wynn-Williams, Lewis and Bowden.[11] Disregarding the slight difference of 0.06 percent between the new and previous value of the energy of the RaC′ alpha-particle, it is seen that no revision of the range-energy curve in the accurately known region is required, because of revision of the fundamental constants.

ENERGY VALUES USED IN SETTING UP THE MASSES

We shall use without comment the two energy values found in this laboratory by electrostatic analysis,[1, 2] namely

$$_4Be^9+{}_1H^1={}_3Li^6+{}_2He^4+2.152\pm0.04\text{ Mev},$$
$$_4Be^9+{}_1H^1={}_4Be^8+{}_1D^2+0.557\pm0.006\text{ Mev}.$$

In addition we will use

$$_3Li^6+{}_1D^2={}_2He^4+{}_2He^4+22.08\pm0.07\text{ Mev}.$$

Oliphant, Kempton and Rutherford[13] compared the range of the alpha-particles from this reaction, when produced with 0.19-Mev deuterons, with the range of 8.62 (extrapolated range) ThC′ particles. They used an absorption tube with thin mica windows for the comparison and report that "the range of the alpha-particles emitted at

TABLE III. *Numerical values useful in computation of the range-energy relation of alpha-particles.*

$e=4.803\times10^{-10}$ e.s.u.	$N=6.0221\times10^{23}$
$c=2.99774\times10^{10}$ cm sec.$^{-1}$	$e/m=1.7597\times10^7$ e.m.u./g
one unit of atomic weight	1.6606×10^{-24} g
mass of the electron	9.11×10^{-28} g
mass of helium atom	6.649×10^{-24} g
one electron volt	1.6022×10^{-12} erg
one unit of atomic weight	9.313×10^8 ev
mass of the alpha-particle	6.647×10^{-24} g
mc^2 for the alpha-particle	5.973×10^{-4} erg
$mc^2/2e$ for the alpha-particle	6.218×10^8 ergs/e.s.u.

[9] S. Rosenblum and G. Dupouy, Comptes rendus **194**, 1919 (1932).

[10] G. H. Briggs, Proc. Roy. Soc. London **A118**, 549 (1928).

[11] Lord Rutherford, C. E. Wynn-Williams, W. B. Lewis and B. V. Bowden, Proc. Roy. Soc. London **A139**, 617 (1933).

[12] W. E. Duncanson, Proc. Camb. Phil. Soc. **30**, 102 (1933).

[13] M. L. E. Oliphant, A. E. Kempton and Lord Rutherford, Proc. Roy. Soc. London **A149**, 406 (1935).

right angles to the bombarding beam is 12.70 ±0.05 cm under standard conditions." The context leaves little doubt that extrapolated range is meant. From Table VI of Duncanson's paper, which applies to extrapolated range, it is found that

$$(v-v')/v_0 = -21.80\times10^{-3},$$

where v is the true velocity, v_0 is the RaC′ alpha-particle velocity of Table IV, and v' is the velocity calculated from the v^3 law, that is,

$$v' = 1.9210\times10^9(12.70/6.945)^{\frac{1}{3}}.$$

One obtains $v = 2.3071\times10^9$, and from the relativistic energy equation, 11.09 Mev. The energy release in the reaction can be calculated by

$$Q = 2(\text{energy of one of the alpha-particles}) - \tfrac{1}{2}(\text{energy of the deuterons}),$$

and one obtains 22.08 Mev, in agreement with the value 22.06±0.07 given by the original authors. It is instructive to note that the slope of the range-energy curve in this region is such that

$$dE/dx = 0.050 \text{ Mev/mm},$$

so that the author's estimated error corresponds to only 25,000 volts. Furthermore if we are to make $_4Be^8$ unstable on the mass scale proposed here by assuming an error in this reaction, we must suppose that the authors made an error of two mm in the range. Livingston and Bethe have discussed corrections for obliquity and thick target effect in this reaction and give an energy release of 22.07±0.07 Mev.

The reactions thus far listed lead to masses of $_3Li^6$, $_4Be^8$, and $_4Be^9$. To include the mass of $_3Li^7$ in our system, we use the reaction

$$_3Li^7 + {}_1H^1 = {}_2He^4 + {}_2He^4 + 17.13\pm0.06 \text{ Mev}.$$

The range of the alpha-particles produced in this reaction lies within the calibrated portion of the range-energy relation, and has been investigated by Oliphant, Kempton and Rutherford.[13] The range is about two mm shorter than that of the well-known ThC′ alpha-particle of 8.764 Mev. Computing directly from their stated mean range of 8.29±0.03 cm at 0.19-Mev protons, we obtain a reaction energy 17.08±0.06 Mev. We adopt the value 17.13±0.06 given by Livingston and Bethe after a consideration of thick target corrections, etc.

To include the masses of the stable boron isotopes in our system, we use two reactions linking them with $_4Be^8$.

$$_5B^{10} + {}_1D^2 = {}_4Be^8 + {}_2He^4 + 17.80\pm0.15 \text{ Mev},$$
$$_5B^{11} + {}_1H^1 = {}_4Be^8 + {}_2He^4 + 8.55\pm0.11 \text{ Mev}.$$

The second of these reactions was investigated by Oliphant, Kempton and Rutherford[3] and the alpha-particles were found to have a mean range of 4.40±0.06 cm with 0.19-Mev protons. Alpha-particles of RaC, having 4.043-cm mean range are known to have an energy of 5.508 Mev, and RaA alpha-particles of mean range 4.620 cm have 5.994-Mev energy. Interpolating between these two points it appears that 4.40-cm particles have an energy of 5.81 Mev. This leads to the reaction energy 8.55 Mev listed above. The original authors gave 8.49 as the reaction energy in Mev.

The first of the above boron reactions was investigated by Cockcroft and Lewis.[14] The high energy alpha-particles were absorbed mostly in mica, which diminishes the accuracy of the range measurement. The most accurate of the various trials they made was with 0.55-Mev deuterons, and the extrapolated range was 14.74±0.05 cm. Again from Duncanson's Table VI, it is found that $(v-v')/v_0$ is -29.25×10^{-3}, and the alpha-particle energy is 12.20 Mev. This gives a reaction energy of 17.88 Mev, and allowing some weight to the other trials of Cockcroft and Lewis,

[14] J. D. Cockcroft and W. B. Lewis, Proc. Roy. Soc. London **A154**, 246 (1936).

TABLE IV. *Effect of new values of e and e/m on the range-energy relationship of the alpha-particle.*

Source	Mean Range	Extrapolated Range	$H\rho\times10^{-4}$	Velocity $\times10^9$	Energy (Mev)	Previous Values	
						Energy	Velocity
Po	3.805	3.848	3.3189	**1.5978**	**5.305**	5.303	1.5976
RaC′	6.870	6.945	3.9928	**1.9210**	**7.678**	7.683	1.9220
ThC′	11.533	11.644	4.6736	**2.2469**	**10.543**	10.538	2.2495

TABLE V. *Reaction energy values used in computation of the masses of* Li^6, Li^7, Be^8, Be^9, B^{10}, B^{11}.

REACTION	ORIGINAL AUTHOR'S ESTIMATE	LIVINGSTON AND BETHE	ADOPTED VALUE MEV	EQUIVALENT MASS, MMU
$_3Li^7(p, \alpha)_2He^4$	17.06 ±0.06	17.13±0.06	17.13 ±0.06	18.40 ±0.07
$_4Be^9(p, d)_4Be^8$	0.557±0.006	——	0.557±0.006	0.598±0.006
$_4Be^9(p, \alpha)_3Li^6$	2.152±0.04	——	2.152±0.04	2.311±0.04
$_3Li^6(d, \alpha)_2He^4$	22.06 ±0.07	22.07±0.07	22.08 ±0.07	23.71 ±0.08
$_5B^{10}(d, \alpha)_4Be^8$	17.5 ±0.15	17.76±0.08	17.80 ±0.15	19.13 ±0.16
$_5B^{11}(p, \alpha)_4Be^8$	8.49	8.60±0.11	8.55 ±0.11	9.18 ±0.12

TABLE VI. *Masses computed from Table V.*

ATOM	ADOPTED MASS	BAINBRIDGE	ASTON	METHOD
$_3Li^6$	6.01670±0.00012			23.71 $+2_2He^4-{}_1D^2$
$_3Li^7$	7.01799±0.00011	7.01818±0.00012		18.40 $+2_2He^4-{}_1H^1$
$_4Be^8$	8.00753±0.00013			$-0.598+{}_4Be^9+{}_1H^1-{}_1D^2$
$_4Be^9$	9.01474±0.00014	9.01516±0.00020		$2.311+{}_3Li^6+{}_2He^4-{}_1H^1$
$_5B^{10}$	10.01579±0.00022	10.01631±0.00020	10.0161±0.0003	19.13 $+{}_4Be^8+{}_2He^4-{}_1D^2$
$_5B^{11}$	11.01244±0.00019	11.01292±0.00016		9.18 $+{}_4Be^8+{}_2He^4-{}_1H^1$

which gave slightly lower values, we arrive at 17.80±0.15. Cockcroft and Lewis gave 17.5 Mev, and Livingston and Bethe on recalculation of their results gave 17.76 Mev as the energy release.

The reactions used and the resultant masses are summarized in Tables V and VI. The uncertainties in the adopted masses are computed from those in the basic data by the formula

$$\epsilon=(\epsilon_1^2+\epsilon_2^2+\cdots)^{\frac{1}{2}}.$$

AGREEMENT WITH OTHER EXPERIMENTS

The masses of Table VI may be used to predict the energy release in nuclear reactions other than those of Table V, and the result compared with experiment. Such a comparison is given in Table VII. It is seen that the calculated and observed values of Q are in agreement within the specified limits.

The extent of the agreement of the adopted masses with certain doublets observed in the mass spectrograph is shown in Table VIII. In these doublets, then, we have agreement between the disintegration results and the mass spectrograph.

In Table VI it is evident that the adopted masses from Li^6 to B^{11} are lower than the mass spectrographic results of Bainbridge. This may be connected with the unexplained discrepancy between Bainbridge's methane-oxygen bracket and Aston's measurement of the same difference.

It is hoped that H^3 and He^3 can soon be added to the list of masses from experiments made with the electrostatic analyzer in our laboratory.

TABLE VII. *Calculated energy releases from Table VI compared with experiment.*

REACTION	CALCULATED Q	OBSERVED Q	REFERENCE
$_4Be^9(d, \alpha)_3Li^7$	7.09±0.17 Mev	7.03±0.12	1
$_3Li^6(d, p)_3Li^7$	4.94±0.11	5.02±0.12	2
$_5B^{11}(d, \alpha)_4Be^9$	7.98±0.23	8.13±0.12	3
$_5B^{10}(d, p)_5B^{11}$	9.26±0.20	9.14±0.06	3
$_5B^{10}(n, \alpha)_3Li^7$	2.71±0.24	2.90	4

[1] M. L. E. Oliphant, A. E. Kempton and Lord Rutherford, Proc. Roy. Soc. **150**, 241 (1935) give 7.21 Mev as the energy release here, which is higher than corresponds to their stated extrapolated range of 3.0 cm at 0.19-Mev deuterons. J. H. Williams, R. O. Haxby and W. G. Shepherd, Phys. Rev. **52**, 1031 (1937) found 2.92 cm mean range at zero deuteron energy, which gives 6.95 Mev. The 7.03 value used here is from a private communication of H. A. Bethe, who applied thick target corrections to the result of Williams, Haxby and Shepherd.

[2] J. D. Cockcroft and E. T. S. Walton, Proc. Roy. Soc. London **144**, 704 (1934) as revised in Livingston and Bethe, reference 6.

[3] J. D. Cockcroft and W. B. Lewis, Proc. Roy. Soc. **154**, 246 (1936) as revised in Livingston and Bethe, reference 6.

[4] W. Maurer and J. B. Fiske, in publication. Made available to us by Dr. W. Gentner. A neutron mass of 1.00897±0.00006 is assumed in the calculated energy.

TABLE VIII. *Comparison of calculated doublet differences with those observed in the mass spectrograph.*

BRACKET	BAINBRIDGE	ADOPTED MASSES
$[Be^9H-B^{9}]$ $[Be^9H-\frac{1}{2}Ne^{20}]-[B^{10}-\frac{1}{2}Ne^{20}]$	6.96±0.20 7.16±0.25	7.08±0.25
$[B^{10}H-B^{11}]$ $[B^{10}H_3-C^{12}]-[B^{11}H-C^{12}]$ $[B^{10}H-\frac{1}{2}Ne^{22}]-[B^{11}-\frac{1}{2}Ne^{22}]$	11.60±0.10 11.61±0.22 11.50±0.52	11.48±0.29

On the Determination of the Signs of Nuclear Magnetic Moments by the Molecular Beam Method of Magnetic Resonance*

S. MILLMAN
Columbia University, New York, New York

(Received February 17, 1939)

It is shown that the molecular beam magnetic resonance method for measuring nuclear magnetic moments is capable of determining the sign of a nuclear moment even though an oscillating perturbing field is substituted for the rotating field required by the theory. The sign determination is obtained from an asymmetry in the resonance curve introduced by the end effects of the oscillating field. The signs of the nuclear moments of Li^6, Li^7 and F^{19} were found to be positive, in agreement with known results.

THE molecular beam magnetic resonance method[1] for determining nuclear magnetic moments measures the Larmor precession frequency of a nucleus in a known strong magnetic field. The theory[2] upon which the method is based, requires the application of a small perturbing field, at right angles to the fixed strong field, rotating with the same frequency and in the same sense as the Larmor precession of the nucleus possessing angular momentum and magnetic moment. If this requirement is fulfilled, the method is capable of measuring not only the magnitude of the nuclear moment but also its sign, since the sense of precession depends upon whether the magnetic moment is in the same direction as the mechanical moment (moment positive) or in the opposite direction (moment negative). However, when an oscillating field is substituted for the rotating field, as has been done in the experiments heretofore described, one effectively introduces two component magnetic fields rotating in opposite directions, one of which rotates in the same sense as the precession and is, therefore, effective in producing the nuclear reorientations that make it possible to identify the Larmor frequency. The other rotating component does not interfere in any way with an experiment designed to measure the magnitude of the magnetic moment, but prevents the determination of the sign of the nuclear moment, since, if the perturbing field is one of pure oscillations along its entire length there is no way of finding out which of the two components is effective in producing transitions. It is the purpose of this note to point out that the two-wire field heretofore used does not, in fact, produce a pure oscillating field over its entire length, and that this feature may be used to determine the signs of nuclear magnetic moments.

A schematic perspective diagram of the hairpin-shaped copper tubes, carrying the oscillating current, in the neighborhood of the molecular beam, is shown in Fig. 1. The center line represents the path of the molecular beam and lies in the horizontal plane defined by the axes of the sections B and B' of the hairpin. The sections A and A' are vertical and lead outside the vacuum system to a turn of copper tubing coupled inductively to the tank coil of the oscillator. The sections C and C' are also vertical and form a loop as shown in the diagram. The strong homogeneous field is horizontal and is perpendicular to the beam axis.

Consider now the magnetic field produced by the oscillating current in the wires. When the current in the tubes is as indicated by the arrows, the directions of the field at representative points along the beam path are as indicated by the circled arrows. At D the contribution to the oscillating field is chiefly from the sections A and A'. The field direction here is approximately that of the beam axis. At E the field makes an angle of about 45° with this axis. In the greater portion of the beam path in the oscillating field, from F to G, the lines of force are vertical. With respect to the moving molecule the field has turned in the sense indicated by the arc of a circle, the plane of which is at right angles to the

* Publication assisted by the Ernest Kempton Adams Fund for Physical Research of Columbia University.

[1] I. I. Rabi, S. Millman, P. Kusch and J. R. Zacharias, Phys. Rev. **55**, 526 (1939).

[2] I. I. Rabi, Phys. Rev. **51**, 652 (1937).

strong homogeneous field. When the current in the wires has reversed, the field directions are as shown by the triangled arrows. Again the field has turned in the same sense as before. Similar considerations show that the turning sense of the lines of force at the detector end of the oscillating field is the same as the one just described for the source end. Thus with respect to the moving molecule the perturbing field is strictly oscillatory only in the region from F to G, while at the end regions the field is a superposition of oscillation and rotation. If we assume that the turning of the field through an angle of 90° takes place in a distance about twice that between the axes of B and B', then for molecules having thermal velocities of the order of 10^5 cm/sec. it is equivalent to a rotational frequency, Δf, of 3×10^4 cycles per second, which is of the order of one percent of the oscillating frequencies, f, used in these experiments. Since the oscillating field can be resolved into two component fields, one rotating in the same direction as the end rotation just described and the other in the opposite sense, the effective perturbing field at the end regions rotates with a frequency $f+\Delta f$ if the Larmor precession is in the same sense as this end rotation, and with a frequency $f-\Delta f$ if the precession is in the opposite sense. A resonance curve plotting intensity against value of strong homogeneous field, H, will show a principal minimum at the position H given by $f=\mu H/Ih$ and an additional minimum (which may or may not be resolved from the principal minimum) at a field value given either by $H+\Delta H=(f+\Delta f)Ih/\mu$ or by $H-\Delta H=(f-\Delta f)Ih/\mu$. Since the sense of the Larmor precession depends only on the direction of H and on the sign of the magnetic moment, μ, we may determine the sign of μ by a mere glance at a resonance curve obtained for a known H direction, or better still by observing two curves corresponding to opposite field directions. Fig. 2 shows a pair of such resonance curves obtained for Li^7 with Li_2 molecules. The experimental conditions were identical for the two curves except that for one curve H was in a direction opposite to that for the other. The additional minimum, in each case at about 30 gauss from the principal minimum, appears on the high field side in one curve and on the low field side in the other. Either curve leads to a positive moment for the Li^7 nucleus, in agreement with results obtained from h.f.s. measurements[3] and from atomic beam determinations.[4]

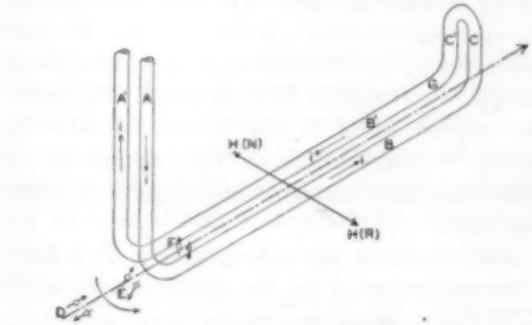

FIG. 1. Schematic perspective diagram of the two-wire oscillating field.

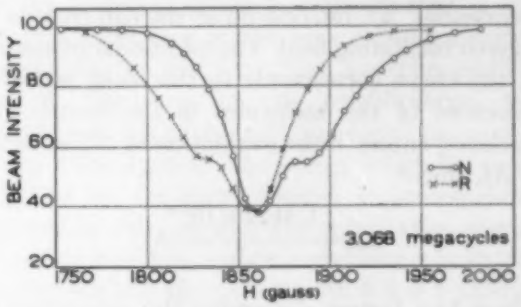

FIG. 2. Pair of Li^7 resonance curves from Li_2 molecules. N refers to the direction of the strong magnetic field, H, as normally used in previous work. It corresponds to the positive Z direction of a right-handed system of axes where the molecular velocity direction is taken as the positive X axis and the vertical downward direction as the positive Y direction. R refers to the opposite direction.

The asymmetry exhibited in either of the two curves in Fig. 1 is the most pronounced ever observed. The curves were obtained under experimental conditions that are particularly favorable for showing to what extent the end effects of the oscillating field can distort the resonance curve. On the other hand the asymmetries in the resonance curves published[1] for Li^6, Li^7 and F^{19} were very slight. For the purpose of obtaining accurate resonance minima locations it is desirable to free the resonance curves from such asymmetries, while for determination of sign it is best to accentuate them. It will be instructive, therefore, to analyze briefly the factors affecting the form of this asymmetry in a resonance curve for any fixed design of the tubes. The principal

[3] L. P. Granath, Phys. Rev. **42**, 44 (1932).
[4] S. Millman and J. R. Zacharias, Phys. Rev. **51**, 1049 (1937).

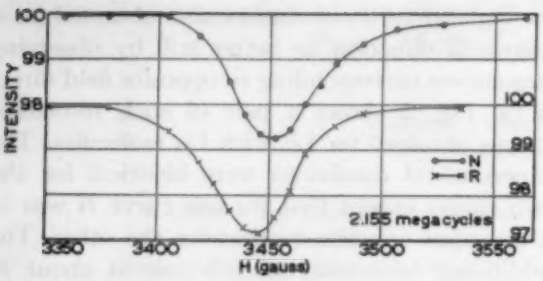

FIG. 3. Pair of Li^6 resonance curves from LiCl molecules. N and R have the same meaning as in Fig. 2.

features are: (1) molecular velocities, (2) value of the nuclear g and (3) amplitude of oscillating current in the tubes. The molecular velocities determine the values of the additional rotating frequencies, Δf, introduced at the end regions of a given oscillating field. The additional minimum in the curve corresponds to the most probable velocities of the molecules in the beam. The nuclear g enters in the evaluation of ΔH in terms of Δf, thus:[4]

$$\Delta H = \frac{1.3122 \times 10^{-3}}{g} \Delta f.$$

These two factors determine the separation in gauss of the secondary minimum from the principal minimum. The last factor will determine how pronounced the subsidiary minimum will be. This can easily be seen by examining the expression for the transition probability near resonance, given for the case $J=\frac{1}{2}$, by[1]

$$P_{(1,-1)} = \frac{\Delta^2}{(1-q)^2+\Delta^2} \sin^2 \Psi$$

with $$\Psi = \pi f(L/v)[(1-q)^2+\Delta^2]^{\frac{1}{2}},$$

where Δ is the ratio of half the amplitude of the oscillating field, H', to the strong field, H; q is the ratio of the applied frequency, f, to the Larmor frequency, $\nu = \mu H/Ih$, and has the value 1 at resonance; L is the length of the oscillating field; and v the molecular velocity. For the purpose of this discussion it will be convenient to divide the field into two parts, L_1 and L_2, L_1 corresponding to the length FG (about 6 cm) and L_2 referring to the sum of the two end regions (about 1 cm). If H' is small enough so that Ψ_{L_1} is approximately $\pi/2$ for $q=1$ and v corresponds to the most probable velocity, the value of Ψ_{L_2} is about $\pi/12$ and $\sin^2 \Psi_{L_2}$ is only 1/15. Such a condition is favorable for accurate location of the principal minimum. As H' is increased the value of $\sin^2 \Psi_{L_1}$ will not change very much. Averaged over a Maxwellian velocity distribution its value will be close to $\frac{1}{2}$ for any large value of H', while $\sin^2 \Psi_{L_2}$ increases with increasing H'. Thus for very large values of H' the subsidiary minimum becomes comparable in magnitude with the main minimum, and since resonance curves tend to broaden for increasing values of H', the two minima may not be distinguishable from one another. The net effect is to shift the resulting apparent minimum either to high field or to low field, depending on the sign of the nuclear moment and on the direction of the strong homogeneous field. Such curves if observed only for one direction of H give no information on the sign of the moment and introduce errors in the measured g values. However, when curves are taken for both field directions the sign of the moment can be determined from the systematic shift of the minima, and the correct g value is given by the average of the two observed values. Fig. 3 shows two such curves observed for Li^6 with LiCl molecules. Here again all experimental conditions were the same for both curves except for the field directions. The shift in apparent minimum position of one curve with respect to that of the other is far beyond experimental error and is observed as often as such pairs of curves are taken.

The sign of the moment of the Li^6 nucleus is positive, in agreement with the result obtained by Gorham,[5] from the atomic beam methods. The same result is obtained for the F^{19} nucleus.

It is seen that by substituting an oscillating field for a rotating field, which results in considerable experimental simplification, the possibility of sign determination was not abandoned as originally thought. In fact, such determinations are obtained in the course of securing accurate measurements of the magnitude of nuclear magnetic moments and require no additional work.

I wish to thank my colleague, Dr. P. Kusch, for his collaboration in the experimental work.

[5] J. E. Gorham, Phys. Rev. **53**, 563 (1938).

The Influence of Chemical Binding and Crystal Structure on X-Ray Absorption Edges

ROLF LANDSHOFF
University of Minnesota, Minneapolis, Minnesota
(Received January 30, 1939)

An attempt is made to explain the positions and the fine structures of x-ray absorption edges, so far as these are not explained by Kronig's theory, by considering that they arise from transitions into a series of discrete states. These are states in which the electron is trapped in the region of surplus positive charge, which is created by the ejection of the electron from the inner shell of the parent ion. To calculate the energy of the trapped states we use a model in which the electron is bound to the positive ions in the neighborhood of the parent ion.

INTRODUCTION

BY THE absorption of an x-ray photon in a solid, an inner-shell electron is lifted into an excited state. Kronig[1] has suggested that we can identify these excited states of the electron with those in which the electron can move more or less freely through the lattice, somewhat like conduction electrons move in metals. Such "traveling wave" states are found to occupy separated bands in the energy spectrum. This should give rise to a sequence of maxima and minima in the absorption spectrum on the short wave side of the edge. For metals which have a relatively simple crystal structure the distribution of states is known fairly well and the calculated absorption curve agrees well with the experimental results. For ionic compounds the situation is more complex. Kronig[2] has also given a qualitative discussion of this problem, and has shown the difficulties caused by the presence of more than one kind of ion. The predictions of this modified theory have been verified in several cases, but contradictory results have been obtained for the structures in the immediate neighborhood of the edges of some K and Cl compounds which have been investigated under high resolving power.[3]

For the absolute positions of the x-ray absorption edges Pauling[4] has developed a theory of great simplicity which agrees satisfactorily with the experimental data. In the picture adopted by Pauling, the lowest excited states of the electron are also identified with traveling wave states, although the method of calculating the energies of these states is quite different from Kronig's. However, objection to this picture can be raised on the following grounds. The removal of the electron from one of the ions creates a region around this ion which contains a surplus positive charge. The ions in the neighborhood will therefore be polarized, and thus lower the energy of the whole system. The energy which has to be supplied by the x-ray photon is consequently reduced by this amount. The polarization energy of an ion which is within a distance r from the surplus positive charge, and which has a polarizability α, is $-\alpha e^2/2r^4$. The total polarization energy is $-e^2/2\cdot\sum_i{}'\alpha_i r_i^4$ where the summation is extended over all points of the lattice. Summations of this kind have been carried through for different types of crystals by J. E. Jones and A. E. Ingham.[5] According to these calculations we can write the polarization energy as $P=-(A'\alpha_+ + A''\alpha_-)e^2/2d^4$ in which α_+ and α_- are the polarizabilities of the positive and the negative ions and d is the distance between nearest neighbors. For crystals of the NaCl type we take from Jones and Ingham[5] the values $A'=13.31$, $A''=9.33$. In Table I we give for several compounds the hypothetical values of the energy (Rydberg units) required to remove an electron from the K shell of the free Cl ion, which would account for the observed frequencies of the edges. In the first line Pauling's original formula has been used, in the second line this formula is corrected for polarization. The energy should of course be the same in all compounds. In the second line of Table I the

[1] R. de L. Kronig, Zeits. f. Physik **70**, 317 (1931); **75**, 191 (1932).
[2] R. de L. Kronig, Phys. Zeits. **36**, 729 (1935).
[3] G. P. Brewington, Phys. Rev. **46**, 861 (1934).
[4] L. Pauling, Phys. Rev. **34**, 954 (1929).
[5] J. E. Jones and A. E. Ingham, Proc. Roy. Soc. **A107**, 640 (1925).

TABLE I. *Hypothetical K absorption edge of free* Cl.

	LiCl	NaCl	KCl	RbCl	CsCl	AgCl
(Pauling)	207.62	207.63	207.60	207.61	207.73	207.75
(Pauling +polarization)	207.86	207.81	207.75	207.77	207.93	208.05

spread between the hypothetical values of the energy is quite large compared with that in the first line. This means that the consistent consideration of polarization terms spoils the good agreement of Pauling's theory with the experimental data.

The fact that the absolute position of the edge and the structure of the absorption spectrum in the immediate neighborhood of the edge do not come out properly in the present theories suggests a reconsideration of the lowest possible excited states. In this article an attempt is made to do this in the light of recent theoretical discussions,[6] which show the existence of a few discrete energy levels below the first continuous band. The region of surplus positive charge created by the removal of the electron can trap an electron so that it cannot travel freely through the crystal. Thus one gets a series of "trapped states" which occupy separated levels below the continuum of energy states in the band. Wannier's argument that these discrete levels will not appear as discrete absorption lines because they are hidden in a superposed band is no restriction in the case of the x-ray absorption because this superposed band is that of the inner shell electrons and its width is negligible. Wannier gives an approximate formula for the energy values of the trapped states. For electrons coming from an inner shell which does not show any spread in energy one has to put $A_g=0$ in his formula (19), and so finds that the states lie within a distance ΔE from the continuum, where ΔE is given by the formula for the electronic levels in the hydrogen atom, in which, however, the electron mass is substituted by an effective mass, which is somewhat heavier. According to this formula the splitting between the two lowest levels is more than ten electron-volts. The observed splitting is smaller however, and it will be necessary to make use of the more detailed information that one can obtain from an atomic picture.[6a] An approach similar to that considered here has been used previously by von Hippel[7] and Klemm[8] in a theory of the ultraviolet absorption of the alkali halides.

[6] J. C. Slater and W. Shockley, Phys. Rev. **50**, 705 (1936). G. H. Wannier, Phys. Rev. **52**, 191 (1937).

THEORY

The states which we shall consider are those in which the ejected electron is captured into the empty place of the series electron at a positive ion. The lowest state will be that in which it is bound to the ion which is nearest to the attracting center, and the other levels arise when it is bound to ions which are farther away. We do not wish to introduce unnecessary complications by attempting to treat the problem in a very general manner, but rather shall limit ourselves to the case in which only one type of positive and one type of negative ion is present.

In case the electron is ejected from a positive ion the lowest state is that in which it stays at the same ion, merely moving to an outer orbit. In this case the considerations are rather simple. The ion does not change its charge and therefore there will be no change in the electrostatic interaction with the neighbors. But there will be a difference in the exchange interaction between the neighbors and the ion in its normal and in its excited state. In many cases this difference in exchange interaction comes out to be too small to be observed. We see for example from a list[9] of wave-lengths of the K edge of K^+ in 27 compounds which have been measured by Stelling, that those of 14 compounds lie between 3427.5 and 3427.9 X.U., the rest are at lower wave-length. In the first group we have all the halides, in the second are typical complex compounds like $K^+[FHF]$. A complex can be suspected of having an electron distribution which is quite extended. It is probably not held together by electrostatic forces alone, since the closed shells in a structure like $F^-H^+F^-$ would have large repulsions, but there is probably some Heitler-London type of attraction for which a rupture of

[6a] Since the Coulomb interaction in a medium with the dielectric constant k is e^2/kr, N. F. Mott recently suggested the formula $\Delta E=-Ry/n^2k^2$. This formula gives the same fine structure for cation and anion, and somewhat too small values, however. N. F. Mott, Proc. Roy. Soc. **167**, 384 (1938).

[7] A. v. Hippel, Zeits. f. Physik **101**, 680 (1936).

[8] W. Klemm, Zeits. f. Physik **82**, 529 (1933).

[9] A. E. Lindh, *Handbuch der Exper. Physik* **24**, 2 Chapter 10, 1 (1930).

the closed shell structure is necessary. This means an increase in volume of the electron cloud. It will then overlap strongly the wave function of the series electron moving around the K^+ and thus shift its state to a higher energy and the absorption edge to a shorter wave-length.

For the calculation of the energy difference between the initial and the final state in case the electron is captured by a different ion, we consider the following effects: (1) The interaction of the ejected electron with the rest of the ion at which it is located, (2) the electrostatic interaction of the electron with the ions to which it is not bound, (3) the polarization energy due to the unsymmetrical arrangement of charges in the final state and (4) the exchange energy. In the following section we give a detailed discussion of these four effects and of their contributions to the initial and final energy of the system, which will be denoted by the letters I and F, respectively.

(1) In the initial state the electron is in one of the lower shells. The energy I_1 with which it is bound to the ion is not affected by the presence of the surrounding ions, inasmuch as these do not affect the charge distribution and therefore the potential close to the nucleus. We conclude that I_1 is equal to the binding energy of the electron to the free ion. This may be expressed in terms of the absorption edge ν_0 of the free ion. We have then $I_1 = -h\nu_0$. It should be noted, however, that ν_0 cannot be determined experimentally. In the final state the electron is bound to the lowest unoccupied level of the cation. The binding energy F_1 is known spectroscopically.

(2) The Madelung potential at a lattice point of an ionic crystal, that is the sum of the potentials of all ions but the one at the considered point, is inversely proportional to the lattice spacing. It is expressible as $-M_+e/d$ at the positive and as M_-e/d at the negative lattice points, with d standing for the distance between nearest neighbors. M_+ and M_- depend on the crystal structure. For a NaCl type with singly charged ions, for example, they would both be equal to 1.748. For the same lattice type but with doubly charged ions as constituents (for example in CaS) this value would have to be multiplied by two. Another example is $SrCl_2$ with $M_+ = 7.56$ and $M_- = 4.067$.

We consider an electron which makes a transition from a negative to a positive ion. In the initial state its electrostatic interaction with the ions to which it is not bound is simply the electronic charge times the Madelung potential at the negative lattice point; that is, $I_2 = -M_-e^2/d$.

For the final state we have to remember that a "positive hole" remains in the lattice after the electron has been ejected. If the electron goes to an ion which is at a distance sd from the ion to which it was bound before the transition occurred, and which is considered as the center of a superposed Coulomb attraction, a term $-e^2/sd$ must be added to the Madelung energy in the final state, so that we obtain $F_2 = (M_+ - 1/s)e^2/d$.

The sum of the two Madelung constants $(M_+ + M_-)$ can be expressed by means of the commonly used Madelung constant M which gives the energy per unit cell as $-Me^2/d$. If n_+ and n_- are the numbers of positive and negative ions per unit cell and Z_+e and $-Z_-e$ their charges, the energy per unit cell is $-\frac{1}{2}(n_+Z_+M_+ + n_-Z_-M_-)e^2/d$. Because of the neutrality of the unit cell we have $n_+Z_+ = n_-Z_-$, which leads to $\frac{1}{2}(M_+ + M_-)n_+Z_+ = M$. Thus we have $F_2 - I_2 = (2M/n_+Z_+ - 1/s)e^2/d$.

(3) In calculating the polarization energy we must consider the fact, that the state of the series electron of the positive ion which is occupied after the transition has occurred has a very high polarizability, so that under the influence of electrostatic attraction alone the electron would be drawn back strongly to the ion from which it came. This tendency is restricted of course, since the electron cannot penetrate into the region where all of the possible states are occupied, and since the unfilled place in the K shell is not available to the ejected electron because of the requirement that the excited state must be orthogonal to the normal state. Anything more than a rather crude treatment of this problem seems to be very difficult. We follow a suggestion by W. Klemm[8] and assume that the series electron is displaced by a distance $d\delta$ in the direction of the resultant electric field so that its energy changes by an amount $F_{3a} = V((s-\delta)d) - V(sd)$. Lacking a model from which to calculate δ, we fix it arbitrarily to be $\delta = 0.5$ when the emitting and the receiving ions are direct neighbors, and $\delta = 0.3$ otherwise. The different choice in δ is

made because of the difference in radii of the ions which are in the way. The emitting ion has its K electron knocked out and therefore it has contracted to a smaller radius. One might argue that δ should depend on the relative sizes of the constituent ions, in such a way perhaps as to give a constant distance of approach for a given ion. But one must consider also the effect of the radius of the orbit of the approaching electron. A large radius of the orbit, or, quantum-mechanically speaking, a large amplitude of the wave function in the region of the ion it approaches, gives a stronger repulsion due to exchange terms, which may be supposed to compensate for the smaller radius of the latter.

In addition to the polarization of the orbit of the emitted electron itself, there should be a polarization of the rest of the ions. At this point, however, it will be necessary to extend our model. An electron bound to a positive ion in the electrically unbalanced region cannot travel freely to the ions which are not in this region, but it can travel easily between ions which are in equivalent positions with respect to the center of the superposed Coulomb field. One should therefore use linear combinations

$$\psi=\sum_s A_s f(r-R_s),$$

as first approximations to the states. The factors A_s should be so determined that the ψ's form sets whose transformations under the rotations of the symmetry group of the crystal are given by the irreducible representations of this group. For the process of absorption of radiation the final state of the electron ejected from the K shell can only be one type of function, in order that the matrix elements giving the transition probabilities may be different from zero. In a cubic crystal these functions are written down quite easily if one considers that they must be antisymmetrical with respect to reflections in one of the principal planes. For a jump to the immediate neighbor for example

$$\psi=\sqrt{\tfrac{1}{2}}(f(x-d, y, z)-f(x+d, y, z))$$

will be one of the functions. While this partition of the electron on two or more ions did not affect our previous considerations, it will be essential for the following. Instead of creating an electric dipole in the lattice, the electron creates a pole of higher order. For the jump that we consider responsible for the first absorption maximum of the K edge of a negative ion, which leads to a place halfway between the center ion and its nearest neighbors, the electric field will be rather small and we shall neglect it altogether. For the following jumps special calculations need to be made.

(4) Finally we must consider the exchange interactions. There are in principle two terms. One is the interaction of the series electron with its negative ion neighbors. The other is the change in interaction of the parent ion with its neighbors, due to its diminished size and to the increase in potential. A direct calculation of the exchange integrals, even approximately, is much too involved to be worth while, but some general statements as to their comparative magnitude can be made. The series electron is repelled by the surrounding ions since the latter do not contain any unpaired electrons. The exchange interaction of the series electron with the neighboring ions will therefore produce a shift towards higher energies. The magnitude of this shift is determined by the amount of overlapping of the respective wave functions. For the interaction of the parent ion and its neighbors, we have to consider first that the influence of the positive hole produces a shift towards higher energies in the final state, while the shrinkage in size of the parent ions has the opposite effect. It appears that the first effect will outweigh the second, so that we again expect a shift toward higher energies.

TABLE II. *K edges of* Cl^- *and of* S^{--} *in several compounds* (ν/R) *and in the free ions* (ν_0/R).

COMPOUND	STRUCTURE	d	Z	ν/R	ν_0/R
LiCl	$B1$	2.57	2	207.871	207.517
NaCl	$B1$	2.81	10	207.867	207.553
KCl	$B1$	3.14	18	207.810	207.515
RbCl	$B1$	3.28	36	207.805	207.524
CsCl	$B2$	3.55	54	207.820	207.553
AgCl	$B1$	2.78	46	207.749	207.625
$SrCl_2$	$C1$	3.02	36	207.867	207.533
BeS	$B3$	2.10	2	182.17	180.85
MgS	$B1$	2.60	10	182.06	180.93
CaS	$B1$	2.84	18	182.01	180.84
BaS	$B1$	3.18	54	181.98	180.88
MnS	$B1$	2.61	23	182.05	180.98
ZnS	$B3$	2.35	28	182.06	181.02
CdS	$B3$	2.57	46	181.97	181.01
Na_2S	$C1$	2.83	10	181.90	180.87

Numerical Application of the Theory

The negative ions for which the influence of the chemical binding on the K absorption edge has been investigated most thoroughly are Cl^- and S^{--}. From the large number of compounds which have been investigated we select those which crystallize in relatively simple systems. In the notation employed in the Landolt Boernstein tables these are the systems $B1, B2, B3, C1$. These symbols and the distances are listed in the second and third column of Table II. The observed frequencies of the K edge which are taken from the Tables 82, 85 and 91 in Lindh's book[9] are given in the fifth column (Rydberg units). In the last column we have the hypothetical value of the x-ray term of the free emitter, which we have to assume to account for the observed frequency of the K edge in the compound under consideration. This value is computed from the formula $h\nu_0 = h\nu - F_1 + I_2 - F_2 - F_3$ that is, with neglect of exchange energy terms. The edge ν_0 of the free ion should, of course, have the same value for all its compounds. For AgCl, MnS, ZnS, Cds, however, the values come out higher than for the other compounds. This can be interpreted as caused by the neglected exchange terms, which are more important in these ions because they overlap their neighbors more than the rest of the ions. The overlapping can be seen by comparing the internuclear distances d with the numbers Z of electrons of the positive ions (see third and fourth column of Table II). For example Ag with its 46 electrons comes closer to the Cl than Na which has only 10 electrons. For the electrons in the closed shells of the positive ion this overlapping does not bring about a higher exchange interaction, because the outer electrons in these particular ions are d electrons which have nodes in the region containing the main portion of the integrand and therefore depress the exchange interaction partly. For the series electron, however, which is an s electron in all cases, there is no counteraction due to nodes and we have to expect higher exchange energies due to the strong overlapping.

If we disregard the compounds for which an exchange interaction is to be expected the values ν_0 are fairly consistent. The discrepancy existing in Pauling's theory in the case of CsCl has disappeared. The mean deviation of the values ν_0/R from their average is 0.014 for Cl^- and 0.025 for S^{--}. For comparison it may be noted that the mean deviation of the corresponding ν/R from their averages is 0.028 and 0.073, respectively. The average value of ν_0 for Cl^- corresponds to a wave-length of the absorption edge of the free ion $\lambda_{free} = 4395.3$ X.U. while Pauling's theory gives a value of 4389.3 X.U.

Next we consider the fine structure at the short wave-length side of the absorption edges. Of course only that type which is not explained by Kronig's theory is considered. We attempt to correlate the maxima to successive trapped states, to explain the structure at the K edge of Cl^- in several alkali chlorides. The compounds which have been investigated[8] are all of the same lattice type as NaCl. The first two maxima in the absorption curve are regarded as being due to transitions to neighboring ions in positions like (100) and (111). In the experimental curves the first maximum is denoted by the letter A and the second one by B, and we shall use the same letters to denote transitions to (100) and (111). F_1 and I_1 are the same for A and B. The electrostatic energy is $F_2 - I_2 = (2M - 1)e^2/d$ for A and $F_2 - I_2 = (2M - 0.577)e^2/d$ for B. The polarization is $F_{3a} = -0.748e^2/d$ and $F_{3a} = -0.139e^2/d$, respectively. For the other part of the polarization energy we have to consider the charge distribution after the transition has taken place. Besides the charge $+e$ in the center, which is created by removing the electron from the K shell, we have the distribution of the charge of this electron. In case A half the charge, that is $-\frac{1}{2}e$ goes to each of the 2 points $((1-\delta), 0, 0)$ and $(-(1-\delta), 0, 0)$, or to an equivalent pair of points on one of the other two axes. In case B the charge $-(1/8)e$ goes to each of the 8 corners $(\pm q, \pm q, \pm q)$ of a cube around the parent ion, with $q = (1 - \delta/\sqrt{3})$. The corresponding polar-

Table III. *Theoretical and experimental energy difference between the first two maxima in the absorption curve.*

	LiCl	NaCl	KCl	RbCl
Δ_1	5.75	5.26	4.61	4.50
Δ_2	0.27	0.26	0.37	0.50
Δ	5.48	5.00	4.24	4.00
$B-A$	3.99	6.37	3.56	4.05

ization energies are $F_{3b}=-0.16\alpha_- e^2/d^4$ and $F_{3b}=-(2.22\alpha_+ + 0.41\alpha_-)e^2/d^4$. α_+ and α_- stand for the polarizabilities of the alkali and the halogen ion. The total energy difference between the two transitions A and B comes out to be: $\Delta = 1.032e^2/d - (2.22\alpha_+ + 0.25\alpha_-)e^2/d^4$. If we express the energy in electron-volts, d in 10^{-8} cm and the polarizabilities in 10^{-24} cm^3, we obtain:

$$\Delta = 14.8/d - (31.8\alpha_+ + 3.58\alpha_-)/d^4 = \Delta_1 - \Delta_2.$$

In Table III we list Δ_1, Δ_2, Δ, and the experimental values $B-A$. The latter two are not equal as they should be, but they are about of the right order of magnitude, which is all we can expect in view of the fact that the polarization energies are calculated from a rather crude model and that the exchange energies are neglected altogether.

In the case of the K edge of the K^+, for which experimental data are available too, a complication arises which makes it difficult to calculate with the above model the separate levels of the trapped states. The terms come out very nearly equal, but since the terms are diagonal elements of the energy matrix, their difference should be large compared with nondiagonal elements. The nondiagonal elements arise from integrals containing products of series electron wave functions which are concentrated around different ions. Without knowing their values numerically, it is reasonable to assume that they are appreciable, since the overlapping of the wave functions of two series electrons from different ions is more prominent than that of closed shells, which are nearer to their respective nuclei. The overlapping of closed shells, however, is responsible for the repulsive forces between the ions, which balance the ionic attraction.

This is not an argument against the assumption that the observed maxima of absorption in the immediate neighborhood of the edge are due to transitions into trapped states, but only against the method of calculating them. Thus, the apparent failure to get a support of the "trapped states theory" in case of the K edge of K^+ does not invalidate the support that we can draw for this theory from the results in case of the fine structure of the Cl^- edge in the alkali chlorides.

APRIL 1, 1939 PHYSICAL REVIEW VOLUME 55

A New Ultraviolet Band System of Silver Iodide

NICHOLAS METROPOLIS
Ryerson Physical Laboratory, University of Chicago, Chicago, Illinois

(Received February 9, 1939)

A new ultraviolet band system of AgI has been photographed in absorption at temperatures 700–900°C. At higher temperatures the system is overlapped by strong continuous absorption, which advances gradually from shorter wave-lengths. The new system lies at 2300A, i.e., at shorter wave-lengths than the known system, and its lower state vibrational constants agree with those given by Brice for the lower state of the longer wave-length system. The rotational structure and the very small isotope effect are not resolved. The equation for the band heads may be written

$$\nu_A = 44{,}724 + 152.8(v'+\tfrac{1}{2}) - 1.1(v'+\tfrac{1}{2})^2 - 205.1(v''+\tfrac{1}{2}) + 0.43(v''+\tfrac{1}{2})^2.$$

This formula is based upon progressions from $v'=0$ to $v'=4$ and from $v''=0$ to $v''=11$. An additional new band system was found at 2150A, and the wave numbers of the band heads may be represented by the following formula:

$$\nu_A = 45{,}487 + 176(v'-b+\tfrac{1}{2}) - 2.5(v'-b+\tfrac{1}{2})^2 - 205(v''-a+\tfrac{1}{2}) + (v''-a+\tfrac{1}{2})^2;$$

the values of a and b could not be determined.

INTRODUCTION

FRANCK and Kuhn[1] were the first to observe bands in the spectrum of silver iodide. They photographed bands in absorption and in resonance in the region 3100–3500A; overlapping continuous absorption was also reported. Additional bands, diffuse in nature, at longer wave-lengths, and a weak continuum having a maxi-

[1] J. Franck and H. Kuhn, Zeits. f. Physik **43**, 164 (1927).

mum at 4000A, were mentioned by Kuhn[2] in a later work. However, it was Brice[3] who first assigned vibrational quantum numbers to the 3.8-ev system. Later he examined the system under high dispersion and succeeded in giving a more complete analysis, aided by the first measurements of the silver isotope effect.[4]

More recently, Mulliken[5] discussed the nature of predicted band systems and continua of silver chloride, bromide and iodide farther in the ultraviolet. Soon after, Jenkins and Rochester[6] reported the existence of a new system of silver chloride in the region 2100–2500A. In the present work, data are presented for a new band system of AgI extending from 2175–2350A. In addition, the analogous system of AgBr has been photographed; the results will be reported in the near future.

Experimental

The silver iodide obtained from Merck was introduced into the quartz absorption tube without further purification. In the early experiments silver iodide was introduced into a cylindrical vessel of transparent, fused quartz, which was then evacuated and sealed while the salt was heated somewhat above its melting point. The diameter of the tube was 2 cm and its length 20 cm. A two-unit cylindrical furnace was constructed so that each end of the tube could occupy the center of one of the units. The results were not entirely satisfactory, because at the necessary temperatures (700–900°C) the salt vapor condensed slightly on the windows and attacked them. The photographs showed that the transmitted intensity was very much reduced in the region under investigation; because, first, the transmission of the quartz at such high temperatures is very poor for these short wavelengths and, second, the loss by scattering by condensed particles of the salt is considerable.

The apparatus was improved by keeping the windows cool. An opaque quartz tube of length 80 cm was wound with Nichrome wire save for 15 cm at each end. Windings were less numerous at the center of the furnace in order to assure a more uniform temperature distribution along the tube. Water-glass was applied to the windings and dried slowly over a flame—this kept the wire in position and in good contact with the surface. Finally the wired portion was wrapped with asbestos to a thickness of three cm. After two hundred hours at temperatures ranging from 700° to 900°C, the tube was still in very good condition. Water-cooled metal sleeves were used at each end of the quartz tube, and to these the windows were fixed with Picein. No clouding of the windows took place, even though the system was evacuated to about one mm Hg pressure to remove the absorption by heated oxygen. The light source was a hydrogen discharge tube of the conventional type, operated at 0.8 amp. and about 3000 volts. The spectra were taken with a Hilger E-3 spectrograph with a slit-width of 0.015 mm; exposures were about fifteen minutes. The plates were measured with copper lines as standards; the accuracy was approximately ± 0.01 mm corresponding to about ± 2.5 cm^{-1}. Some experiments were tried on a Bausch and Lomb large Littrow spectrograph to utilize the latter's high resolving power and dispersion.[7] The resolution would have sufficed to permit measuring the isotope effect for making the vibrational quantum number assignment definite, but the intensity of the light source unfortunately proved insufficient.

[2] H. Kuhn, Zeits. f. Physik **63**, 456 (1930).
[3] B. A. Brice, Phys. Rev. **35**, 960 (1930).
[4] B. A. Brice, Phys. Rev. **38**, 658 (1931).
[5] R. S. Mulliken, Phys. Rev. **51**, 310 (1937).
[6] F. A. Jenkins and G. D. Rochester, Phys. Rev. **52**, 1141 (1937).

[7] I wish to thank Dr. Mark Fred of the Standard Oil Company of Indiana for the use of the spectrograph, and also for his very kind cooperation.

Table I. *Vibrational analysis of 5.52-ev system of silver iodide.*

v'	$v''=0$	1	2	3	4	5	6	7	8	9	10	11
0	44695	44492	44289	44087	43886	43686	43486	43285	43087	42890		
1	44845	44642	44439	44236	44037	43837	43638	43436	43238	43041	42842	
2	44993	44791	44589	44386	44187	43984			43387	43190	42991	42794
3	45139	44936	44735							43337	43138	
4	•	•								43484	43285	43086

• Blended.

Results and Analysis

The plates show in the region below 2400A features which are now observed for the first time. When the temperature of the AgI is raised, a continuum advances from the short wave-length side. At a temperature of 775°C the region below 2260A showed seventy-five percent or more absorption; fifty percent absorption was estimated for the region 2260–2360A, and very little absorption above 2360A. Superimposed on this continuum, sharp band heads appear in the region 2175–2350A. The bands degrade to the red and form sequences. The most intense bands are near 2230A. The analysis of this system is given below. The wave numbers of its band heads are given in the conventional arrangement in Table I. The general formula for the wave numbers of the band heads of the new system is

$$\nu_A = 44{,}724 + 152.8(v'+\tfrac{1}{2}) - 1.1(v'+\tfrac{1}{2})^2 - 205.1(v''+\tfrac{1}{2}) + 0.43(v''+\tfrac{1}{2})^2. \quad (1)$$

The lower state vibrational constants are identical[8] with those given by Brice for the lower state of the longer wave-length system. Hence the lower state of the new system is the normal state. The $v'=0$ level is 5.52 ev above the ground level and 1.68 ev higher than the zero vibrational level of the previously known excited state. From application of the Franck-Condon principle to the observed intensities, the equilibrium distance of the new electronic state should be larger than that of the normal state.

Absorption Bands in Other Spectral Regions

Several additional band heads, beyond those given above, were observed. They were diffuse in nature, and accurate measurements could not be made. The results, which may be in error by several wave numbers, are given in Table II.

Table II. *Wave numbers of band heads that are part of another electronic band system whose excitation energy is greater than 5.6 ev.*

v'	$v''=a$	$a+1$	$a+2$	$a+3$
b		45270		
$b+1$	45641	45439	45239	
$b+2$		45598	45401	45210
$b+3$			45561	45363

[8] The fact that band heads, and not band origins, are measured may account for the difference of 1 cm^{-1} in ω''.

It appears that they are transitions to a new electronic state of higher excitation energy. The lower level should be the known ground level of AgI. With this assumption, supported by observed $\Delta\nu$'s, the following formula represents the observations:

$$\nu_A = 45{,}487 + 176(v'-b+\tfrac{1}{2}) - 2.5(v'-b+\tfrac{1}{2})^2 - 205(v''-a+\tfrac{1}{2}) + (v''-a+\tfrac{1}{2})^2, \quad (2)$$

where a and b are integers that could not be determined. The accuracy is approximately ± 5 cm^{-1}.

The possibility that iodine bands in this spectral region originating from iodine formed by the thermal decomposition of silver iodide might account for part of the observed spectrum was checked by taking photographs of iodine vapor of 0.2-mm pressure at 850°C. No absorption by I_2 was found below 5000A.

On some plates the NO γ-bands were observed in absorption. Evidently NO was formed from the residual air in the hot quartz tube, probably under the action of the ultraviolet irradiation.

In the visible region there is absorption, with a maximum at 4000A, at the same vapor pressure[9] necessary for photographing the band system of Franck and Kuhn. One or more band systems are evident, covering the whole range between the 3.8-ev system and the visible absorption bands of iodine. The diffuse bands reported by Kuhn[9] represent only a part of the very numerous band heads appearing in this region. The bands are of nearly equal intensity and more or less evenly spaced, showing a slow convergence at shorter wave-lengths. The absence of apparent sequences or progressions cannot be explained easily.

A new thermodynamical calculation of the dissociation energy of AgI has been made recently by Beutler and Metropolis, and a value of 2.93 ev is found for the dissociation energy, higher than previously supposed. In connection with a report on this calculation, it is planned to give the analysis of the band system in the region of 4000A and a discussion of the potential energy curves of the several AgI states now known.

The writer wishes to acknowledge the encouragement and the invaluable suggestions of Professor Robert S. Mulliken and of Dr. H. G. Beutler.

[9] Contrary to the report of H. Kuhn, Zeits. f. Physik **63**, 469 (1930) that very high temperatures are required.

The *E* Region of the Ionosphere

E. O. HULBURT
Naval Research Laboratory, Washington, D. C.
(Received February 16, 1939)

Comparison of *E* region observations from 1930 to 1938 of ionosphere stations scattered over the earth with the theory of ionization caused by solar radiation absorbed exponentially in a relatively quiet terrestrial atmosphere yielded the conclusions: (1) the diurnal variation of y_m, the maximum-with-height value of the equivalent electron density, during daylight is in close accord with the theory with the recombination coefficient α proportional to y_m^2 and equal to 2×10^{-6}, or perhaps greater; (2) y_m at night was not in accord with the theory, but the data do not preclude a night value of $\alpha=2\times10^{-6}$ or greater provided suitable hypotheses are added to the theory; (3) the morning increase in y_m was observed at Washington near midsummer to begin about 35 minutes before ground sunrise, whereas the theory put it about 20 minutes; (4) the seasonal variation of noon y_m agrees with the theory at stations in latitudes from 12° S to 80° N; (5) at any season noon y_m falls off with latitude more rapidly than the theoretical expectation. A relation between noon y_m and sunspots is given.

THE *E* region of the ionosphere is situated at about 100 to 130 km above sea level. It is the lowest in altitude and usually the least densely ionized of the three main ionospheric regions, and the most regular. *E* ionization experiences regular changes through the day, with the season and with sunspots; it is subject to erratic short period variations. It has often been shown[1] that average daily and seasonal changes in *E* ionization are in approximate accord with simple relations of the theory that the ionization is caused by solar radiations, probably ultraviolet light, absorbed exponentially in a relatively quiet terrestrial atmosphere. In this paper *E* region observations from ionosphere stations scattered over the earth are compared with fully developed theoretical derivations. In certain cases good agreement is found, in other instances discrepancies are noted.

Short period fluctuations in *E* ionization may or may not be associated directly with fluctuations in solar radiation, and therefore may or may not fall within the scope of the present theoretical comparisons. It has been established with considerable certainty by Dellinger[2] that the sudden increases in ionization near, and probably slightly below, *E* levels associated with radio "fade outs" are due to eruptions of solar radiations which move approximately with the velocity of light. The cause of the suddenly appearing *E* echoes,[3] known as "sporadic" *E*, is not yet clearly understood, although a reasonable suggestion has been made[4] that attributes the echoes to scattering by ionic clouds or irregularities of size comparable with the radio wavelengths. Sporadic *E* phenomena are local, not frequent near the equator, increase in frequency with latitude, and in temperate latitudes occur both night and day. The *E* region perturbation, described as "turbulence," [5] occurs during strong magnetic disturbance.

It is of interest to remark that, although an ultraviolet solar radiation origin of *E* ionization is reasonably probable, no detailed theory has yet been outlined due to lack of knowledge of photochemical reactions; no contribution to this aspect of the theory is offered here. Thus it is not known what radiations cause *E* ionization or what atmospheric gases are ionized. A calculation[6] based on equations of astrophysics indicated that the *F* regions were oxygen and nitrogen ionized by frequencies in the continua above the series limits at 910 and 860A, but gave no information about *E* region. Wulf and Deming[7] have given reasons for suggesting that *E* ionization is molecular oxygen ionized by wave-lengths from about 1100 to 1300A. Recent experiment[8]

[1] For example, S. S. Kirby and E. B. Judson, Proc. Inst. Rad. Eng. **23**, 733 (1935); E. O. Hulburt, Terr. Mag. **40**, 193 (1935).
[2] J. H. Dellinger, Proc. Inst. Rad. Eng. **25**, 1253 (1937).
[3] T. R. Gilliland, S. S. Kirby, N. Smith and S. E. Reymer, Nat. Bur. Stand. J. Research **20**, 627 (1938); L. V. Berkner and H. W. Wells, Terr. Mag. **42**, 73 (1937).
[4] H. G. Booker and H. W. Wells, Terr. Mag. **43**, 249 (1938).
[5] S. S. Kirby, N. Smith and T. R. Gilliland, Phys. Rev. **54**, 234 (1938).
[6] E. O. Hulburt, Phys. Rev. **53**, 344 (1938).
[7] O. R. Wulf and L. S. Deming, Terr. Mag. **43**, 283 (1938).
[8] H. Raether, Zeits. f. Physik **110**, 611 (1938).

has shown that ultraviolet wave-lengths, believed to be in the neighborhood of 800 to 1000A, from a spark can penetrate several cm of air and cause ionization. The thickness of the atmosphere above 100 km is equivalent to several cm of air.

Theoretical

The fact that the variation of the virtual height of E region with the solar zenith angle is in agreement[5] with deductions from the ultraviolet theory indicates that diurnal and seasonal temperature changes in levels from the stratosphere to about 100 km are not great. Therefore, as a working hypothesis, an atmosphere is assumed relatively undisturbed by winds and at a temperature 219°K constant with altitude from 20 to 100 km for day and night at all latitudes. It is assumed that the atmospheric gases are completely mixed. The density n of the air molecules is expressed as a function of the height z by

$$n = n_0 \epsilon^{-pz}, \tag{1}$$

in which z is measured from the height where $n = n_0$; for $z = 20$ km, $n = 1.86 \times 10^{18}$. The term $p = mg/kt$, where m is the mass of the average air particle and t the temperature. For $t = 219°$K, $p = 1.54 \times 10^{-6}$.

It is assumed that the atmosphere is ionized by the absorption of solar ultraviolet frequencies of effective average molecular or atomic absorption coefficient β, and that all of the absorbed energy causes ionization. The number q cm^{-3} sec.$^{-1}$ of electron-ion pairs produced is

$$q = ni\beta/\chi, \tag{2}$$

where i is the intensity of the light at a level z where the molecular density is n and χ is the ionizing energy per molecule or atom. If i_0 is the intensity outside of the atmosphere and $\bar{n}$ is the total number of absorbing particles traversed by the light in its path from outside of the atmosphere to the level z,

$$i = i_0 \exp(-\beta\bar{n}). \tag{3}$$

The evaluation of $\bar{n}$ for various zenith angles ζ was accomplished by working out two cases, a flat earth and a curved earth, the one exact at $\zeta = 0°$ and the other at $\zeta = 90°$, which approached each other at ζ about equal to 75°. It is assumed that there is no refraction of the solar ionizing rays in the atmosphere. For the case of a flat earth consider an element dx of a solar ray at angle ζ with the vertical. Then $dx = dz/\cos\zeta$, and $\bar{n}$ for a point in the atmosphere at an altitude z and molecular density n is

$$\bar{n} = \int_z^\infty n\,dx = \int_z^\infty (n_0 \epsilon^{-pz} dz)/\cos\zeta = n/p\cos\zeta. \tag{4}$$

When applied to a curved earth (4) is exact only for $\zeta = 0°$ and becomes too large by an amount that increases to ∞ as ζ increases to 90°. However, as shown later, the amount is less than one percent for $\zeta < 75°$.

To determine $\bar{n}$ for a curved earth consider the ray AP, Fig. 1, which passes within a distance z_1 of the surface of the earth SS. Let n_1 and n refer to A and P, respectively; let the altitudes of A and P be z_1 and $z + z_1$, the zenith angle of the ray AP at P be ζ, the radius of the earth be $r = 3670$ km and the distance AP be x. From Fig. 1,

$$x^2 = (r + z_1 + z)^2 - (r + z_1)^2. \tag{5}$$

Let $r_1 = r + z_1$. Then (5) is

$$x^2 = 2r_1 z(1 + z/2r_1). \tag{6}$$

Also
$$\cos\zeta = [1 - r_1^2/(r_1 + z)^2]^{\frac{1}{2}}. \tag{7}$$

For $z \ll r_1$ (6) is approximately

$$x = (2r_1 z)^{\frac{1}{2}}(1 + z/4r_1). \tag{8}$$

By differentiation (8) yields

$$dx = (r_1/2)^{\frac{1}{2}}\{z^{-\frac{1}{2}} + 3z^{\frac{1}{2}}/4r_1\}dz, \tag{9}$$

and if (1) is put into (9) we obtain

$$n\,dx = n_1(r_1/2)^{\frac{1}{2}}\{z^{-\frac{1}{2}}\epsilon^{-pz} + 3z^{\frac{1}{2}}\epsilon^{-pz}/4r_1\}dz. \tag{10}$$

By writing $s = pz$ and integrating, one obtains from (10)

$$\int n\,dx = n_1\left(\frac{r_1}{2p}\right)^{\frac{1}{2}}\left\{\left(1 + \frac{3}{8r_1 p}\right) \times \int s^{-\frac{1}{2}}\epsilon^{-s}ds - \frac{3s^{\frac{1}{2}}\epsilon^{-s}}{4r_1 p}\right\} \tag{11}$$

$$= D\left\{E\int s^{-\frac{1}{2}}\epsilon^{-s}ds - F\right\}, \tag{12}$$

where D, E and F are defined by identifying (11) and (12). Now

$$\bar{n} = \int_A^\infty n\,dx \mp \int_A^P n\,dx, \tag{13}$$

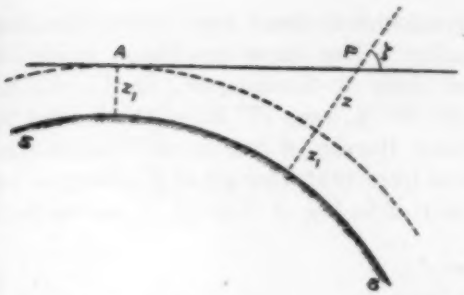

FIG. 1. Solar ray AP in the terrestrial atmosphere.

Here the − and + signs refer, respectively, to P and the sun on the same side of A, and on opposite sides. At A and ∞, s is 0 and ∞, respectively; in each case F is zero. Then from (12) and (13)

$$\bar{n}=D\left\{E\int_0^{\infty}s^{-\frac{1}{2}}\epsilon^{-s}ds\mp E\int_0^{s}s^{-\frac{1}{2}}\epsilon^{-s}ds\pm F\right\}. \quad (14)$$

The first integral of (14) is $\Gamma(\frac{1}{2})=\pi^{\frac{1}{2}}$. The second integral is an incomplete gamma-function; upon substitution of a new variable $\sigma=s^{\frac{1}{2}}$ it is transformed[9] to an error function, the values of which are given in mathematical tables.[10] Eq. (14) becomes

$$\bar{n}=D\left\{E\Gamma(\tfrac{1}{2})\mp ZE\int_0^{s^{\frac{1}{2}}}\epsilon^{-\sigma^2}d\sigma\pm F\right\}. \quad (15)$$

Eq. (15) is exact for $\zeta=90°$ and merges asymptotically into (4) at about $\zeta=75°$. The asymptotic approach of the two functions may be shown analytically by expanding (15) in a semi-convergent series. The ratio of $\bar{n}$ of (15) to $\bar{n}$ of (4) is 0.46, 0.87, 0.94, 0.98 and 0.998 at $\zeta=89°$, 86°, 83°, 80° and 77°, respectively. For ζ from 0° to 75° $\bar{n}$ was calculated from (4) and for ζ from 75° to 105° from (15). The results are accurate within one percent. It does not seem probable that the assumption of no atmospheric refraction of the solar ionizing rays introduces an important error.

From the values of $\bar{n}$ thus calculated q was determined by means of (2) and (3) as a function of ζ, or the time t, for each altitude z; the (q, t) curves are not shown here. For each value of z above a station the (q, z) curve is symmetrical about local noon.

Recombination of electrons and positive ions is assumed to take place at the rate of αy^2, where α is the recombination coefficient and y is the electron density. Then at any point in the atmosphere

$$dy/dt=-\alpha y^2+q, \quad (16)$$

where q is a function of z and the time t. At night $q=0$, and (16) becomes

$$y=1/(1/y_1+\alpha t), \quad (17)$$

where y_1 is the value of y at nightfall.

Since q was determined in the form of (q, t) curves for each value of z (16) could not be integrated explicitly. Therefore the (y, t) curves were obtained graphically by following the course of dy/dt, which could be done with desired precision.[11] The (y, t) curves are not shown here. The envelope of the family of (y, t) curves gave the curve of (y_m, t), where y_m denotes the maximum-with-height value of y for any t. (y_m, t) curves were computed for various values of α for comparison with observation.

A special case is of interest, namely, when recombination is very rapid or $\alpha=\infty$. Then in (16) $dy/dt=0$ and

$$q=\alpha y^2. \quad (18)$$

From (2), (3), (4) and (18)

$$y=\{(ni_0\beta/\alpha\chi)\epsilon^{-\beta n/p\cos\zeta}\}^{\frac{1}{2}}. \quad (19)$$

The maximum-with-height value of y of (16) occurs at a value of n, corresponding to an altitude z, obtained by equating the exponent of ϵ to unity. Therefore

$$y_m=(pi_0/\alpha\chi\epsilon)^{\frac{1}{2}}(\cos\zeta)^{\frac{1}{2}}, \quad (20)$$

at

$$n=(p\cos\zeta)/\beta. \quad (21)$$

Eq. (20) may be written

$$y_m=y_0(\cos\zeta)^{\frac{1}{2}}, \quad (22)$$

where

$$y_0=(pi_0/\alpha\chi\epsilon)^{\frac{1}{2}}, \quad (23)$$

is the value of y for $\zeta=0$. Eqs. (19) to (23), are

[9] The general transformation is discussed by E. T. Whittaker and G. N. Watson, *Modern Analysis* (1927), fourth edition, p. 341.

[10] For example, B. O. Pierce, *A Short Table of Integrals* (1929), third edition p. 116.

[11] M. V. Wilkes, Proc. Phys. Soc. London **51**, 138 (1938) used a Bush Harmonic Analyser to determine (y, t) curves; S. Chapman, Proc. Phys. Soc. London **43**, 26 and 483 (1931), determined (y, t) curves by a method of successive trials.

valid only for ζ less than about 80° since they are based on (4). During the daylight hours the variation of y_m of (22) with ζ or t is symmetrical about local noon. As α decreases from ∞ the (y_m, t) curve is distorted and its maximum is displaced into the afternoon; the amount of displacement increases with decreasing α.

The Diurnal Variation of y_m of E

Routine ionosphere data are usually reported as critical frequencies f_c for each ionospheric region for each hour of the day averaged over a month. Unless otherwise stated monthly average values are used throughout this paper. From f_c the equivalent electron density y_m was calculated from the dispersion formula[12] which, for the ordinary component of polarization, leads to

$$y_m = \pi m f_c^2 / e^2 c^2, \qquad (24)$$

where e and m refer to the electron and c is the velocity of light. In Figs. 2 and 3 are plotted y_m values for the first three months of 1938 from the ionosphere station at Huancayo, Peru, lat. 12° 2.7′ S, long. 20′.4 W, of the Carnegie Institution.[13] New automatic recording equipment was placed in operation at the station in November, 1937. The daytime data of Fig. 2 are symmetrical about noon within the error of variation.[14] The same conclusion holds for E region data at Washington, D. C., U. S. A., lat. 38° 50′ N, long. 77° W, of the United States National Bureau of Standards,[15] which are continuous from 1931. One set of Washington values are plotted in Fig. 4. The (y_m, t) curves for four values of α, namely, ∞, 2×10^{-8}, 10^{-8} and 2×10^{-9}, were passed through the points of Figs. 2 and 3. The curves were based on values of ζ for February 15, 1938; since Huancayo is near the equator the use of ζ for January 15 and March 15 would lead to but slight deviation from the curves of Fig. 2.

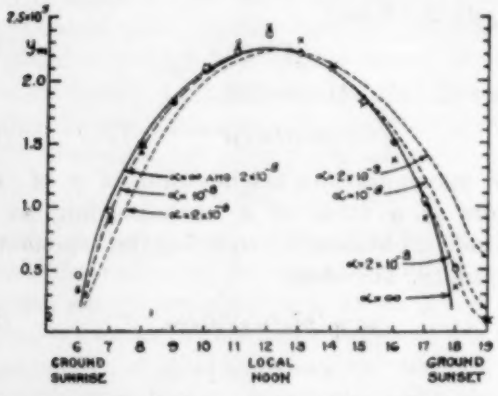

Fig. 2. E data (reference 13) at Huancayo, Peru, for January, February and March, 1938, shown by circles, dots and crosses, respectively. Theoretical curves from (16).

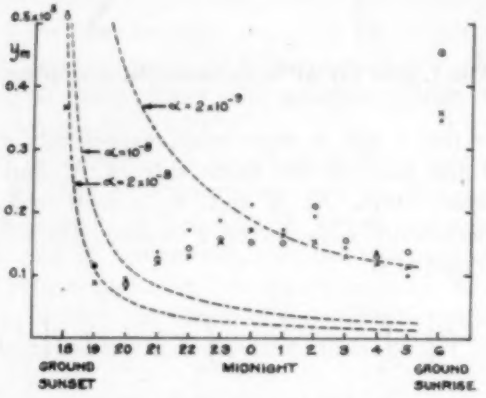

Fig. 3. E data (reference 13) at Huancayo, Peru, through the night, continued from Fig. 2. Theoretical curves from (16).

It is seen that the (y_m, t) curve of Fig. 2 for $\alpha = 2\times10^{-8}$ is in best agreement with the observations. During most of the daylight hours the difference between the curves for $\alpha = 2\times10^{-8}$ $\alpha = \infty$ is imperceptible on the scale of Fig. 2; $\alpha = \infty$ is, of course, impossible physically. We conclude that available data favor $\alpha = 2\times10^{-8}$ but do not preclude an even higher rate of recombination. With $\alpha = 2\times10^{-8}$ and $y_0 = 2.25\times10^5$ at 100 km we obtain from (19) to (22) $\beta = 2.23\times10^{-10}$ and $i_0/\chi = 1.8\times10^9$. For an energy of ionization $\chi = 14$ electron-volts, $i_0 = 4\times10^{-2}$ erg cm^{-2} sec.$^{-1}$, which, on the assumption that the sun radiates as a blackbody at 6000°K, is the

[12] The discussion continues concerning whether the value of a in the H. A. Lorentz dispersion theory is 0 or $\frac{1}{3}$ or some intermediate value: see H. G. Booker and L. V. Berkner, Terr. Mag. **43**, 427 (1938); D. F. Martyn and G. H. Monro, Nature **142**, 1159 (1938). The difficulty arises from ignorance of the exact nature of collision between ionized and neutral particles. In (24) a is 0; if a were $\frac{1}{3}$, values of y_m mentioned here would be increased by 50 percent, but all conclusions would remain unaltered.

[13] H. W. Wells and H. E. Stanton, Terr. Mag. **43**, 467 (1938).

[14] One cannot speak of "error of observation" for such a quantity is not reported. The irregularity in an average datum is due to error of observation and to natural fluctuation of the ionization.

[15] Now published each month by T. R. Gilliland, S. S. Kirby and N. Smith in the Proc. Inst. Rad. Eng. Their papers are in the Nat. Bur. Stand. J. Research.

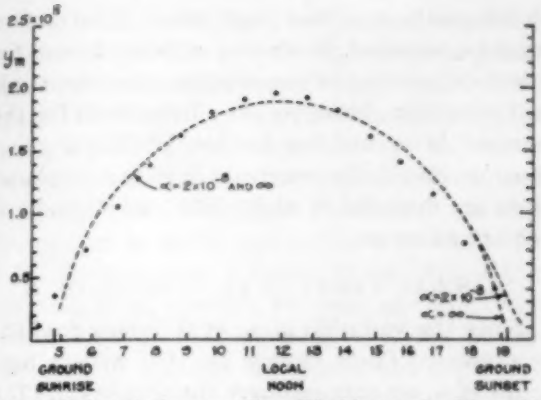

FIG. 4. E data (reference 15) at Washington for May 1938 shown by dots. Theoretical curves from (16).

solar energy falling on the top of the atmosphere in the wave-length region from about 960A to 0, or in a band about 10A wide at 1000A, or in a narrower band at a longer wave-length.

In turning to the night E values of Fig. 3 it is manifest that a simple theory of ionic recombination during the night, as (17), with no other changes cannot account for the facts. The value of y_m is observed to increase after sunset to a mild maximum around midnight, whereas (17) calls for a steady decrease in y_m through the night. Whether the nocturnal increase of y_m at Huancayo is peculiar to that station or occurs elsewhere is not known. Whether it is similar to "sporadic" E ionization[3] at higher latitudes is not yet reported; Kirby and Judson[1] expressed the opinion that most night-time E reflections at Washington were of a sporadic type. Whether the increase is caused by effects in the atmosphere, as ionic clouds and scattering centers due to winds ("white cap" theory), generation of ionization by collision of excited or combining atoms ("spontaneous generation" theory), night cooling of an E region warmed during the day ("contraction" theory), or by effects external to the atmosphere, as meteors ("interplanetary debris" theory), or by some other effect ("angel" theory), cannot be said. Be this as it may, the facts at present do not necessarily imply a value of α during the night which is different from its day value.

It has long been known[15, 16] that E ionization begins to increase during morning twilight before ground sunrise but no continuous accurate measurements have been made of the effect. A series of data was obtained at Washington by the United States National Bureau of Standards for the purpose of comparison with the present theory. Their data are given in Fig. 5 for three mornings, May 11 and 18 and June 1, 1938, that appeared to be relatively free from sporadic E phenomena and magnetic disturbance. In Fig. 5 y_m is plotted against ζ and a scale of t is appended that was approximately the same for all three mornings. The monthly average hourly values of y_m for May,[10] assumed to apply to May 15, 1938, were used. These are plotted in Fig. 4 and the (y_m, t) curve for $\alpha = 2\times10^{-8}$ was passed through them. This determined all the constants of (16) and underlying equations. Since the (y, z) curve at 30 minutes before ground sunrise was not known, a (y, z) curve was assumed with $y_m = 0.4\times10^4$ in agreement with the observed values of Fig. 5. The curve is drawn in Fig. 6; but what follows does not depend at all critically on the assumed form of the curve. The (y, z) curves at succeeding epochs up to sunrise were calculated from (16); they are given in Fig. 6. From them the (y_m, t) curve was determined and is plotted in the curve of Fig. 5 for $\alpha = 2\times10^{-8}$. It does not agree with the observations. The entire calculation was repeated with $\alpha = 4\times10^{-8}$, the resulting curve is given in Fig. 5 and again is discordant with

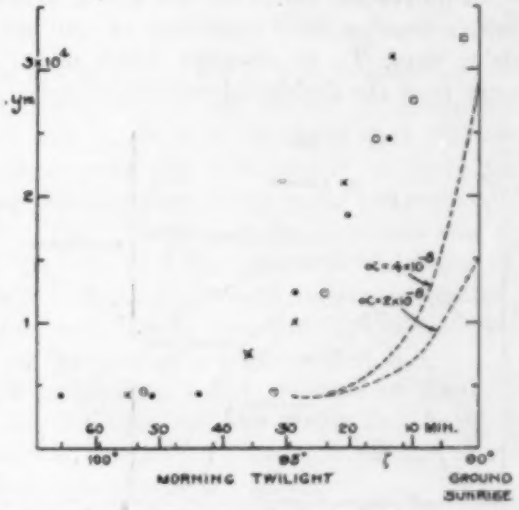

FIG. 5. Pre-dawn E data at Washington for May 11 and 18 and June 1, 1938, shown by dots, crosses and circles, respectively. Theoretical curves from (16).

[16] S. K. Mitra, Science and Culture **3**, 496 (1938); J. E. Best, F. T. Farmer and J. A. Ratcliffe, Proc. Roy. Soc. **A164**, 96 (1938).

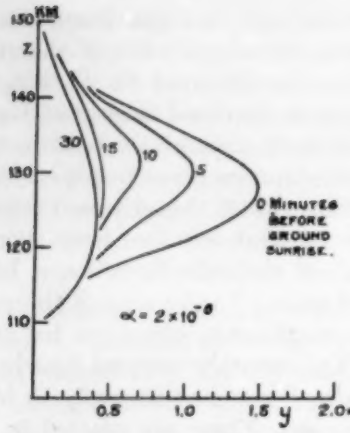

FIG. 6. Theoretical (y, z) curves from (17) during morning twilight at Washington, May 15, 1938.

observation. There is also a difficulty with virtual heights; these were observed to be about the same, within 10 km, during morning twilight as they were during the day, whereas the theoretical virtual heights from the curves of Fig. 6 are 20 km or more above the day values.

It is concluded that the simple theory does not yield exact agreement with the observed morning twilight augmentation of y_m of E. It is not safe to generalize too much from data of only three mornings at one station; further data, accurate and closely spaced, of all ionospheric regions would be desirable. If the discrepancy is found to persist, three effects, among those omitted from simple theory, come to mind toward its elucidation. They are winds, atmospheric refraction and scattering of the solar ionizing rays. To be effective winds must be greater than the peripheral velocity of rotation of the earth, or a very high index of refraction must be assumed. Scattering appears to call for a less extreme set of assumptions than do winds and refraction. However, any hypothesis for the purpose of accounting for the pre-dawn effect must necessarily be uncertain as long as explanations are doubtful of night-time and sporadic E echo phenomena.

SEASONAL VARIATION OF NOON y_m OF E

Since the variation of y_m of E during daylight is expressed fairly closely by (16) with a high value of α, we may compare the simple Eq. (22), $y_m = y_0(\cos\zeta)^{\frac{1}{2}}$, with average monthly noon values of y_m observed at various stations scattered over the earth. Since E ionization varies with the sunspot cycle it is convenient to make the comparison for each year separately. Results for 1936, 1937 and 1938 are given in Fig. 7, in which the smooth curves for each station are from (22) and the observed points are shown by the initial letter of each station. In more detail, the curve of (22) was passed through the Washington observations, which determined y_0 for the year; with this value of y_0 and with ζ from the latitude of the station the curve of (23) for the station was drawn. The data of Fig. 7 were from Washington,[15] Huancayo,[16] Tromsö[17] and Northeast Land.[18] Measurements were made at Wuchang,[19] China, lat. 30° 34′ N for a few months in 1937 and 1938. Comparisons similar to those of Fig. 7 were prepared for the years

[17] L. Harang, Terr. Mag. **43**, 41 (1938).
[18] A. B. Whitman and R. A. Hamilton, Proc. Phys. Soc. London **50**, 217 (1938).
[19] P. L. Sung and C. T. Kwei, Terr. Mag. **43**, 453 (1938).

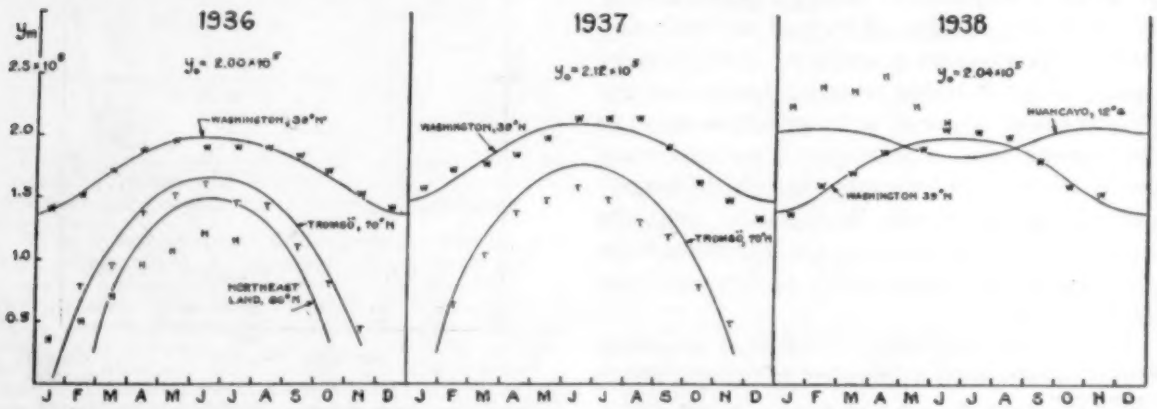

FIG. 7. Observed average monthly noon values of y_m of E shown by the initial letter of the station. Theoretical curves from (22).

1931 to 1935, inclusive. The Washington observations were continuous throughout these years. Data were available from Slough,[20] lat. 51° 30′ N, and Tromsö[20] for the year from August 1932 to August 1933; from Deal,[21] lat. 40° 15′ N for the year from March 1933 to March 1934; and for Slough[19] for 1934. These comprise practically all reported monthly average noon values of y_m of E. The conclusion was that at any station the variation of y_m through the year agreed closely with (22) but that between stations widely separated in latitude the agreement with (22) was far from close. The discrepancy in 1938 between Huancayo and Washington is particularly noticeable. These are accurate stations; it is to be remembered that Huancayo has been operating on its present schedule for only about a year. The discrepancy appears to be that noon y_m of E falls off more rapidly with increasing latitude than would be expected from (22); y_m is below the value from (22) by roughly 0, 10, 20 and 30 percent at latitudes 0°, 40°, 70° and 80°, respectively. If the discrepancy turns out to be real, additional theoretical hypotheses may be called for.

In this connection a suggestion, albeit vague and qualitative, may be in order. The assumption was made that the atmosphere of the E region was the same at all latitudes. It may be necessary to depart from the assumption to some extent and to assume that the character of the atmosphere changes from the equator to the poles. For example, sunlight may cause excitation or may dissociate molecular oxygen or nitrogen, or both, to the atomic condition, the amount of excitation or dissociation being a function of the latitude. Therefore the absorption and recombination coefficients, in short the entire photochemistry of the E region, may vary sufficiently with latitude to account for the departures from the simple photochemistry underlying the present calculations.

Variation of y_0 of E with Sunspots

The values of y_0 of E were determined from the Washington[14] observations for the years 1931 to 1938, which cover a portion of a sunspot cycle. In Fig. 8 y_0 is plotted with the yearly average relative sunspot number[22] s; it is seen that y_0 and s rise and fall together. A theoretical relation between y_0 and s may be derived as follows: From (23) $y_0 \sim i_0^{\frac{1}{4}}$, where i_0 is the intensity of the solar radiation which causes E ionization. Assume that $i_0 \sim (s+b)$, where b, a constant, is introduced in recognition of the fact that y_0 and i_0 have values other than zero when s is zero, i.e., when there are no sunspots. Then

$$y_0 = a(s+b)^{\frac{1}{4}}. \tag{25}$$

The dotted curve of Fig. 8 is plotted from (25) with $a = 0.154 \times 10^5$ and $b = 78.6$; it agrees fairly well with y_0. It may be noted that (25) with different constants was found[23] to agree with long distance short wave radio communication data. The difference in the constants was due to the facts that the radio data depended in a complex manner on the F regions as well as E region and that the variation of F with sunspots is not the same as the variation of E.

In conclusion, it is a pleasure to thank Dr. J. H. Dellinger and the Radio Section of the National Bureau of Standards for the unpublished data plotted in Fig. 5.

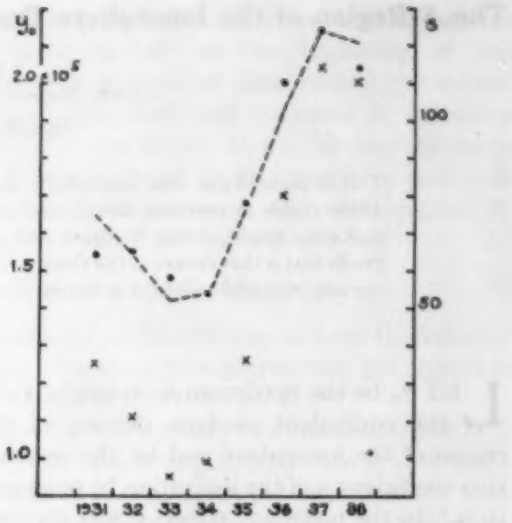

Fig. 8. Dots, y_0 of E from Washington observations (reference 15); crosses relative sunspot numbers (reference 22) s. Dotted curve from (25).

[20] E. V. Appleton, R. Naismith and L. T. Ingram, Phil. Trans. Roy. Soc. **236A**, 218 (1936–1938); E. V. Appleton and R. Naismith, Proc. Roy. Soc. **A150**, 685, (1935).

[21] J. R. Schafer and W. M. Goodall, Proc. Inst. Rad. Eng. **23**, 670 (1935).

[22] W. Brunner, each volume of Terr. Mag.

[23] L. C. Young and E. O. Hulburt, Phys. Rev. **50**, 45 (1936).

The *E* Region of the Ionosphere During the Total Solar Eclipse of October 1, 1940

E. O. HULBURT
Naval Research Laboratory, Washington, D. C.
(Received February 16, 1939)

It is pointed out that ionospheric observations during the total solar eclipse of October 1, 1940, visible in northern Brazil, may provide data for an exacting test of the theory of solar radiation origin of the *E* region and may yield a precise value of the ionic recombination coefficient α that occurs in the theory. To this end *E* region ionization curves are worked out for various assumed values of α during the eclipse.

LET y_m be the maximum-with-height value of the equivalent electron density of the *E* region of the ionosphere and let the recombination coefficient α of the ionization be proportional to y_m^2. In the preceding paper[1] it was shown that the observed variation of y_m during the daylight hours was in close agreement with the theory that the ionization was caused by solar radiation absorbed exponentially in a relatively quiet terrestrial atmosphere. A value for α of 2×10^{-8} was indicated but the accuracy of the experimental data did not preclude the possibility of an even higher value. It is doubtful that a more exact value of α can be obtained from diurnal measurements in view of the relatively slow change in solar radiation intensity due to the diurnal variation of solar zenith angle. During an eclipse of the sun the solar radiation intensity changes rapidly and it appears that y_m data obtained at a station in the path of totality may offer a more precise determination of α and a more exacting test of the theory. Although ionosphere observations have been made during epochs of solar eclipses,[2] there exist no measures of y_m by a station in the path of totality.

A total eclipse of the sun occurs on October 1, 1940, under circumstances favorable to an ionosphere experiment. The complete elements of the eclipse will be published soon by the United States Naval Observatory. The central line of totality runs along the northern edge of Brazil.[3] At Pernambuco, Brazil, totality occurs at about 10 A.M., local time, of duration about 5 minutes, the solar zenith angle being about 35°.

In Fig. 1 are given y_m curves for the period of the eclipse calculated for various values of α. In order to make the calculations, eclipse conditions were assumed that approximate those of the actual eclipse. Exact calculations for the actual eclipse can be made when the location of the observing station is known. Assume that the station is at latitude 8° S and longitude 35° W, as near Pernambuco, and that the first, second, third and fourth contacts occur at 9, 10, 10.04 and 11.04 A.M., local time, respectively. Since the apparent diameters of the sun and moon are approximately equal and since the moon moves uniformly across the sun, the fraction f of the exposed disk of the sun is expressed as a function of the time t seconds by

$$f=1-(2/\pi)\{\cos^{-1}T-T(1-T^2)^{\frac{1}{2}}\}. \quad (1)$$

Between first and second contacts, t is measured from the first contact, $T=1-t/3600$; and between second and third contacts, t is measured from the third contact, $T=t/3600$. Here t refers to the ionospheric level under investigation and not to the surface of the earth.

Let q ion-electron pairs sec.$^{-1}$ cm^{-3} be the rate of production of ionization at the y_m level and ζ be the zenith angle of the sun. From Eqs. (2), (3) and (4), reference 1,

$$q=q_0\cos\zeta, \quad (2)$$

where q_0 is the value of q for the sun overhead. In general, from Eq. (16), reference 1,

$$dy_m/dt=-\alpha y_m^2+q. \quad (3)$$

On a day with no eclipse, from (2) and (3),

$$dy_m/dt=-\alpha y_m^2+q_0\cos\zeta, \quad (4)$$

and during the eclipse, from (1), (2) and (3)

$$dy_m/dt=-\alpha y_m^2+fq_0\cos\zeta, \quad (5)$$

[1] E. O. Hulburt, Phys. Rev. **55**, 639 (1939).
[2] S. S. Kirby, T. R. Gilliland and E. B. Judson, Nat. Bur. Stand. J. Research **16**, 213 (1936), and references *infra*.
[3] L. T. Comrie, Roy. Astron. Soc., M. N. **93**, 181 (1932–33).

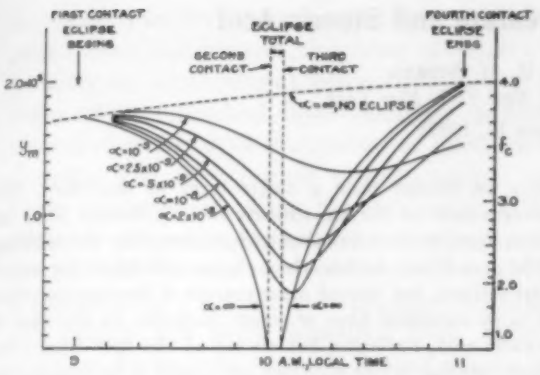

FIG. 1. Theoretical ionization of E region at Pernambuco, Brazil, during the eclipse of October 1, 1940.

on the assumption that the intensity of the ionizing radiation is proportional to f.

For α very great, practically infinite, the ionization is approximately in equilibrium with the radiation which produces it and $dy_m/dt=0$. Eqs. (4) and (5) become, respectively, for no eclipse

$$y_m=[(q_0 \cos \zeta)/\alpha]^{\frac{1}{2}}, \tag{6}$$

and during the eclipse

$$y_m=[(fq_0 \cos \zeta)/\alpha]^{\frac{1}{2}}. \tag{7}$$

In Fig. 1 y_m from (6) and (7) is plotted in the two curves marked $\alpha=\infty$; the constant q_0 is adjusted to make $y_m=2\times10^5$ at 11 A.M., which is probably near to the actual value for the E region. The other curves of Fig. 1 were worked out from (5) with the various values of α designated; for each curve q_0 was chosen to give $y_m=1.74\times10^5$ at the beginning of the eclipse. The method of determining the curves has been described[1] and consisted in following graphically the course of dy_m/dt step by step. The datum observed by an ionosphere station is the critical frequency f_c for each region of ionization, where for the ordinary ray

$$f_c^2=ye^2c^2/\pi m; \tag{8}$$

e and m refer to the electron and c is the velocity of light. A scale of f_c in megacycles per second is marked on the right of Fig. 1.

From Fig. 1 it appears that measurements of f_c during the eclipse might determine α with some degree of precision. It would be important that the E region during the eclipse be free from sporadic effects and magnetic disturbance. The assumption in (5) of uniformity of ionizing radiation over the solar disk must be borne in mind. Near the edge of the disk the assumption may fail. In any case analysis of the observations might give information about the intensity distribution over the face of the sun. As said before, if observations are made by an ionosphere station in the path of totality, exact calculations similar to those of Fig. 1 can be made referring to the location of the station. The foregoing discussion has been directed to consideration of the E region, but with appropriate changes it applies equally well to the other regions of the ionosphere.

Rubbed Films of Barium Stearate and Stearic Acid

L. H. GERMER AND K. H. STORKS
Bell Telephone Laboratories, New York, New York

(Received February 17, 1939)

Films of barium stearate and of stearic acid have been prepared on polished chromium and on smooth natural faces of silicon carbide crystals. After these films have been rubbed with clean lens paper, electron diffraction patterns are obtained from them by the reflection method. *Well rubbed films* give patterns characteristic of a single layer of molecules standing with their axes approximately normal to the surface; the hydrocarbon chains of barium stearate are found to be more precisely oriented than those of stearic acid; exactly the same difference exists between unrubbed single layers of molecules of barium stearate and of stearic acid deposited by the Langmuir-Blodgett method. Thickness of rubbed films on chromium has been found, by the Blodgett optical method, to be the same as that of unrubbed single layers of molecules. *Lightly rubbed films* may be thicker than a single layer of molecules. The arrangement of barium stearate in such thicker films has been found to have been somewhat altered by the rubbing. The axes of the hydrocarbon chains still stand normal to the surface, but lateral arrangement is less regular than it is in unrubbed films of equal thickness. In the case of stearic acid, molecules left on top of the first layer after light rubbing in one direction are found to lie inclined by about 8° to the surface and to point outward against the rubbing direction (Fig. 7); they are arranged in crystals having a structure different from that of the film before rubbing. Such "upset" films of stearic acid are completely removed by very light rubbing in the direction opposite to that of the original rubbing, but they are rather resistant to light rubbing in the same direction.

IN MULTILAYERS of barium stearate or of stearic acid, built by the Langmuir-Blodgett method, the orientation of the molecules of the first layer is dependent upon the substratum. Upon clean metal these molecules are always oriented with their carboxyl or metal ends against the surface; upon an organic material having a hydrophobic surface they are, in general, turned the other end up, with the carboxyl or metal ends pointing outward.[1]

We have shown[2] that, when paraffin ends are against a surface, stearic acid molecules of the first layer stand with their axes inclined to the surface normal and are built into true crystals characteristic of the acid, and barium stearate molecules of the first layer stand with their axes parallel to the surface normal and are arranged laterally in characteristic fashion. On the other hand our experiments have shown that, on metal surfaces, the molecules of the first layer are packed closely together laterally, but without any regular arrangement. It seems probable that this absence of ordered arrangement in the first layer on metal surfaces is accounted for by the fact that the molecules are anchored to the surface by their chemically active ends. Paraffin ends upon the surface of an organic material are not so firmly anchored. Thus molecules oriented with their paraffin ends against a surface are free to arrange themselves under the influence of the lateral forces exerted by their neighbors, and under these circumstances molecules of the first layer form true crystals or pseudo-crystals.

These observations are consistent with the known fact that all but one layer of stearic acid or barium stearate molecules can be easily wiped from a metal surface, but the first layer is not readily removed. Consideration of these matters, and of their possible importance from the standpoint of lubrication, led us to experiment upon films of barium stearate and stearic acid which had been rubbed in various ways. We have obtained electron diffraction patterns from rubbed films on polished chromium and on very smooth natural faces of silicon carbide crystals, and we have measured thicknesses of rubbed films upon polished chromium by the Blodgett optical method.[3]

Our experiments show that even a single moderately vigorous rub with clean lens paper is often sufficient to remove all but one layer of barium stearate or of stearic acid molecules from a chromium or silicon carbide surface. This remaining layer of molecules is arranged upon the surface just as are the molecules of a single layer deposited by the Langmuir-Blodgett

[1] K. B. Blodgett, J. Am. Chem. Soc. **57**, 1007–1022 (1935).
[2] L. H. Germer and K. H. Storks, J. Chem. Phys. **6**, 280–293 (1938).
[3] K. B. Blodgett, J. Phys. Chem. **41**, 975–984 (1937).

method. Further vigorous rubbing with lens paper does not remove this layer of molecules, or alter its arrangement perceptibly; the molecules of this residual layer seem to be firmly anchored either upon chromium or upon silicon carbide, and they remain on the surface with their axes approximately parallel to the surface normal. It turns out, furthermore, that for stearic acid the same result is obtained by rubbing a film built by the Langmuir-Blodgett method or one which has been deposited from benzene solution. In the case of thick films of stearic acid and light rubbing in one direction some of the material may, however, be left piled up in a different fashion on top of the first layer of molecules; this can be removed by one or two rubs in the opposite direction. Some of the electron diffraction patterns upon which these conclusions are based are reproduced here.

Studies of Well Rubbed Films

The patterns of Fig. 1 were obtained from a film composed of seven layers of stearic acid molecules upon chromium; Fig. 1(a) was obtained before rubbing and Fig. 1(b) from the same film after a single downward rub with clean lens paper under moderate pressure. Patterns identical with Fig. 1(b) were obtained from the same block after further rubbing which was very vigorous. The two patterns of Fig. 1 are characteristic, respectively, of a number of layers of stearic acid molecules, and of a single layer upon a metal. (See Figs. 7 and 5, reference 2.) The thickness of a well rubbed film of stearic acid has been found to be 25 ± 2A by optical measurement with polarized sodium light. The method of measurement has been described by Blodgett.[3]

Patterns from barium stearate films are reproduced in Figs. 2 and 3. The pattern of Fig. 2 (from a built-up film which had been dipped into benzene to demonstrate the failure of benzene to change a barium stearate film) is similar to a previously published pattern from a barium stearate multilayer (see Fig. 3, reference 2). The patterns of Fig. 3 were obtained from built-up films which had been very vigorously rubbed with lens paper and exhibit the diffraction bands characteristic of a single layer of barium stearate molecules (see Fig. 1, reference 2); in Fig. 3(b) there appear also lines from the underlying silicon carbide crystal.

In our earlier paper we established a difference between the arrangement of barium stearate molecules in a single layer and the arrangement

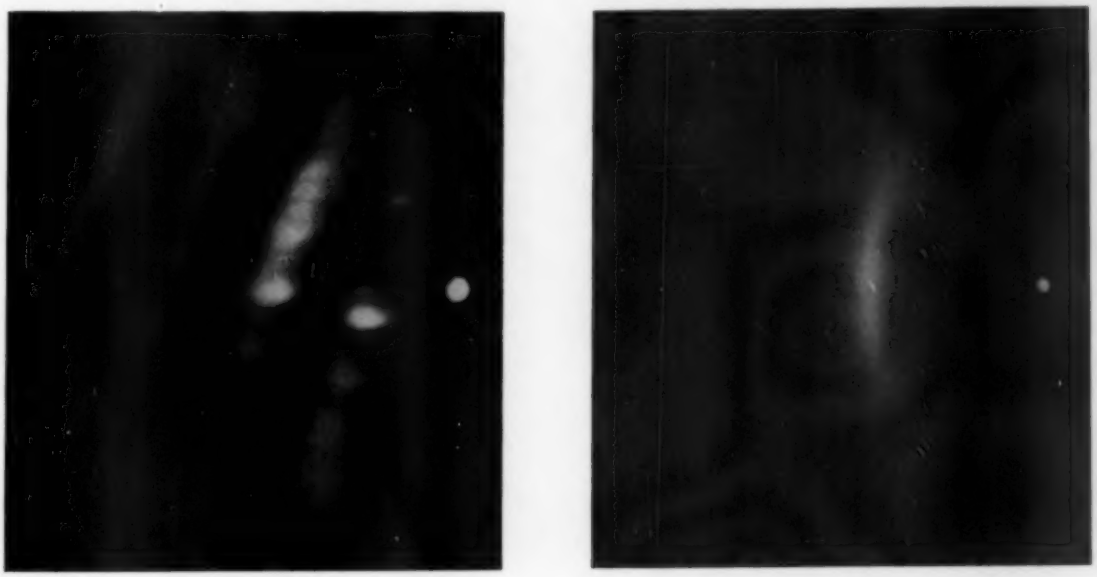

(a) Before rubbing. (b) After single rub with lens paper.

Fig. 1 Electron diffraction patterns from a chromium surface upon which have been deposited 7 layers of stearic acid molecules. Electron beam normal to direction of dipping when the layers were formed, and patterns reproduced here with dipping direction downward. ($L\lambda = 3.205\times10^{-4}$ mm^2.)

FIG. 2. Diffraction pattern from 7 layers of barium stearate molecules (obtained after the built-up film had been dipped into benzene). ($L\lambda = 3.205 \times 10^{-4}$ mm².)

of stearic acid molecules in a single layer (reference 2, the corresponding diffraction patterns are reproduced as Figs. 1 and 5, respectively); barium stearate molecules are oriented with their axes rather accurately normal to the supporting surface, whereas molecules of stearic acid are less precisely arranged. It is interesting to point out that exactly the same difference exists between *rubbed films* of barium stearate and stearic acid; Figs. 1(b) and 3(a) exhibit the same difference as do Figs. 5 and 1 of the earlier paper.

Studies of Lightly Rubbed Films

When a rather thick film of barium stearate or stearic acid upon chromium is rubbed sufficiently lightly, enough material may be left on the surface to be visible. Ten layers of molecules can be seen easily, and under good conditions five layers. Electron diffraction studies of such residual films have been carried out.

A film of 61 layers of barium stearate molecules was first built upon a chromium surface. After this film had been rubbed with lens paper very lightly in one direction until the remaining material was barely visible, the diffraction pattern of Fig. 4 was obtained from it. One concludes from this pattern that the molecules of this rubbed film are standing with their axes normal to the surface, as they were before rubbing. Furthermore it is clear, from comparison of Figs. 2, 3(a) and 4, that the regularities which were initially present in the lateral arrangement of the molecules have been largely, but not entirely, destroyed by rubbing. The comparative lack of lateral regularity is due to rubbing, not to thinness of the remaining film; this is proved by the fact that the pattern of Fig. 4 exhibits less marked indications of lateral regularities than does a pattern from only three built-up layers of molecules (reference 2, Fig. 3), although the film which produced the pattern of Fig. 4 was visible and contained on the average from 5 to 10 layers. The structure of the final film is apparently independent of the direction of rubbing.

The effect of light rubbing upon thick films of stearic acid is markedly different, and the direction of rubbing is important. The pattern of Fig. 5 was produced by a film of stearic acid which had been rubbed lightly in a direction normal to the primary electron beam, and parallel to the paper and upward as the pattern is reproduced here. We have shown that rubbing in the opposite direction, downward but still normal to the electron beam, results in a pattern which is an image of Fig. 5 mirrored by the horizontal center line passing through the primary beam position. These diffraction patterns obtained after rubbing are unrelated to the original inclination of the molecules before rubbing. We have proved this by studying diffraction patterns from films consisting originally of 61 layers of stearic acid molecules, built by the Langmuir-Blodgett method, which have been rubbed in the direction of the inclination of the hydrocarbon chains and opposite to the direction of inclination, and from rubbed films of stearic acid deposited by evaporation from benzene solution. Each of these films was rubbed lightly in one direction only, and in each case the pattern from the rubbed film was determined completely by the rubbing.

The rubbed film which produced the pattern of Fig. 5 was barely visible and must therefore have had an average thickness corresponding to somewhat less than 200A, (10 layers of molecules as they are arranged before rubbing). This estimate is confirmed by the fact that in Fig.

5(a) can be seen weakly a diffuse band at the position of the strong second-order band from a single layer of stearic acid molecules. The fact that the pattern from the first layer of molecules is not quite obliterated by the material lying upon it is adequate basis for an estimate of thickness of somewhat over 100A. (This is based upon the earlier paper.[2])

The pattern of Fig. 6 was obtained from a film, consisting initially of 51 layers of molecules, which had been rubbed very lightly in the downward direction just until no material could be seen on the surface. It is clear that this is predominantly the pattern of a single layer of molecules. The weak spot pattern in Fig. 6 is like the mirror image of the pattern of Fig. 5(a); it must arise from an "upset" film of stearic acid, less on the average than 20A in thickness, resting on top of the first layer of molecules.

The most prominent features of Fig. 5(a) are readily interpreted. There is a film line pointing toward the primary beam position and making an angle of 42° with the vertical, and there are four parallel lines separated from it by multiples of 5.0 mm. A portion of the line pointing toward the primary beam position is clearly resolved into 14 spots which are equally spaced at separations of 0.57(7) mm, and the parallel lines are also resolved into spots, but much more imperfectly. The 14 spots, which appear more clearly in the enlargement of Fig. 5(b), are reflections from widely spaced crystal planes standing normal to the lines. It is clear that the poor resolution of spots along lines not passing through the primary beam position is due to the fact that we are not dealing with a perfect single crystal. The pattern is that of a mass of crystallites distributed over a small angular domain about a mean position. Rotation about a line normal to the paper would result in rotation of the diffraction pattern about the line normal to the paper through the primary beam position. The effect of such rotation is very obvious in Fig. 5(a); each diffraction spot is clearly an arc about the primary beam position, with an angular extent of perhaps 5°. This rotation does not affect the resolution of spots along the line through the primary beam position, but smears together spots along parallel lines.

In these experiments the Bragg formula can be written, $Rd = L\lambda$, where values of R represent separations of diffraction spots, d corresponding crystal plane spacings, and $L\lambda$ a constant of the apparatus determined, for Fig. 5, to be 2.345×10^{-6} mm² by calibration against a foil of gold. From this formula one finds that the crystal planes which give rise to the line of spots are separated by distances equal to $2.345\times10^{-6}/0.577 = 4.06\times10^{-6}$ mm = 40.6A, and that the edge of the unit cell which lies in one of these planes and parallel to the plane of the paper has the length $2.345\times10^{-6}/5.0 = 4.69$A or a multiple of this.

In Fig. 5(a) one observes diffuse parallel bands about 9.3 mm apart and inclined by about 8° to the horizontal. The spots which make up the fine lines are very intense only where they cross these bands. The bands, which correspond to rows of atoms separated by distances of $2.345\times10^{-6}/9.3 = 2.52$A, undoubtedly represent the positions at which the alternate carbon atoms in each stearic

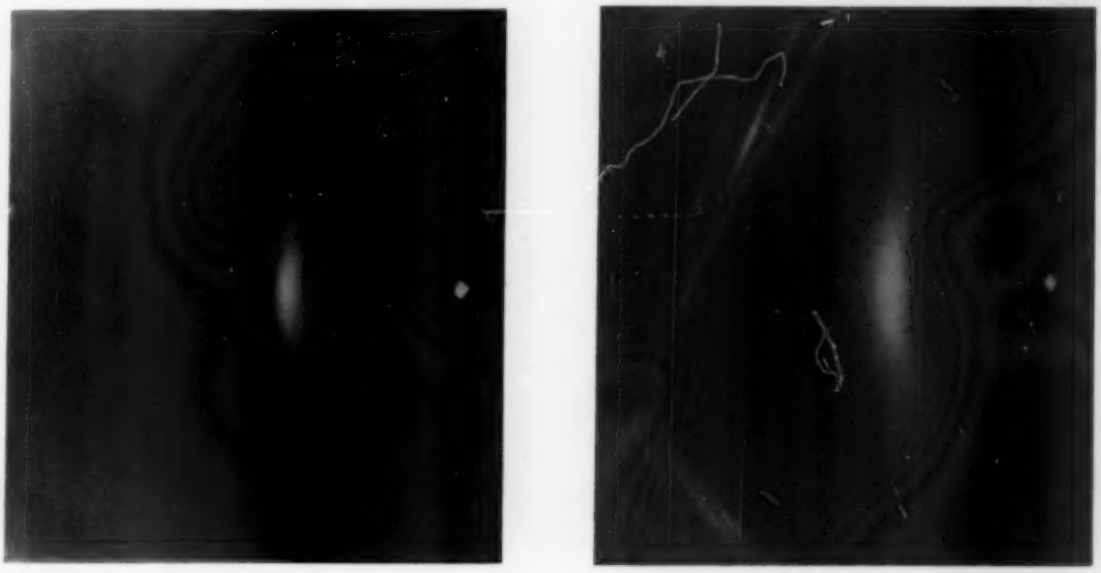

(a) Upon chromium. (b) Upon silicon carbide.

FIG. 3. Diffraction patterns from built-up films of barium stearate which have been virogously rubbed with lens paper. ($L\lambda = 3.205\times10^{-6}$ mm².)

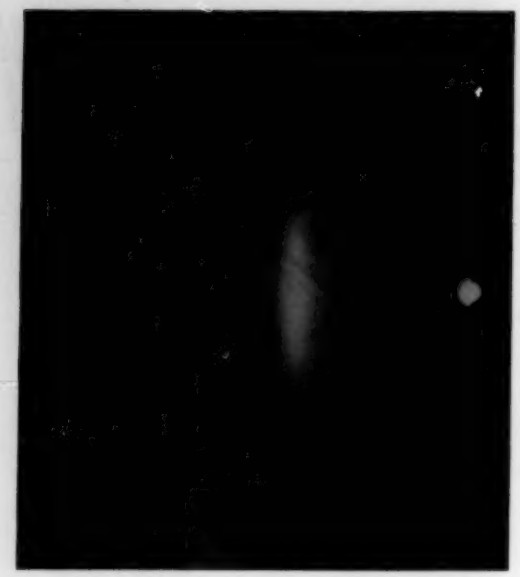

FIG. 4. Diffraction pattern from a thick built-up film of barium stearate, obtained after it had been rubbed down to a thickness of somewhat less than 10 layers of molecules. ($L\lambda = 3.205 \times 10^{-6}$ mm².)

acid molecule scatter in phase, and the direction of the normal to the bands is parallel to the axes of the molecules. These molecular axes are thus inclined by 42°–8° = 34° to the normals to the widely spaced planes.

It is conventional to designate crystal axes in such a way that the long spacing (40.6A) represents separations between the *ab* planes, and, assuming monoclinic structure which has been established for at least two of the polymorphic forms of stearic acid, the *b* axis is normal to the other two. With this description of axes the spots making up the inclined line through the primary beam position in Fig. 5 are (0 0 *l*) reflections, and spots on parallel lines are (*h* 0 *l*) reflections with a particular value of *h* applying to each line. The length of the edge of the unit cell parallel to the *a* axis is then 4.69A, or a multiple of this. The direction of the *c* axis and the length of the edge of the unit cell parallel to it are somewhat arbitrary. If we choose this direction parallel to the axes of the hydrocarbon chains we obtain $\beta = \pi/2 - 34° = 56°$, $c = 40.6/\sin\beta = 49.0$A.

Examining again the pattern of Fig. 5(a) one observes that there are other spots lying upon the diffuse and nearly horizontal "molecular bands" in addition to those occurring at intersections with the inclined (*h* 0 *l*) lines. These extra spots appear to lie upon other inclined lines. In all probability these are (*h* 1 *l*) and (*h* $\bar{1}$ *l*) lines, and occur because we are dealing not with a single crystal but with a mass of crystallites many of which are slightly rotated about the mean position. On this assumption one can calculate from positions of these spots the separation of the *ac* planes. One discovers that the (*h* 1 *l*) lines are spaced half as far apart as are (*h* 0 *l*) lines and that the *ac* plane separation is about 5A, although, determined in this manner, this value has low precision. All of the additional reflections are accounted for in this way and there are no missing (*h* 1 *l*) lines in the intense part of the pattern. The fact that (*h* 0 *l*) lines have separations which are twice those of (*h* 1 *l*) lines must be interpreted as meaning that (*h* 0 *l*) reflections occur only for *h* even, and that $a = 2(4.69) = 9.38$A rather than half this value.

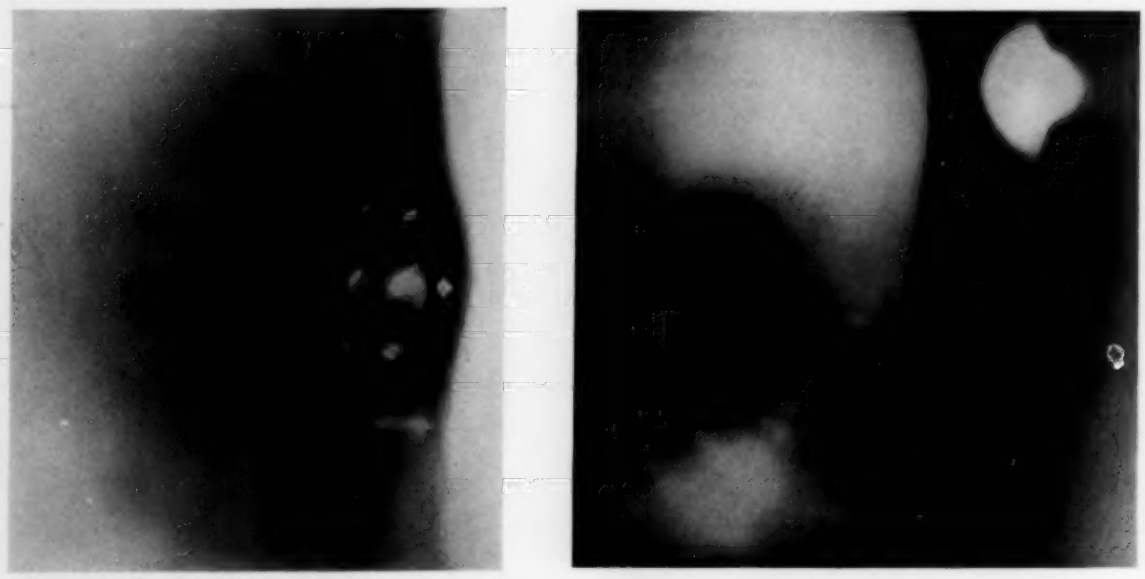

(a) (b)

FIG. 5. Diffraction pattern from film of stearic acid rubbed lightly normal to the primary electron beam and upward as the pattern is reproduced here. ($L\lambda = 2.345 \times 10^{-6}$ mm².) ((b) Enlarged portion of Fig. 1(a) to show the closely spaced (0 0 *l*) reflections.)

FIG. 6 Diffraction pattern from film of stearic acid rubbed lightly just until no more film can be seen on the surface. ($L\lambda = 3.205 \times 10^{-4}$ mm².)

Collecting the data obtained from Fig. 5 we have: $a = 9.38$A, $b \sim 5$A, $c = 49.0$A, $\beta = 56°$. (h 0 l) reflections occur only for h even. These data are in excellent agreement with those published for the "α" or "ϵ" form of stearic acid.[4]

The stearic acid films, upon which the rubbing experiments reported here were performed, gave before rubbing diffraction patterns like that of Fig. 1(a). This is characteristic of one of the polymorphic forms which we have studied (column 2, Table V, reference 2). Lightly rubbed films, however, have a structure which is entirely different. It is interesting and surprising to find that light rubbing not only turns over the stearic acid molecules but also changes the crystalline form.

The sketch of Fig. 7 illustrates schematically the effect of light rubbing upon unit cells of stearic acid crystals. The cross-hatched area at the right represents the first layer of stearic acid molecules upon a chromium or silicon carbide surface. The inclined parallelograms *A* and *B* represent unit cells of stearic acid standing upon this first layer. After light rubbing in the direction of the arrow the resulting unit cell is depicted by the parallelogram *C*, quite irrespective of how *A* or *B* is turned about the surface normal.* If there were no change of crystal form we can see that *A* could be rotated by rubbing directly into the position *C*, but *B* could not be so turned. The fact that *B* as well as *A* is found experimentally to be changed into *C* is, however, not so surprising as it would be if this were not accompanied by change in structure. Light rubbing produces not only an overturning of the molecules but also a rearranging of the molecules within each unit cell.

Films in the condition *C* in Fig. 7 have been found to be fairly resistant to repeated light rubbing in the direction of the arrow. They are, on the other hand, removed with extreme ease by rubbing in the opposite direction; two or three rubs with lens paper under pressure which is barely perceptible are often sufficient to remove all except the first layer of molecules. In one case

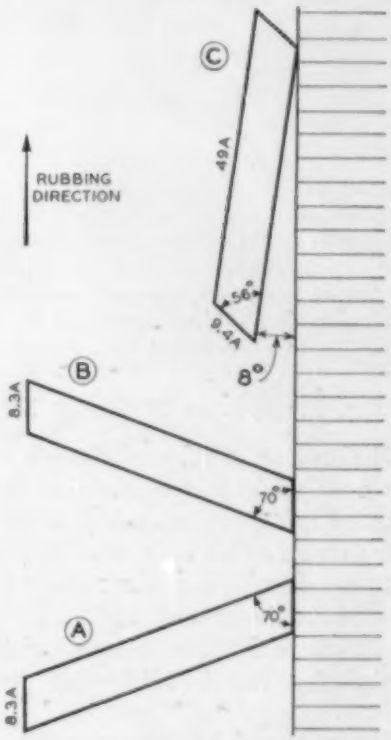

FIG. 7. Representation of unit cells in stearic acid films, A and B before rubbing, C after light rubbing in the direction of the arrow.

[4] L. H. Germer and K. H. Storks, Proc. Nat. Acad. **23**, 390–397 (1937). Also column 3, Table V, reference 2.

* We have pointed out above that the direction of the long axis is somewhat arbitrary. It is drawn here parallel to the axes of the hydrocarbon chains. Perhaps a more pleasing choice of the c axis for the rubbed film would make it parallel to the surface and inclined by 8° to the chain axes.

in which the "upset" molecules were not completely removed by light reversed rubbing the orientation of the remaining material was found to have been unaltered by the second rubbing. It seems quite possible that the material which was not removed had never been actually touched by the lens paper.[5]

It may be interesting to describe a mechanical model which might be expected to exhibit similar different responses to rubbing. If very soft bristles were supported in an inclined position in small holes in a solid surface, rubbing in the direction of their inclination would remove many bristles but rubbing in the opposite direction would only wedge them in more tightly.

It may be possible to carry the analysis of diffraction patterns like that of Fig. 5 considerably farther than has been done here. Also diffraction patterns from lightly rubbed films obtained with the primary beam parallel to the rubbing direction would yield precise values of the "*b*" spacing and probably other data. Intriguing as these matters are, they seem to us to be unrelated to the purpose of this simple study of rubbed films.

[5] Finch has reported very briefly [G. I. Finch and S. Fordham, Chem. and Ind. **56**, 637 (1937); G. I. Finch, J. Chem. Soc. 1144 (1938); Nature **141**, 547 (1938)] similar orientation of stearic acid molecules produced by rubbing. Our observations differ from his in some ways. From his very brief published statements we understand that his rubbed films are fairly resistant to rubbing in the opposite direction; this we do not find.

APRIL 1, 1939 PHYSICAL REVIEW VOLUME 55

On the Origin of Great Nebulae

G. GAMOW AND E. TELLER
The George Washington University, Washington, D. C.

(Received February 4, 1939)

The formation of condensation due to gravitational instability is discussed in a uniformly expanding space. It is shown that such condensations cannot be formed at the present stage of the development of the universe but could have been formed in the past when all linear dimensions were 600 times smaller. This corresponds to the stage at which, according to astronomical observations, nebulae have been separated from each other. To get the correct dimensions of nebulae it is necessary to accept that the velocities of particles at the moment of separation were about 140 km/sec. which strongly suggests that these particles were stars and not atoms. The type of expansion necessary for the formation of nebulae indicates that space is infinite and unlimitedly expanding.

I. General Properties of Great Nebulae

DURING recent years, considerable progress has been made in the study of great (or extragalactic) nebulae, due mainly to the investigations of Hubble.[1] We know that these objects represent immensely large accumulations of matter scattered in general uniformly through space, the average distance between neighboring nebulae being about 1.7×10^{6} light years or 1.6×10^{24} cm.

The nebulae themselves possess radii varying from one thousand light years (10^{21} cm) for spherical forms up to four or five thousand light years for very elongated nebulae which are usually accompanied by more or less opened spiral arms. (These arms often extend for more than forty thousand light years from the center.) It is usually accepted that different shapes of nebulae are due to rotation, and the spiral arms represent the material thrown out by centrifugal force from the equatorial plane. The study of nebular rotation permits estimation of their masses which come out of the order of 10^{9} sun masses.[1] The observed total luminosities average 10^{9} suns and the spectral class varies between *F*9 and *G*4 indicating an effective temperature slightly lower than that of the sun. From these data it can be definitely concluded that we must consider great nebulae as consisting of separate stars analogous to those of our own galaxy. In fact, if we would suppose that nebulae are continuous masses of gas emitting a continuous spectrum, then the luminosity of nebulae as

[1] E. Hubble, *The Realm of the Nebulae* (Yale University Press, 1936).

compared to that of the sun would be roughly proportional to the ratio of the surfaces. However, although the radii of nebulae are 10^{10} times larger than the sun's radius, their luminosities are not 10^{20} but only 10^{9} times larger, indicating that only 10^{-11} part of their surface is actually luminous. If, on the other hand, we suppose that nebulae consist of separate stars with average luminosity somewhat smaller than that of the sun, their masses and luminosities can be easily understood.

One of the most important discoveries concerning the nebulae is that they show a definite recession-effect, which is usually interpreted in terms of the expanding universe. The velocity of recession (v) increases proportionally to the distance and we can write

$$v = \alpha R, \tag{1}$$

where α has (at present) the numerical value 1.8×10^{-17} sec.$^{-1}$.

A random motion of nebulae is superimposed on this recession but is comparatively so small that it overbalances the recession of neighboring nebulae in only a few cases.

From the values of recession velocities it can be concluded that nebulae separated from each other about 1.8×10^{9} years ago, if we suppose that the relative velocity of two neighboring nebulae did not change since the time of separation (uniform expansion). Before that time, space must have been uniformly populated by stars, or by gas molecules, if we suppose that the formation of stars took place after the separation of nebulae.

II. Formation of Nebulae in an Expanding Space

We want to consider now the conditions under which the continuous distribution of matter will show the tendency to form separate nebulae. Let us consider space uniformly populated by particles (stars or molecules) moving with certain random velocities (V). The condition for the formation of condensation due to gravitational instability[2] can be written in the form

$$\frac{G\rho(4\pi R^3/3)}{R} \geqslant \frac{V^2}{2}, \tag{2}$$

where G is Newton's constant of gravitation, ρ is the density at the time in question, and R is the radius inside of which the condensation will take place. It is clear that condition (2) can always be satisfied if we choose R sufficiently large. Thus, if space was originally filled with a gas at any given temperature, the condensation of sufficiently large masses into stars was always taking place. The size of stars formed by such a process must be limited by the fact that the nuclear energy, liberated in central regions of too massive condensations, makes them unstable and leads to splitting up into smaller stars.

The situation, however, will be rather different if we accept that the distribution of matter in space is in the state of a permanent expansion as given by formula (1). In fact, under such conditions the effective velocity of particles at large distances will be mainly given by the expansion velocity, $v=\alpha R$. Substituting this velocity into Eq. (2) we obtain

$$\frac{G\rho(4\pi R^3/3)}{R} \geqslant \frac{\alpha^2 R^2}{2} \tag{3}$$

or

$$\rho \geqslant 3\alpha^2/8\pi G = \rho_0. \tag{4}$$

This formula[3] no longer contains the radius of the condensing region. It shows that in an expanding space the formation of gravitational condensations can take place only when the average density is above a certain critical density ρ_0. Substituting $\alpha=1.8\times10^{-17}$ sec.$^{-1}$ and $G=6.7\times10^{-8}$ cm^3 sec.$^{-2}$ g^{-1} we obtain $\rho_0=0.6\times10^{-27}$ g cm^{-3}. This density is much smaller than the present mean density in space. In fact according to astronomical estimates, the mean density of matter in space is of the order of magnitude 10^{-30} g/cm^{-3};[4] and we must conclude that, *under present conditions the formation of condensations in the universe on a great scale is impossible whatever the masses or velocities of particles may be.* Thus the great nebulae must have been formed before the average density of the universe reached a certain critical value ρ_0'.

[2] J. H. Jeans, *Astronomy and Cosmogony* (Cambridge University Press, 1928).

[3] A similar formula has been derived by G. Lemaître (National Academy of Science 20, 12 (1934)) but his interpretation of its role in the problems pertaining to the great nebulae is rather different from ours. In his work particular attention is paid to nebular clusters.

[4] The density may be much larger if a considerable amount of dark matter is present in the intranebular space. However, there is no direct experimental evidence of such matter.

It can also be shown that existing nebulae could not have been formed a long time before the critical value of density was attained. In fact, for accumulations formed due to gravitational instability at such early stage of expansion the velocity between two neighbors would not be large enough according to (3) to separate them entirely. Therefore separation becomes possible only if the random velocities of the newly formed condensations are larger than the expansion velocities. A system of nebulae receding from each other without a strong random motion can thus be formed only when the density is close to the critical value corresponding to the given stage of expansion.

In order to find when in the past development of the universe the condition for the formation of nebulae was satisfied, we must make a definite hypothesis concerning the rate of expansion during this time. We shall accept here that *the expansion is uniform in time;* i.e., *that the relative velocity of two nebulae always remains constant.* According to (1) this means that the value of α is inversely proportional to the "dimensions" of the expanding universe. If we denote by l the length, the change of which characterizes the expansion, and denote by primed symbols the quantities corresponding to a certain passed time, we may write

$$\alpha' = \alpha l/l'; \tag{5}$$

similarly

$$\rho' = \rho(l/l')^3. \tag{6}$$

Now we can write our condition for the formation of nebulae in the form

$$\left(\frac{l}{l'}\right)^3 \rho = \frac{3}{8\pi}\frac{\alpha^2}{G}\left(\frac{l}{l'}\right)^2 \tag{7}$$

or

$$\frac{l}{l'} = \frac{3}{8\pi}\frac{\alpha^2}{G\rho} = \frac{\rho_0}{\rho}. \tag{7'}$$

Substituting numerical values for ρ and ρ_0 we find $l/l' \sim 600$, i.e., formation of nebulae took place when all linear dimensions were six hundred times smaller than at present. Since after separation the nebulae should have kept roughly their original dimensions,[5] the size of nebulae should be about six hundred times smaller than present internebular distances. This is in agreement with observation.

We proceed now to calculate the velocity of particles at the moment of formation of nebulae necessary to secure the observed dimensions of nebulae. This can be estimated from the relation:

$$V = \alpha' R = \alpha(l/l')R. \tag{8}$$

If R (the radius of a nebula) is assumed to be

$$\frac{1}{2} \times \frac{1}{600} \times 1.7 \times 10^6 ly = 1.4 \times 10^3 ly,$$

$$V = 1.8 \times 10^{-17} \times 600 \times 1.3 \times 10^{21} = 100 \text{ km/sec.} \tag{8'}$$

This velocity is common in the world of stars.[6] On the other hand if we assumed that the particles participating in the formation of nebulae were gas molecules, the temperature of the gas must have been around one million degrees. At such temperatures and and at densities corresponding to the present mean densities in nebulae the mass of the radiation would be more than 10^9 times that of matter. Therefore we conclude that *most of the stars have been formed before the separation of nebulae* though, of course, further formation might continue in separate nebulae even at present.

III. Cosmological Consequences

As we have seen in the previous section, our theory of nebular formation requires that the velocity of expansion remain nearly constant while the distances between nebulae increase by a factor 600. According to the general relativistic theory of the expanding universe,[7] the factor representing the time dependence of linear dimension, usually denoted by $e^{\frac{1}{2}\varphi(t)}$, is given by the equation:

$$\frac{d}{dt}e^{\frac{1}{2}\varphi(t)} = \pm\left(\frac{8\pi G}{3}\rho e^{\varphi(t)} - \frac{c^2}{\mathfrak{R}^2}\right)^{\frac{1}{2}}, \tag{9}$$

[5] Because at the time of separation they were in dynamical equilibrium and the loss of energy through various processes is relatively small.

[6] Actually observed stellar velocities in our galaxy are grouped around 30 km/sec. However, we should not forget that stars near our sun are located rather eccentrically relative to the center of galaxy and might therefore possess smaller velocities. The second reason for the present velocities of stars to be smaller than at the time of the formation of nebulae is that during its life a nebula might lose rapidly moving stars. The average velocity is thus reduced.

[7] R. C. Tolman, *Relativity, Thermodynamics and Cosmology* (Oxford, Clarendon Press, 1934).

where the cosmological constant Λ is taken to be zero.

If we use for the present mean density $\rho = 10^{-30}$ g cm^{-3} and for the present expansion velocity $\alpha = (d/dt) \log e^{\frac{1}{3}\sigma(t)} = 1.8 \times 10^{-17}$ sec.$^{-1}$, Eq. (9) is inconsistent with the real value of $\mathfrak{R}$ (closed space) and also with $\mathfrak{R} = \infty$. The only remaining possibility is to assume an imaginary value of $\mathfrak{R}$. This gives for sufficiently late stages of expansion a constant expansion velocity, i.e., an infinite infinitely expanding space. For sufficiently early stages of expansion the Eq. (9) approaches the condition (4), and small density fluctuations in these early stages could have given rise to the condensations discussed above. Thus *in order to understand the formation of great nebulae and to satisfy the condition of continuity at the moment of their separation, it is necessary to accept the hypothesis that space is infinite and ever expanding.*

The only way to estimate the type of the curvature of our universe from direct observations is, at present, the method of Hubble and Tolman[8] based on the changes of observed density distribution of nebulae at great distances. Their analysis indicates that the apparent density of nebular distribution increases with increasing distance, which brings them to the conclusion that our universe has positive curvature and is closed in itself. However, we must notice that these conclusions are based on the hypothesis that the absolute luminosities of nebulae, which they use for the estimate of distances, do not change with the age of the nebulae. *If, however, we suppose that the absolute luminosities of very distant nebulae are slightly higher, because we see them at an earlier stage of evolution, the observational material no longer contradicts the assumption of an opened hyperbolic space.* At the present stage of our knowledge it is, of course, difficult to predict the expected changes of nebulae with their age, but since we deal with a period comparable to the total age of nebulae small changes are quite plausible. For example a decrease of luminosity might be accounted for by the above-mentioned possibility that the nebulae are permanently losing stars possessing too large velocities to be kept back by the gravitational attraction of the nebula.

We consider it our pleasant duty to express thanks to Mr. C. G. H. Tompkins for having suggested the topic of this paper and to H. A. Bethe for valuable discussions.

[8] E. Hubble and R. C. Tolman, Astrophys. J. **82**, 302 (1935).

APRIL 1, 1939 PHYSICAL REVIEW VOLUME 55

Perpendicular Vibrations of the Ammonia Molecule

E. F. Barker
University of Michigan, Ann Arbor, Michigan

(Received January 5, 1939)

The vibration frequency ν_2 of NH_3 is identified by means of the combination bands $\nu_2 \pm \nu_3$ at 2.2μ and 4.0μ, in each of which the spacing between component bands is about 16 cm^{-1}. From the difference band the numerical value of ν_2 is fixed at 3415 cm^{-1}. The fundamental band may be recognized in the weak and complex background of the absorption at 3μ. The coefficient ζ_3 of the vibrational angular momentum is approximately +0.6.

The second perpendicular fundamental band at 6μ is partially resolved, and is in good agreement with the expected pattern if ζ_4 equals −0.3. The indicated value of ν_4 is 1628 cm^{-1}. The numerical values of ζ_3 and ζ_4 do not agree well with those predicted theoretically.

The parallel component of $2\nu_4$ is found at 3220 cm^{-1}, and two pairs of parallel combination bands, $\nu_1 + \nu_3$ at 4270 and 4303 cm^{-1} and $2\nu_4 + \nu_3$ at 4177 and 4217 cm^{-1}.

THE four atoms in the ammonia molecule, as is well known, form a pyramid with axial symmetry, and must have four different fundamental vibration frequencies. All four should be active both in infra-red and in Raman spectra. Two of these, represented by the bands at 3μ and at 10μ, involve oscillations parallel to the axis of symmetry and are readily identified. Each gives rise to a double band with P, Q and R branches, the levels occur in pairs because of the two potential minima defining alternative equilibrium positions for the nitrogen atom. A third

band, found at 6μ, must be associated with vibrations normal to the axis, and its structure, as described below, is in accord with this view. Regarding the position of the fourth fundamental there has been considerable difference of opinion,[1, 2] and until now the experimental evidence has not been conclusive. Unpublished observations by Stinchcomb and Barker in 1929 seemed definitely to exclude as a possibility the strong band at 2.2μ because of its complexity and the relative intensities of its component lines.

Raman observations upon gaseous ammonia contribute very little to this question, since scattering due to perpendicular vibrations has not been detected. The measurements of Lewis and Houston[3] showed two lines in the neighborhood of 3μ, of which the one displaced by 3334 cm^{-1} is the parallel frequency ν_1, indicated by infra-red measurements at 3337 cm^{-1}. These authors suggested that the second line, displaced by 3219 cm^{-1}, might represent the perpendicular band ν_3. This clearly is not the case however, as the infra-red measurements show, and the line 3219 cm^{-1} must be the parallel component of the harmonic of ν_4 (1628 cm^{-1}), probably intensified somewhat by resonance interaction with ν_1. The Raman spectrum of liquid ammonia shows three neighboring frequencies, 3216, 3304 and 3380, corresponding exactly to the lines appearing in the liquid methyl halides[4] where interaction of the type mentioned has been well established. In every case the highest of the three frequencies, observed only in the liquid, corresponds to a perpendicular vibration.

The similarity between NH_3 and CH_3 follows also from a mechanical treatment of the problem of vibration. Utilizing forces of the valence type, Howard[5] has obtained a potential function involving two constants, which may be so chosen as to yield the frequencies of ν_1 (3334) and ν_4 (1626). The other two frequencies, which may then be predicted approximately, are $\nu_2=3370$ and $\nu_3=1050$. The observed value for the latter is about 950. Since 3370 is not far from the value suggested by Raman observations on liquid NH_3, it may be considered as a fair approximation. Three important factors were neglected in the computation, however, and it is difficult to estimate how much they may affect the result. They are anharmonicity, resonance interaction, and the double minimum.

A convincing argument supporting this approximate value of ν_3 has recently been provided by measurements upon ND_3,[6] where all four of the fundamentals may be observed. If the three above-mentioned conditions are neglected, a

[1] Cl. Schaefer and F. Matossi, *Das Ultrarote Spektrum* (Berlin, Julius Springer, 1930), p. 250.
[2] H. Verleger, Physik. Zeits. **38**, 83 (1937).
[3] C. M. Lewis and W. V. Houston, Phys. Rev. **44**, 903 (1933).
[4] A. Adel and E. F. Barker, J. Chem. Phys. **2**, 627 (1934).
[5] J. B. Howard, J. Chem. Phys. **3**, 207 (1935).
[6] M. V. Migeotte and E. F. Barker, Phys. Rev. **50**, 418 (1936).

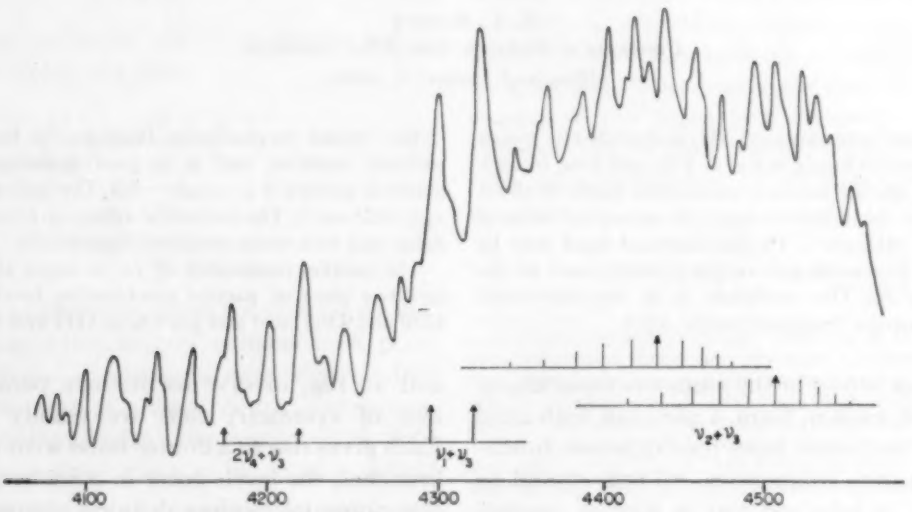

FIG. 1. The band at 2.2μ.

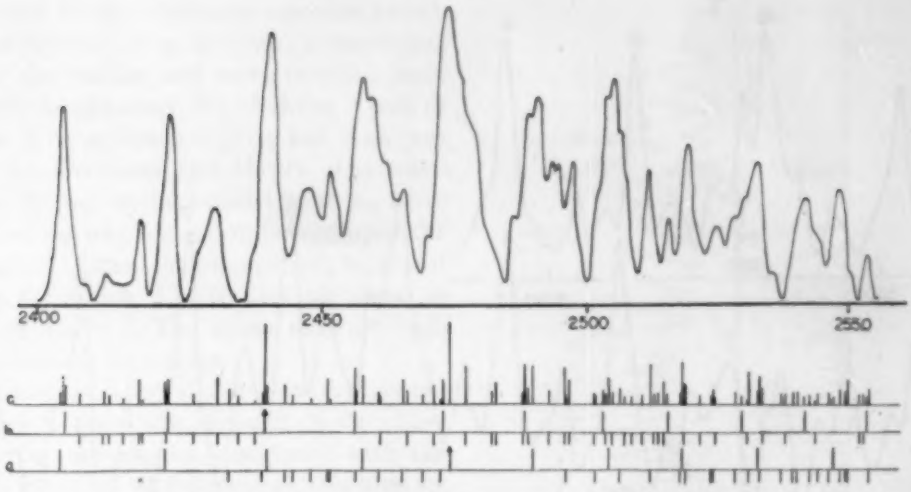

FIG. 2. The difference bands $\nu_2-\nu_3$. a and b represent the high and low frequency components, respectively. c represents the combination, with intensities roughly indicated. For $\Delta J=0$ marks extend upward, for $\Delta J=\pm 1$ downward.

simple numerical relation may be obtained between the values of ν_2 and ν_4 for NH_3 and for ND_3. This yields for ν_2 (NH_3), when the other three known frequencies are introduced, a value of approximately 3400. The evidence is strong, therefore, that in NH_3 the frequencies ν_1 and ν_2 are close together, and that, since the latter has not been positively identified in the infra-red, it must be represented by a band of relatively small intensity. Hence the strong band at 2.2μ may be interpreted as a superposition of $\nu_1+\nu_3$, $\nu_2+\nu_3$ and $2\nu_4+\nu_3$. A superficial examination at once indicates that the first of these cannot provide the major part of the absorption. Apparently, therefore, ν_2 combines strongly with ν_3.

THE COMBINATION BANDS $\nu_1+\nu_3$ AND $\nu_2\pm\nu_3$

The 2.2μ band has been re-examined with results quite in accord with earlier (unpublished) measurements. The absorption due to 25 cm of gas at 60 cm pressure, as observed with a grating having 4800 lines per inch, is indicated in Fig. 1. The slit includes 4 cm^{-1}, and the resolution is far from complete. Certain features may be recognized, however. At 4294 and 4319 cm^{-1} a pair of zero branches appear which must correspond to $\nu_1+\nu_3$. The positions would be $3337+933=4270$ and $3337+966=4303$ if interaction is neglected. The change in character of the motion reduces the separation of the two ν_3 levels, as might be expected, from 33 cm^{-1} to 25 cm^{-1}, and the value of x_{13} is negative. A second pair of maxima at 4177 and 4217 cm^{-1} ($\Delta\nu=40$) may be the zero branches of the parallel type component of $2\nu_4+\nu_3$. The main portion of the band consists of a number of lines at intervals of approximately 16 cm^{-1} which form two distinct groups, the maxima of which occur at 4434 and 4506. These apparently constitute the bands $\nu_2+\nu_3$, but do not yield precise values of ν_2 since x_{23} is unknown. The very wide separation, $\Delta\nu=72$ indicates either an amplitude of vibration of the N atom parallel to the symmetry axis

TABLE I. *Lines assigned to the transitions $\Delta J=0$ in the bands $\nu_2-\nu_3$, ν_2 and $\nu_2+\nu_3$.*

2441 band ν	$\Delta\nu$	2473 band ν	$\Delta\nu$	3407 band ν	$\Delta\nu$	4470 band ν	$\Delta\nu$
2404.0		2405		3352		4360	
	17.0		17		21		24
2423.0		2422.0		3373		4384	
	17.2		18		16		16
2440.8		2440.0		3389		4400	
	16.9		17		18		16
2457.7		2457.0		3407		4416	
	15.6		16.3		16		18
2473.3		2473.3		3423		4434	
	14.9		16.4		16		18
2488.2		2489.7		3439		4452	
	14.7		14.5		15		24
2502.9		2504.2		3454		4476	
	13.7		14.8				17
2516.6		2519.0				4493	
	13.4		13.0				13
2529.0		2532.0				4506	
	11.1		15.0				15
2540.1		2547				4521	

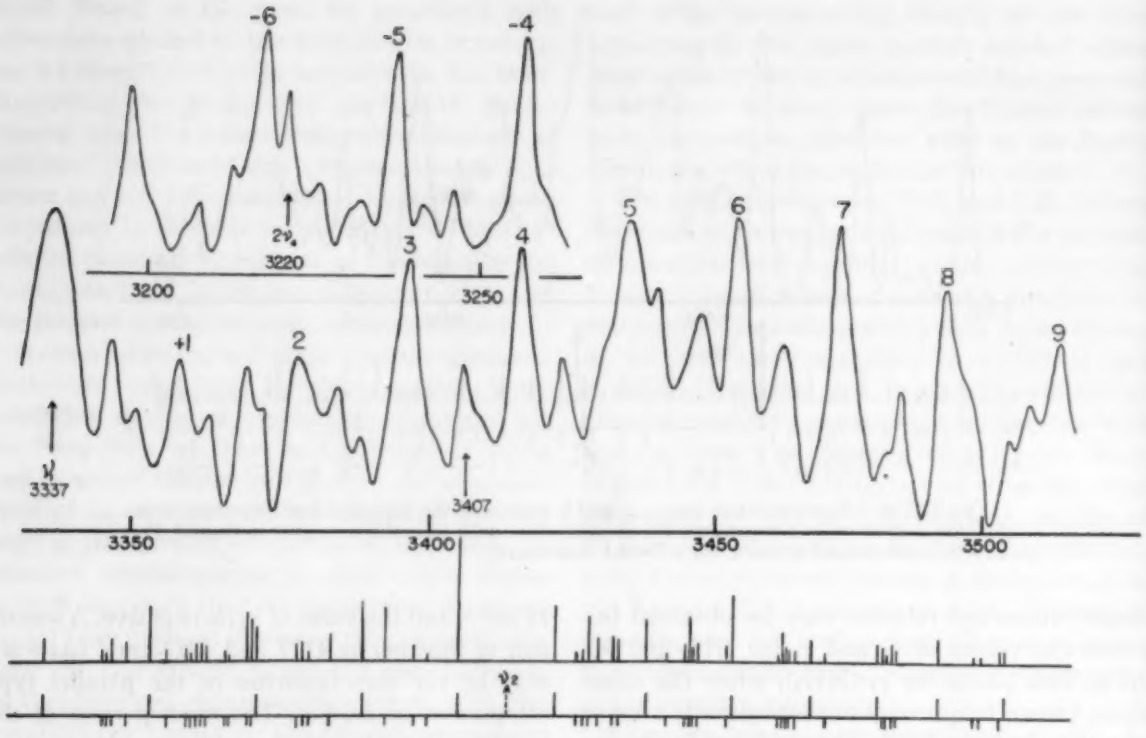

FIG. 3. A part of the 3μ band, including ν_1 and ν_3.

which is greater than for ν_3 alone, or a decrease in the hump separating the two potential minima, or both.

This pair of bands consists of two sets of zero branches forming the prominent maxima, each of which is the center of a component sub-band. These are indicated diagrammatically in Fig. 1 underneath the curve. While some convergence is apparent, a numerical evaluation of the coefficients for the quadratic terms is hardly justifiable. The observed positions of the lines appear in Table I, column 7.

The difference band, $\nu_2-\nu_3$, appears at 4μ. To observe it a four-meter cell was used, filled by displacement to a concentration of about 50 percent NH_3. It had mica windows. The resulting absorption is presented in Fig. 2. Again the lines show intervals of about 16 cm^{-1}, but now the separation between the two component bands is exactly the ν_3 interval, i.e., 33 cm^{-1}, since in the ν_2 levels the spacing does not differ much from that of the ground state. The central maxima lie at 2440.8 and 2473.3 cm^{-1}, which indicates that the corresponding line for ν_2 occurs at 3407 cm^{-1}.

In diagram a of Fig. 2, the lines drawn upward represent the transitions $\Delta J=0$, and those drawn downward represent $\Delta J=\pm 1$, for the band of higher frequency. Diagram b of Fig. 2 represents the lower frequency band, and the two are combined in c, where the lengths of the line segments indicate approximately the expected intensities. Because of the strong CO_2 band near 4.3μ it is not possible to extend the measurements to lower frequencies with an open spectrometer. The line at 2404 cm^{-1} is more intense than might have been expected. At exactly this position, however, one component of the difference band $\nu_1-\nu_3$ should appear $(3337-933=2404)$. The positions of the lines $\Delta J=0$ are indicated in Table I, columns 1 and 3. In these measurements the slit included 1.5 wave numbers.

THE FUNDAMENTAL ν_2

In the earliest observations upon the 3μ band of NH_3 a lack of symmetry was noted. The high frequency side not only has a greater intensity, but also includes many lines not assignable to ν_1. This is also clear in the measurements by

Dennison and Hardy.[7] Without a precise knowledge of the position of ν_2, however, a convincing analysis of the weaker and more complex band could hardly be obtained. Fig. 3 shows a part of this region at a resolution slightly less than that employed by Dennison and Hardy. The numbered lines belong to the parallel band ν_1, while the predicted pattern for ν_2 is indicated upon the lower diagram. Lines drawn upward represent transitions for which $\Delta J=0$, and are given in column 5 of Table I. The upper diagram indicates approximate intensities.

The frequency interval between component bands depends upon the amount $\zeta h/2\pi$ of internal angular momentum associated with the degenerate vibration. If ζ were zero, this interval would be $(1/C-1/A)h/4\pi^2$, or approximately 8 cm^{-1}. In order to explain the displacements of approximately 16 cm^{-1} between component bands it is necessary to assign to ζ_2 the value $+0.6$, while that predicted by Johnston and Dennison[8] is -0.004. The vibration frequency itself has a value higher than that corresponding to the most intense zero branch by one-half interval, i.e., $\nu_2=3415$ cm^{-1}.

The low frequency side of this 3μ band is also complicated by the harmonic of ν_4, consisting of a parallel and a perpendicular component. A strong maximum at 3220 cm^{-1}, near the line -6, probably indicates the center of the parallel band, in agreement with the Raman observations already mentioned.

The Fundamental ν_4

The most intense absorption in the ammonia spectrum occurs in the region of 6μ. When examined at moderate dispersion it has the appearance of a parallel band with an intense central maximum.[9] Higher resolution shows, however, that this is not a typical zero branch, but consists rather of a group of strong lines at intervals of four or five wave numbers, with intensities decreasing rapidly in both directions from the center. This is exactly the situation predicted by Dennison for the perpendicular

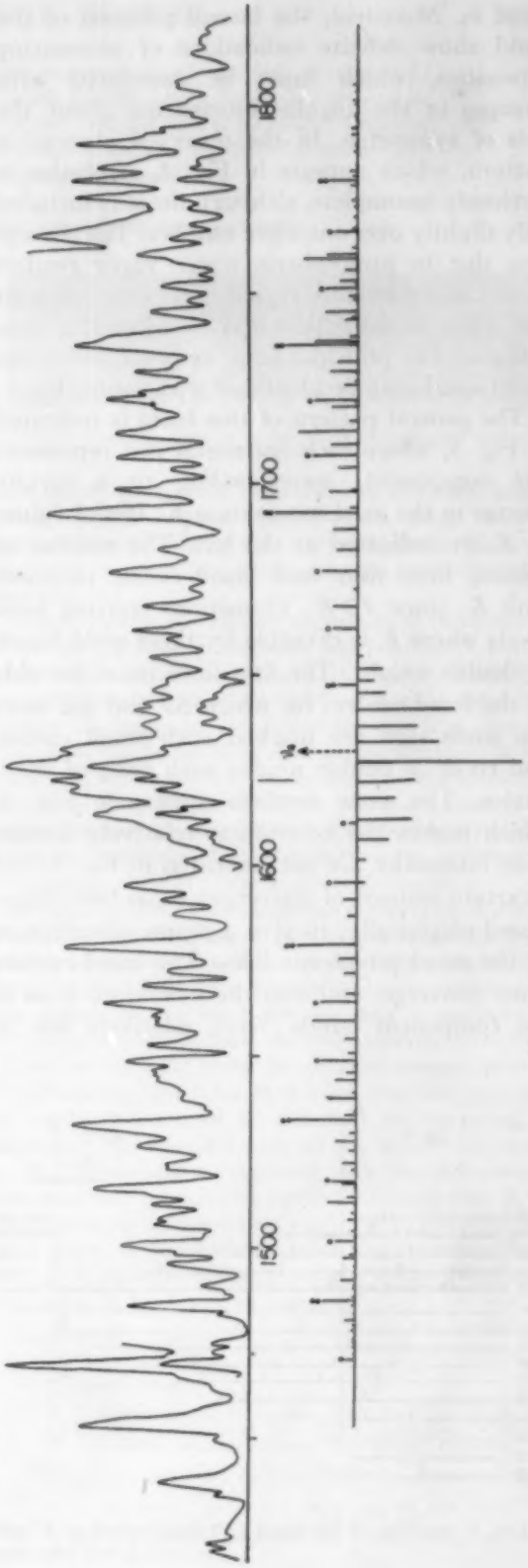

FIG. 4. The band ν_4 at 6μ, as observed and as predicted.

[7] D. M. Dennison and J. D. Hardy, Phys. Rev. **39**, 938 (1932).
[8] M. Johnston and D. M. Dennison, Phys. Rev. **48**, 868 (1935).
[9] R. Robertson and J. J. Fox, Proc. Roy. Soc. **A120**, 161 (1928).

band ν_4. Moreover, the lateral portions of the band show definite indications of alternating intensities, which must be associated with changes in the angular momentum about the axis of symmetry. In the observed absorption pattern, which appears in Fig. 4, resolution is obviously incomplete, although the slits included only slightly over one wave number. The absorption due to atmospheric water vapor renders observations in this region somewhat difficult and a few minor details may be subject to later revision. The principal lines, however, stand out clearly and may be identified with confidence.

The general pattern of this band is indicated in Fig. 5, where each horizontal row represents one component, corresponding to a certain change in the axial momentum K. Initial values of K are indicated at the left. The number of missing lines near each band center increases with K, since $J \geqslant K$. Transitions starting from levels where K is divisible by three yield bands of double weight. The first lines on either side of the band centers for which ΔJ and ΔK have the same sign are marked with small circles, and those of double weight with pairs of small circles. The same symbols appear in Fig. 4, which makes the correlation relatively simple. Line intensities are not indicated in Fig. 5, but a certain amount of convergence has been introduced empirically, to give a proper distribution of the more prominent lines. The band centers must converge, and also the individual lines in the component bands. Since relatively few of these lines can be identified with certainty, and the positions of the various zero branches are not fixed with great precision, no attempt has been made to evaluate the quadratic coefficients. The wave numbers for some of the lines are listed in Table II. Since the most intense zero branch occurs at 1626 cm^{-1}, one-half space from the band center, the value of ν_4 is 1628 cm^{-1}. From the observed band spacing it follows that ζ_4 is approximately -0.3, instead of -0.17 as predicted.

TABLE II. *Wave numbers and assignments of lines in the band ν_4. Columns headed J and K indicate quantum numbers of the initial state; the appended sign designates + or − transitions.*

J	K	ν	J	K	ν
0_0	0+	1626.4	1+	1+	1661.7
2−	2−	1594.9	1+	0+	1667.4
2−	1−	1591.1	2+	2+	1676.6
2−	0+	1587.3	3+	3+	1691.8
3−	3−	1579.8	2+	3+	1698.7
6−	6−	1532.8	4+	4+	1707.0
7−	7−	1516.2	3+	4+	1713.3
8−	8−	1501.0	5+	5+	1722.2
9−	9−	1485.3	6+	6+	1736.6
10−	10−	1470.0	7+	6+	1760.0
11−	11−	1454.0	9+	9+	1779.5

The experimental values of ζ_2 and ζ_4 are not only very different from those theoretically expected; they are also inconsistent with the prediction requiring their sum to equal $(C/2A)-1$. This suggests that some revision is necessary, either in the interpretation of the data, or in the mechanical treatment of the interaction between vibration and rotation.

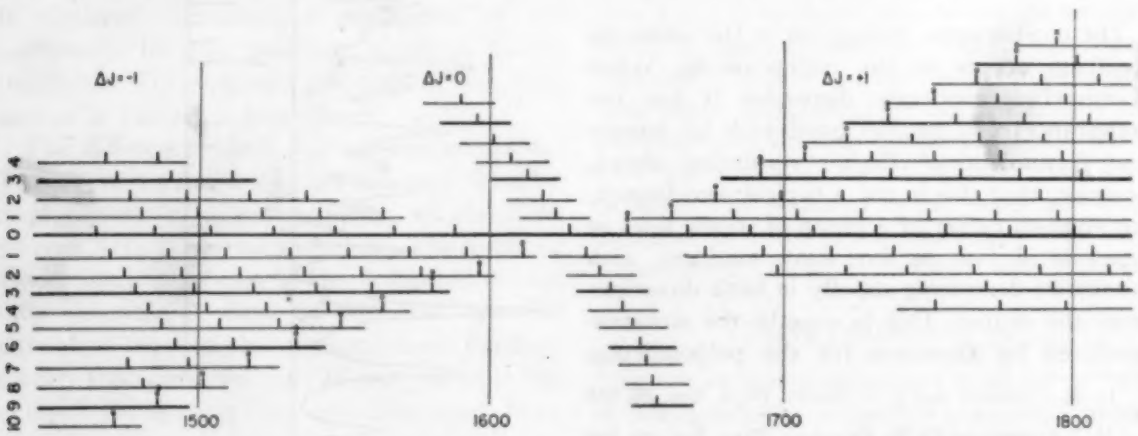

FIG. 5. Analysis of the band ν_4. Initial values of K indicated at the left. $\Delta K = +1$ for horizontal rows 0 and above. $\Delta K = -1$ for horizontal rows below 0.

LETTERS TO THE EDITOR

Prompt publication of brief reports of important discoveries in physics may be secured by addressing them to this department. Closing dates for this department are, for the first issue of the month, the eighteenth of the preceding month, for the second issue, the third of the month. Because of the late closing dates for the section no proof can be shown to authors. The Board of Editors does not hold itself responsible for the opinions expressed by the correspondents.

Communications should not in general exceed 600 words in length.

Spark Discharge on Surfaces

It has been shown by a number of different workers,[1] by means of a rotating lens or film camera, that the initiation of a lightning flash consists of two principal stages. First, a so-called leader which usually, although not always, starts from the cloud and progresses toward the earth with a velocity between 10^7 and 5×10^9 cm/sec. This leader is relatively faint and normally on the first flash shows on the photographs as "stepped." Second, following the arrival of the leader at the earth, a very intense "return stroke" occurs which moves in the opposite direction to the leader but over the same path at a much higher velocity. The same type of phenomenon has been shown to occur in both long[2] and short sparks,[3] in air as well as in the discharge tube.[4] In the latter two cases the leader may or may not be stepped, depending upon the characteristics of the electrical circuit. The purpose of this note is to report observations with the rotating mirror of the same kind of phenomenon in the spark discharge on surfaces. In order to obtain sufficient luminosity in the leader stroke, the usual method for the production of surface discharges was modified. A wash tub 2½ feet in diameter was half-filled with a dilute solution of $CuSO_4$ in water. A ¼" brass rod about one foot long was then mounted horizontally just below (3–6 mm) the surface of the liquid along the diameter of the tub. One end of this rod was near the axis of the tub and the other was connected to the grounded terminal of the circuit. The discharge occurred along the surface of the water solution above this rod. The high voltage electrode was a small metal rod mounted with its axis vertical and its lower end about a millimeter above the water surface, and directly above the end of the horizontal rod which was nearest the axis of the tub. A third electrode, connected to the tub, was mounted vertically with its lower end just touching the water so that it could be moved along directly over the horizontal rod. When voltages of 10 kv were applied impulsively from a one-mf condenser, surface discharges 25 cm in length were obtained. If either the capacity or voltage was increased, the maximum length of the surface discharge was increased. If the distance between the two vertical rods was made greater than the maximum length of the spark, only the leader discharge occurred.

FIG. 1. Leader stroke with branches. Stationary camera.

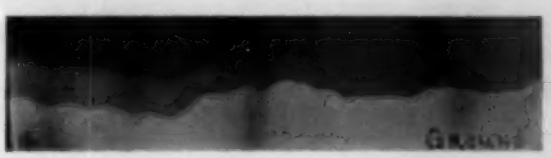

FIG. 2. Discharge along the water surface photographed with a revolving mirror.

Figure 1 shows a stationary photograph of these leaders when the high voltage electrode was positive. It will be observed that the main path of the leader follows the surface directly above the horizontal grounded wire. Clearly the reason for this is that the field is greatest at the tip of the leader along this direction because if the horizontal rod is removed, various leaders move in random directions along the surface. Also, branching takes place in the direction of propagation. A statistical study of this branching indicates that the number of branches is roughly proportional to the length of the leader.

Figure 2 shows a rotating mirror photograph of a non-oscillatory discharge along the surface when the high voltage electrode was positive. It will be observed that a leader starts at the high voltage electrode, moves along the surface of the water solution until it reaches the vertical grounded electrode. An intense return stroke then occurs. In Fig. 2 the leader travels at an average speed of 5×10^6 cm/sec., but it has been found that this speed can be markedly increased or decreased by increasing or decreasing the current supply to the leader. The same general phenomena are observed with the high voltage electrode either positive or negative, although they differ considerably in certain details which will be described in a later paper. If the horizontal rod was removed and a drop of oil placed on the liquid surface, the leader followed the outline of the water, oil interface.

Rouss Physical Laboratory,
University of Virginia,
Charlottesville, Virginia,
March 3, 1939.

L. B. SNODDY
J. W. BEAMS

[1] B. F. J. Schonland and H. Collens, Proc. Roy. Soc. **A143**, 654 (1934); **A152**, 595 (1935); **A164**, 132 (1938); McEachron, J. Frank. Inst. **227**, 149 (1939); Workman, Beams and Snoddy, Physics **7**, 375 (1936).

[2] T. E. Allibone and J. M. Meek Proc. Roy. Soc. **A166**, 97 (1938); **A169**, 246 (1938).

[3] L. B. Snoddy and C. D. Bradley, Phys. Rev. **45**, 432 (1934); **47**, 541 (1935); H. Raether, Zeits. f. Physik **107**, 91 (1937).

[4] J. W. Beams, Phys. Rev. **36**, 997 (1930); Snoddy, Beams and Deitrich, Phys. Rev. **50**, 469 (1936).

The Delayed Neutron Emission which Accompanies Fission of Uranium and Thorium

In our previous letter[1] we suggested that the delayed neutrons produced by neutron bombardment of uranium might originate either in direct neutron emission (by one of the disintegration products), or in a photodisintegration process. Further evidence has now been obtained which indicates that direct neutron emission is responsible for the delayed neutrons which we observed.

All elements except uranium, carbon, and hydrogen (in paraffin) were eliminated as a source of the delayed neutrons by changing the neutron detector from a boron-lined brass chamber to one of aluminum lined with lithium. The detecting apparatus was located at a distance from the bombarding position at the high voltage target. Furthermore, cloud-chamber photographs of hydrogen recoils from the delayed neutrons showed no appreciable diminution in the number of recoils when one inch of lead was interposed between the chamber and the activated uranium, although the gamma-ray intensity was greatly decreased. The remaining possibility of photodisintegration in the uranium itself was eliminated by surrounding a small amount of the activated uranium with a large quantity of normal uranium. No observable increase in the number of delayed neutrons was produced by the additional uranium.

In comparing the periods of the delayed neutrons and gamma-rays from uranium several longer periods were observed for the gamma-rays but not for the neutrons. The complexity of the gamma-ray decay makes it difficult to determine any of the periods accurately, but there seems to be evidence for at least three periods considerably longer than the short period previously reported.

It was found that the delayed neutrons and all the gamma-ray periods were produced by both thermal and high energy neutrons but not by the medium energy neutrons from carbon. These conditions are the same as for the uranium fission process.

The cross section for the production of delayed neutrons by lithium-neutron bombardment of uranium (high energy neutrons) was measured by comparing the number of delayed neutrons with the number observed from a calibrated radon-beryllium source. By neglecting the asymmetry of the lithium-neutron source and using the yield curves of Amaldi, Hafstad, and Tuve,[2] the cross section was found to be about 4×10^{-26} cm^2 which is roughly one-half the reported cross section for fission when fast radon-beryllium neutrons are used.[3] This large cross section is further evidence that the 15-sec. gamma-rays cannot be the cause of the neutrons.

Cloud-chamber observations of the recoils from the delayed neutrons indicated that their energy is less than one million electron volts and probably near one-half million electron volts.

Delayed neutrons were also observed from thorium nitrate which had been activated by fast lithium neutrons. The intensity was roughly one-fourth of that observed from uranium. The period seemed to be roughly the same as that of the delayed neutrons from uranium.

We are greatly indebted to Professor J. R. Dunning for the radon-beryllium neutron source used in the cross section determination, and to Dr. F. Kracek for the loan of material which made the measurements on thorium possible.

R. B. Roberts
L. R. Hafstad
R. C. Meyer
P. Wang

Department of Terrestrial Magnetism,
Carnegie Institution of Washington,
Washington, D. C.,
March 10, 1939.

[1] R. B. Roberts, R. C. Meyer, P. Wang, Phys. Rev. **55**, 510 (1939).
[2] E. Amaldi, L. R. Hafstad, and M. A. Tuve, Phys. Rev. **51**, 896–912 (1937).
[3] H. L. Anderson and others, Phys. Rev. **55**, 511–512 (1939).

The Determination of Force Fields from Scattering in the Classical Theory

Although mutual scattering of nuclei provides one of the most important sources of information on nuclear force fields, no systematic method has so far been developed for the determination of these fields from the observed angular distributions. In a recent conversation Dr. O. Klein suggested to me that a method devised by him[1] for the determination of the potential curves of diatomic molecules from their band spectra might be useful in this connection. A slightly modified form of this method proves, indeed, to be applicable to the scattering problem, but only insofar as the results are interpreted according to classical mechanics. In spite of this serious limitation, a brief account of the method should be of interest.

For scattering by a fixed force center with potential function $V(r)$, the effective potential U for the radial motion of particles with angular momentum L and mass m is $U=V(r)+L^2/2mr^2$, where r is distance from the force center. The angular deflection θ of such particles is determined by their energy E, and for present purposes is most conveniently measured by the "deflection parameter" $\rho=\pi/2-\theta/2$. It is readily shown that ρ can be expressed in the form

$$\rho(E)=-[L/(2m)^{\frac{1}{2}}]\int_{\infty}^{r_0} dr/r^2(E-U)^{\frac{1}{2}},$$

where r_0 is the distance of closest approach, for which $E=U$. If the equation of the potential function be taken in the form $f(U)=1/r$ so that $dr/r^2=-f'(U)dU$, the above relation may be written

$$\rho(E)=\frac{L}{(2m)^{\frac{1}{2}}}\int_0^E \frac{f'(U)dU}{(E-U)^{\frac{1}{2}}}.$$

This functional equation connecting $\rho(E)$ and $f(U)$ is of the Abelian type encountered by Klein and can be solved for $f(U)$ to give the equation of the potential curve in the form

$$\frac{1}{r}=f(U)=\frac{(2m)^{\frac{1}{2}}}{\pi L}\int_0^U \frac{\rho(E)dE}{(U-E)^{\frac{1}{2}}}.$$

The function $\rho(E)$ (angular deflection as a function of the energy for a fixed angular momentum) can, in principle, be determined from the scattering data in the follow-

ing way. From elementary mechanical considerations it can be shown that $\sigma(\theta)\sin\theta=(1/4mE)(d/d\theta)L^2$ where σ is the scattering cross section per unit solid angle. Integration gives

$$L^2=4mE\int_0^{\pi-2\rho}\sigma(\alpha)\sin\alpha d\alpha,$$

which establishes a functional relation between ρ, E and L from the angular distribution curves at different energies. From it the function $\rho(E)$ (for constant L) can be deduced, and the field can then be obtained by a graphical integration. The classical problem of determining the force field from the scattering data can thus be regarded as solved in principle.

It is obvious that such a classical method can give no information on the internal "potential wells" that are assumed for nuclear scattering. Attention has been called to it in the hope that a similar method may be devised which is valid in quantum mechanics to within the limits of the WKB method.

F. C. Hoyt

Ryerson Physical Laboratory,
University of Chicago,
Chicago, Illinois,
March 15, 1939.

[1] O. Klein, Zeits. f. Physik **76**, 226 (1932).

Electric Quadrupole Moment of the Deuteron

Kellogg, Rabi, Ramsey, and Zacharias[1] have pointed out that their observations on the magnetic moments of H_2, D_2 and HD molecules can be accounted for if the deuteron is assumed to have an electric quadrupole moment of magnitude

$$Q=(3z^2-r^2)_{Av}\sim 2\times10^{-27}\ \text{cm}^2.$$

If this interpretation is correct, the interaction between the proton and the neutron must contain, besides the usual Majorana and Heisenberg forces, a force which mixes some D state wave function with that of the normal S state of the deuteron. Neither the Thomas precession, which gives no mixing of S with higher states, nor the interaction between the magnetic moments of neutron and proton, which gives much too small a mixing, can account for the observed quadrupole moment. However, a spin-orbit interaction of the form

$$J(r)(\boldsymbol{\sigma}_p\cdot\mathbf{r}_1)(\boldsymbol{\sigma}_n\cdot\mathbf{r}_1), \qquad (1)$$

where $\boldsymbol{\sigma}_p$, $\boldsymbol{\sigma}_n$ are the spins of proton and neutron, respectively, $\mathbf{r}_1$ is a unit vector along their relative coordinate, and $J(r)$ is the radial dependence of the interaction, similar to that which arises in the first-order terms of the Yukawa[2] mesotron theory of nuclear forces, gives a quadrupole moment of the observed magnitude if the strength of this force is assumed to be about equal to that of the Majorana force.

Since the quadrupole moment is small compared to the area of the deuteron, the change in the wave function by this interaction must be small and the use of perturbation theory for the calculation is justified. The usual interaction between the proton and the neutron was taken as a rectangular potential hole of depth D and width a, and $J(r)$ in (1), as a rectangular hole of the same width a but of depth K.[3] The integration over the positive energy of the D state of the deuteron had to be carried out numerically. By taking the binding energy of the deuteron as $\epsilon=2.15$ Mev, and the range of the nuclear forces as $a=2.2\times10^{-13}$ cm we find

$$Q=(3z^2-r^2)_{Av}=(K/D)\times1.9\times10^{-27}\ \text{cm}^2.$$

By taking the value of Q given by Rabi and his associates,[4] we obtain

$$K/D\sim1.$$

Thus the strength of the spin-orbit interaction must be about equal to that of the ordinary interaction.

A rough idea of the magnitude of the spin-orbit interaction and its dependence on a can be obtained by taking some suitably chosen average energy $\bar{E}$ for the D state in the denominator of the energy integral and then using the completeness relation for the wave functions. It gives

$$Q=(2/75)(K/D)(D/(\epsilon+\bar{E}))a^3/(a+\alpha),$$

where $\alpha=4.36\times10^{-13}$ cm is the "radius" of the deuteron. This estimate shows that K/D varies approximately as $1/a^3$ so that if a were taken to be 2.7×10^{-13} cm we would get $K/D\sim\frac{1}{2}$.

It is interesting to note that the ratio between the strength of the spin-orbit interaction, calculated in this way, and the strength of the Heisenberg force between the proton and neutron, determined from the position of the singlet S state of the deuteron, is in rough agreement with the same ratio derived from Yukawa's theory. The experiments quoted above, however, indicate that Q is positive, whereas the Q calculated from Yukawa's spin-orbit interaction (which is repulsive) is negative.

If it is true that there is a spin-orbit interaction of strength comparable with that of the ordinary interaction, then there is an important consequence that the total spin of the particles in a nuclear system will not be, even approximately, a constant of the motion. There can thus be no selection rules for spin.

We wish to thank Professor J. R. Oppenheimer for suggesting this problem and for much helpful advice, and Dr. L. I. Schiff for many illuminating discussions.

R. F. Christy
S. Kusaka

University of California,
Berkeley, California,
March 7, 1939.

[1] J. M. B. Kellogg, I. I. Rabi, N. F. Ramsey and J. R. Zacharias, Phys. Rev. **55**, 318L (1939).
[2] H. Yukawa, S. Sakata and M. Taketani, Proc. Phys. Math. Soc. Japan, **20**, 319 (1938). Such interactions have been considered by J. Schwinger, Phys. Rev. **55**, 235 (1939).
[3] This schematic form for K was chosen for convenience since divergences render questionable the form of the terms given by Yukawa's theory (reference 2).
[4] In this formula, s and r are coordinates of the proton in the reference frame with origin at the center of gravity of the deuteron; and, in using the value of the quadrupole moment given by Rabi and his associates, we assumed that their value is given in terms of these coordinates. If, on the contrary, their s and r are coordinates of the distance of the proton from the neutron, then the value of K/D given here should be divided by 4.

Internal Conversion Electrons from Br^{80}

Segrè, Halford and Seaborg[1] have recently reported that the 18 min. Br^{80} isomer is formed by the decay of the 4.4-hr. activity. They have concluded that the 4.4-hr. isomer has the greater energy. This is in agreement with the proton threshold measurements reported by Buck.[2] They also conclude that the 4.4-hr. radiation is probably composed entirely of low energy internal conversion electrons.

We have produced $Br^{78, 80, 82}$ by proton bombardment of thin selenium films mounted on 2.5μ Al foil. The negative electron spectra were examined in the region 13 kev to 150 kev with a β-ray spectrograph. We find two strong lines of electrons at 44±1 and 33.5±1 kev, respectively. These are accompanied by a third much weaker line at 21.5±2 kev. We have shown definitely that the 44 and 33.5 kev lines belong to the 4.4-hr. Br^{80} period. The 21.5 kev line belongs either to the 4.4-hr. Br^{80} or to the 33-hr. Br^{82} with a much greater probability in favor of its belonging to Br^{80}.

We exposed four plates to different relative intensities of the various activities of $Br^{78, 80, 82}$ as follows:

Exposure	Plate No.	1	2	3	4
6.3 min. Br^{78}		70	130	0	0
18 min. Br^{80}		330	1140	0	0
4.4 hr. Br^{80}		52	450	455	0
33 hr.		2.5	48	250	300

The exposure figures given refer to measurements of the total radiation emitted by each isotope as measured with a N_2-filled ionization chamber. Plates 2 and 3 are reproduced in Fig. 1 and microphotometer measurements of these plates are shown in Fig. 2. It should be noted that (1) Plates 2 and 3 were exposed to the same intensity of 4.4-hr. activity and show the 44 and 33.5 kev lines at the same intensity, (2) Plate 2 was exposed to only 20 percent as much Br^{82} radiation as was Plate 3, yet shows the 21.5 kev line equally strong. Plate 1 was blank. Plate 4 was exposed the most intensely of all the Plates to Br^{82} radiation, yet shows only a small and questionable maximum around 20 kev.

The 44 kev and 33.5 kev lines agree within the experimental error with the expected values for L and K conversion in bromine of a gamma-ray of about 45 kev. The 21.5 kev line is either the result of L conversion of a 23 kev gamma or K conversion of a 34 kev gamma-ray. Since the existence of this 21.5 kev line is important to the theory of isomers we shall complete its examination shortly.

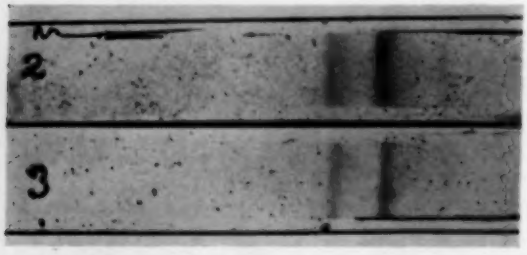

Fig. 1.

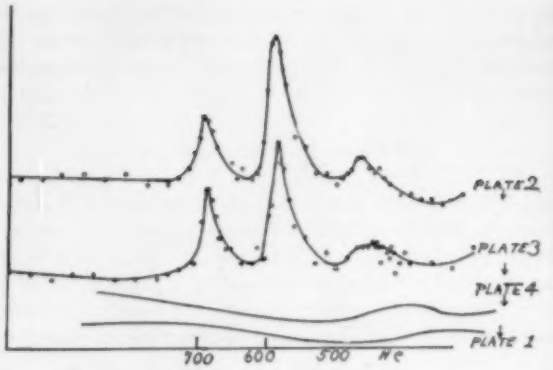

Fig. 2. Microphotometric measurements of the plates.

We wish to thank Professor L. A. DuBridge for suggesting this problem and to thank Dr. J. H. Buck for the selenium films.

G. E. Valley
R. L. McCreary

Physics Department,
University of Rochester,
Rochester, New York,
March 15, 1939.

[1] E. Segrè, R. S. Halford, and G. T. Seaborg, Phys. Rev. **55**, 321 (1939).
[2] J. H. Buck, Phys. Rev. **54**, 1025 (1938).

On the Nuclear Magnetic Moment of Beryllium*

The molecular-beam magnetic-resonance method, discussed in the preceding issue of the *Physical Review*,[1] measures g, the ratio of the magnetic moment to the angular momentum of a nucleus. For the nuclei therein reported the spins are known, and the magnetic moments were obtained directly from the product of the spins and the measured g values. Elsewhere in this issue a method of measuring the sign of the nuclear moment is described.[2] We have applied these methods to the study of the gyromagnetic properties of the beryllium nucleus, $_4Be^9$.

The molecules used in our experiments were sodium beryllium fluoride ($NaF \cdot BeF_2$) and potassium beryllium fluoride ($KF \cdot BeF_2$). The resonance minima we obtain yield values of $\mu/hI = f/H$ for the constituent nuclei of the molecules. There were two different values of f/H common to both molecules. One of these values agreed closely with that previously found for F^{19}. The other value must therefore be ascribed to Be^9. The value of f/H for Be^9 was found to be constant to 0.2 percent for frequencies ranging from 0.9×10^6 to 3.0×10^6 cycles per second. The value of g of Be^9 is 0.783±0.003 when referred to that of Li^7 ($g = 2.167$).[1]

The sign of the moment of Be^9, as determined from the systematic shifts of the positions of the resonance minima when the direction of the homogeneous field is reversed[2] is found to be negative. This is the first nucleus investigated by molecular-beam magnetic-resonance methods for which a negative magnetic moment has been found.

Since our experiment does not measure spin and since no

reliable value of the spin exists in the literature we cannot ascribe a definite value to the moment of this nucleus. However, it is highly improbable that the spin is $\frac{1}{2}$. If the nuclear state were $P_{\frac{1}{2}}$ the neutron spin would be directed oppositely to the orbital angular momentum and since the neutron moment is negative[3] the resultant would be positive. If the state were $S_{\frac{1}{2}}$ the resultant moment would indeed be negative but equal to $-0.783\times\frac{1}{2}=-0.392$ which is to be compared with the expected value of the neutron moment of -1.9.[4] A value of $\frac{3}{2}$ for the spin would be much more plausible. In this case the nuclear moment would be -1.175 nuclear magnetons. This is to be compared with the theoretical prediction of Rose and Bethe[5] which is -1.65. The lack of agreement may arise from the value of the neutron moment which these authors assumed as equal to -2.0. Recent work on the H and D nuclei shows that the deuteron possesses a quadrupole moment,[6] which indicates that there is an orbital contribution to the moment of the D nucleus. Such an orbital contribution would decrease the absolute value of the moment of the neutron which is obtained by comparing the moments of H and D.[7] Our present results are in agreement with this view. The research has been aided by a grant from the Research Corporation.

P. Kusch
S. Millman
I. I. Rabi

Columbia University,
New York, New York,
March 15, 1939.

* Publication assisted by the Ernest Kempton Adams Fund for Physical Research of Columbia University.
[1] I. I. Rabi, S. Millman, P. Kusch and J. R. Zacharias, Phys. Rev. 55, 526 (1939).
[2] S. Millman, Phys. Rev. 55, 628 (1939).
[3] O. R. Frisch, H. von Halban and J. Koch, Phys. Rev. 53, 719 (1938).
[4] J. M. B. Kellogg, I. I. Rabi, N. F. Ramsey, Jr. and J. R. Zacharias, Bull. Am. Phys. Soc. 13, No. 7, Abstract 24; Phys. Rev. 55, 595 (1939).
[5] M. E. Rose and H. A. Bethe, Phys. Rev. 51, 205 (1937).
[6] J. M. B. Kellogg, I. I. Rabi, N. F. Ramsey, Jr. and J. R. Zacharias, Phys. Rev. 55, 318 (1939).
[7] J. Schwinger, Phys. Rev. 55, 235 (1939).

New Periods of Radioactive Tin

We have found in the tin precipitate, prepared by bombardment of tin with five-Mev deuterons, radioactivities with half-lives 9 minutes (−), 40 minutes (−), 26 hours (−), 10 days (−), about 70 days (−) and at least 400 days (sign unknown). All but the very longest period have also been obtained with slow neutrons on tin. One of the deuteron activated samples is over two years old and is still measurably active.

Previous reports on tin activities have been made: Naidu[1] found 8 and 18 minutes while Nahmias[2] gives 6 minutes, both after slow neutron activation of tin; we have quoted[3] half-lives of 12 minutes, 45 minutes, 28 hours and several months, obtained with deuterons on tin; Pool, Cork and Thornton have found[4] a 47-minute period with fast neutrons on tin; Barnes obtains[5] radioactive tin with half-lives 20 minutes (+) and 50 days (−) from protons on indium. All of these activities, except the 20-minute positron emitter, are probably to be identified with the periods quoted in the first paragraph.

The unstable tin isotopes to which these activities could be assigned are Sn^{113}, Sn^{121}, Sn^{123} and Sn^{125}. One must of course also consider the possibility that some of them may be due to excited forms of stable tin, similar to that of indium recently described.[6, 7] A few identifications can be made reasonably.

Inasmuch as neither we nor Pool, Cork and Thornton observe the 9-minute period when fast neutrons from Li+D are used, it is plausible to assign this period to Sn^{125}, obtained as the result of neutron capture by the heaviest stable isotope. Barnes' two activities should both belong to Sn^{113} (provided the longer period decays by K-electron capture) and our 70-day activity may perhaps be the same as that given by him as a 50-day period. We will give further evidence for this below. (The fact that the 20-minute activity is not obtained after deuteron or slow neutron bombardment of tin is probably explained by the low abundance of Sn^{113} and the high intensity of the observed short lived products.) We have reason to believe that an early report[8] by one of us of a 24-hour tin formed by $Sb^{121}(d, \alpha)Sn^{121}$ is in error, so that the 26-hour tin isotope from tin plus deuterons or neutrons is not necessarily associated with Sn^{121}, although it may be.

The isotopic constitution of the neighboring elements is such that little additional aid in assignment is obtained by studying the transmutations of elements close to tin. The only unstable tin isotope common to the reactions (Sn, dp)Sn and Cd(α, n)Sn is Sn^{123}. A chemical separation for tin after activation of cadmium with 16-Mev helium ions does in fact give a precipitate which contains an activity with a half-life of about 70 days (sign unknown). This is additional evidence that Sn^{113} has this period, and perhaps decays by K-electron capture to stable In^{113}. This tin fraction also contains activities with half-lives of 25 minutes (−), 3 hours (−) and 13 days (−). The question as to whether this 25-minute activity is to be identified with Barnes' 20-minute period cannot be decided from the present data since our magnetic deflection experiments show the predominant sign of the 25-minute period to be negative, while Barnes reports that positrons were observed. No assignment can be attempted for the 3-hour and 13-day activities. They may be formed from the rare isotopes Cd^{108} or Cd^{106} (abundance about one percent, compared to the 12.8 percent of Cd^{110} which gives rise to the 70-day Sn^{113}) and hence would be involved in multiple decays leading back to stable Cd^{111} or Ag^{109}.

We wish to extend our thanks to the Research Corporation for its support in this work.

J. J. Livingood*
G. T. Seaborg

Radiation Laboratory, Department of Physics, (J.J.L.)
Department of Chemistry, (G.T.S.)
University of California,
Berkeley, California,
March 9, 1939.

[1] R. Naidu, Nature 137, 578 (1936).
[2] M. Nahmias, Comptes rendus 202, 1050 (1936).
[3] J. J. Livingood and G. T. Seaborg, Phys. Rev. 50, 435 (1936).
[4] M. L. Pool, J. M. Cork and R. L. Thornton, Phys. Rev. 52, 237 (1937).
[5] S. W. Barnes, Phys. Rev. 55, 241 (1939).
[6] M. Goldhaber, R. D. Hill and L. Szilard, Phys. Rev. 55, 47 (1939).
[7] S. W. Barnes and P. W. Aradine, Phys. Rev. 55, 50 (1939).
[8] J. J. Livingood, Phys. Rev. 50, 425 (1936).
* Now at Harvard University.

Gamma-Rays from Uranium Activated by Neutrons

A search has been made for gamma-rays emitted during the bombardment of uranium by neutrons. Uranium nitrate enclosed in a lead envelope 3 cm×12 cm and 0.85 mm thick was waxed to the inside wall of a cloud chamber filled with air and alcohol vapor in a magnetic field of 1500 gauss and bombarded with neutrons produced by 350 kilovolt deuterons on a heavy ice target. Out of 532 photographs 118 beta-ray tracks with energies in excess of 2.2 Mev were measured. The majority of the tracks originated in the walls of the chamber (or perhaps in the heavy material outside) and are attributed to recoils from gamma-rays and not to betas coming directly out of the uranium.

The experiment was repeated with the same amount of lead in the chamber but without the uranium. There were 238 photographs made and 23 recoils were measured whose energies exceeded 2.2 Mev. In Fig. 1 is plotted an integral curve for each of the runs. The upper curve shows the results with uranium in the cloud chamber. The lower curve represents the results without the uranium reduced to the same number of photographs as the upper curve and to approximately the same neutron intensity. (An estimate of the relative neutron intensities in the two experiments was made by comparing the number of recoil protons observed in an equal number of pictures. The ratio of the number of recoil protons without uranium to the number with uranium in the chamber was 1.5.)

Part of the difference in the number of low energy gamma-rays in the two cases might be attributed to radiative neutron capture in the uranium, but it seems quite clear that certainly the gamma-rays above 4 or 5 Mev are associated with the fission process, and probably are emitted by the excited products of the ruptured uranium nucleus. If in the products of the uranium disintegration, as in other excited nuclei, the gamma-ray energy is distributed over several quanta, one can conclude that these nuclei are in a very highly excited state after the fission in view of the high energy gamma-rays observed.

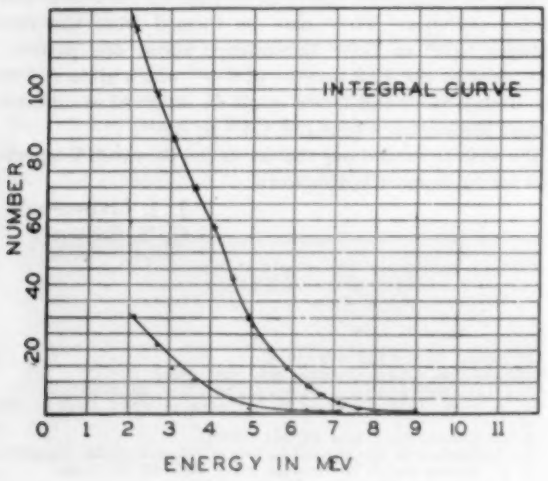

FIG. 1.

Because very few tracks came out of the lead envelope the present experiment might indicate that there are very few high energy beta-rays emitted during the actual fission. A few practically straight beta-ray tracks were observed in the cloud chamber, but it is possible that they were due to cosmic-ray shower particles, and consequently these were not included in the data in Fig. 1.

The data shown in Fig. 1 are not to be interpreted as representing a true distribution of the gamma-ray energies because only direct views of the tracks were photographed in the cloud chamber whose sensitive region was approximately 3 cm deep; and all tracks which could be measured, regardless of their lengths, were included in the data.

We wish to acknowledge the financial aid of the Duke University Research Council, and the helpful discussion of members of the Physics Department in this work.

J. C. MOUZON
R. D. PARK
J. A. RICHARDS, JR.

Physics Department,
Duke University,
Durham, North Carolina,
March 15, 1939.

Influence of Frequency on the Electro-Optical Effect in Colloids

Colloidal clay was separated into various particle sizes by centrifuging by the technique of Hauser and Reed.[1] A 1-percent suspension of particle size approximately 1500A was subjected to alternating electric fields from 30 to 12,000 cycles. The electro-optical effect on light moving perpendicular to the electric field between crossed Polaroids oriented at 45° to the field was observed. The transmitted light was measured by a photo tube and recording meter as the frequency was changed continuously. The r.m.s. field was held constant at 25 volts/cm and the temperature was 30°C.

As Mueller[2] reports, there is an enormous "Kerr" effect. (See Fig. 1.) Furthermore the continuous record shows one frequency where there is no light response to the voltage applied, although there is response at higher

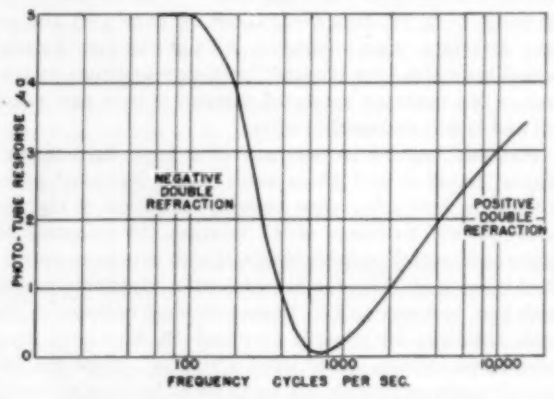

FIG. 1. Electric double refraction of colloidal clay.

and lower frequencies. The recorded minimum at 630 cycles is for a material called "colloidal talc" or "white bentonite." It is mainly magnesium silicate with very low iron content. Similar effects are shown by the ordinary yellow bentonite which is mainly aluminum silicate.

It was also found that on d.c. and at frequencies below the minimum the sol showed negative double refraction, and at frequencies above the minimum the double refraction was positive. Vanadium pentoxide sol was similarly examined and found to have a flat frequency characteristic with positive double refraction as does nitrobenzene. The position of the minimum and details of the bentonite curves were found to depend on the age and other characteristics of the particular sol. Double refraction was determined by a double quartz wedge.[3]

This effect is similar to the anomalous change in the Kerr effect found by Kitchin and Mueller[4] with rosin, and Raman and Sirkar[5] with octyl alcohol.

FRANCIS J. NORTON

Research Laboratory,
General Electric Company,
Schenectady, New York,
March 16, 1939.

[1] Hauser and Reed, J. Phys. Chem. **40**, 1169 (1936).
[2] H. Mueller, Phys. Rev. **55**, 508 (1939).
[3] Hull and Burger, Rev. Sci. Inst. **7**, 98 (1936); Baldwin, G. E. Rev. **40**, 319 (1937).
[4] D. W. Kitchin and H. Mueller, Phys. Rev. **32**, 986 (1928).
[5] Raman and Sirkar, Nature **121**, 794 (1928).

Raman Effect in Difluorochloromethane

We have observed thirteen Raman shifts in difluorochloromethane. The results are shown in Table I. The equipment used was described earlier.[1]

Three exposures were made by using Eastman Spectroscopic Plates Type 1J. Exposure times employed were 10.3, 27 and 36 hours.

Since difluorochloromethane boils at −40.8°C, a modification of our low temperature apparatus[2] was used to maintain the substance in the liquid state. The average temperature employed during these runs was −55°C.

The difluorochloromethane was furnished by the E. I. duPont de Nemours Company and was specified "Plant Product, refrigerator grade, probably 99 percent pure or better." About 50 grams of sample were available. The sample was supplied in a steel tank; connection to the cooling system was made by a Pyrex seal to a specially prepared copper fitting. Thus all connections were metal or glass, no pressure tubing, which might contaminate the sample, was used for joints. The sample was perfectly dust-free and gave spectrograms entirely devoid of background.

TABLE I. *The Raman shifts of difluorochloromethane.* $a = 4358.34$A; $b = 4046.56$A; $c = 4077.8$A.

Raman Shift in cm^{-1}	Percent Mean Deviation	Exciting Lines	Number of Readings	Average Relative Intensity
3032.2	0.04	*a*, *b*	6	8 (*b*)
1353.6	0.22	*a*, *b*	4	3
1310.5	0.14	*a*, *b*	6	4
1127.9	0.24	*a*, *b*	3	0.5
1085.3	0.20	*a*, *b*	4	0.5
830.9	0.18	*a*, *b*	4	3
799.6	0.14	*a*, *b*, *c*	7	9 (*b*)
596.5	0.18	*a*, *b*	6	8
456.4	0.01	*a*	2	1
436.3	0.00	*a*	2	0.5
415.9	0.22	*a*, *b*, *c*	7	10 (*b*)
409.1	0.15	*a*	3	1
369.2	0.10	*a*	3	7

We wish to express our gratitude to Dr. A. F. Benning of the Jackson Laboratory for the loan of this substance. Further details concerning these results will be published later.

GEORGE GLOCKLER
J. H. BACHMANN

University of Minnesota,
Minneapolis, Minnesota,
February 3, 1939.

[1] G. Glockler and J. H. Bachmann, Phys. Rev. **54**, 970 (1938).
[2] G. Glockler and M. M. Renfrew, Rev. Sci. Inst. **9**, 306 (1938).

Constancy of K^{40}

W. R. Smythe[1] has recently concluded that KCl prepared from old and deeply covered granite has essentially the same beta-ray activity as ordinary potassium salts. While this result alone appears to preclude the possibility of formation of K^{40} by present day processes associated with cosmic rays, it seems advisable to mention several experiments performed in this laboratory to test this very point.

A mass-spectrographic investigation of the relative abundance of K^{40} in comparatively fresh Vesuvius lava and in various clay soils failed to detect any measurable difference in the abundance ratio. In making these tests the samples were not subjected to any chemical treatment. In a further set of experiments the beta-rays of pure KCl extracted from Saratoga Spring water were contrasted with beta-rays of potassium from various commercial sources. The Saratoga Springs KCl was prepared by Dr. Oskar Baudisch who used the perchlorate method. The beta-ray measuring technique was the same as that described previously.[2] No detectable difference was observed between the various samples. These results are of interest since the best available geological information[3] indicates that Saratoga Spring waters derive their mineral content from deeply covered Pre-Cambrian formations. If the radioactivity is enhanced by any processes continually going on at the surface a change in the beta-ray emissivity should have been detected.

While these results are purely negative, they indicate, in agreement with those of Smythe, that the K^{39}/K^{40} abundance ratio is comparatively constant throughout nature. It seems justifiable, therefore, to use the $K^{40}-Ca^{40}$ ratio in estimating the age of matter.[4]

A. KEITH BREWER

Bureau of Chemistry and Soils,
U. S. Department of Agriculture,
Washington, D. C.,
March 7, 1939.

[1] W. R. Smythe, Phys. Rev. **55**, 361 (1939).
[2] A. Bramley and A. Keith Brewer, Phys. Rev. **53**, 502 (1938); J. App. Phys. **9**, 778 (1938).
[3] Rudolph Ruedeman, Science **86**, 531 (1937).
[4] A. Keith Brewer, Ind. and Eng. Chem. **30**, 893 (1938).

Further Products of Uranium Cleavage

Recent work has demonstrated conclusively that when uranium is irradiated by neutrons, elements of much smaller atomic number are produced.[1] In this laboratory we have already found in the products of uranium disintegration a three-day tellurium which decays into a 2½-hour iodine.[2] Further experiments now demonstrate the presence of additional radioactive antimony, tellurium and iodine isotopes. Of these three elements the most thoroughly studied so far is iodine. A table of activities follows.

Antimony		Tellurium		Iodine
<15 min.	→	72 hr.	→	2½ hr.
				8 day
		40 min.	→	54 min.
		1 hr.	→	22 hr.
4.6 hr.	→	70 min.		
5 min.				
40 min.				

As previously pointed out the 72-hour tellurium and the 2½-hour iodine correspond to bodies formerly identified as "transuranic elements."[3] It is of interest to note that the 72-hour activity does not grow from a one-hour period as was reported by Meitner, Hahn and Strassmann. This was shown by making a series of quantitative tellurium extractions from an irradiated sample at 15-minute intervals. The eight-day iodine correspond to the known[4] I^{131}. Absorption measurements were made under identical geometrical conditions on samples of the eight-day iodine produced both by neutron activation of uranium and by deuteron activation of tellurium. The beta-ray absorption curves were identical. The 40-minute tellurium was established through quantitative iodine extractions from tellurium, which had been precipitated from an activated uranium sample. A series of as many as twenty iodine extractions were made from the tellurium at definite intervals. Decay curves of these extractions were followed and analysis showed two main components of 54-minute and a 22-hour half-life. It is barely possible that the 22-hour activity and the 54-minute body are isomers with the 54-minute activity having the highest energy state. The iodine was separated from tellurium by carbon tetrachloride extraction and by distillation of a solution containing dilute nitric acid. If some of the active iodine were converted to iodate and later converted into free iodine through recoil the observed results would be found. The 4.6-hour antimony activity was shown to decay into a 70-minute tellurium. Since it seemed possible that the 70-minute body might be the parent of the 22-hour iodine, this possibility was investigated with a negative result. The 70-minute activity could be[4] Te^{129} but that possibility has not been investigated. The five-minute and the 40-minute periods have not been completely identified as antimony. In the chemical procedure followed, germanium also appears with antimony. The five-minute activity could be the parent of the 72-hour tellurium. I wish to express my thanks to Professor E. O. Lawrence for his interest in this experiment and to the Research Corporation for financial support.

PHILIP ABELSON

Radiation Laboratory,
Department of Physics,
University of California,
Berkeley, California,
March 13, 1939.

[1] O. Hahn and F. Strassmann, Naturwiss. **27**, 11 (1939).
[2] P. Abelson, Phys. Rev. **55**, 418 (1939).
[3] L. Meitner, O. Hahn and F. Strassmann, Zeits. f. Physik **106**, 249 (1937).
[4] J. J. Livingood and G. T. Seaborg, Phys. Rev. **54**, 775 (1938). The same authors have made further investigations (unpublished) which prove the 8-day iodine to be I^{131} and that a 70-minute tellurium activity is Te^{129}.

Proceedings of the American Physical Society

Minutes of the New York, New York, Meeting, February 23–25, 1939

THE 226th regular meeting of the American Physical Society was held in New York City on Thursday, Friday and Saturday, February 23, 24 and 25, 1939 as a joint meeting with the Optical Society of America and the Inter-Society Color Council. The presiding officers at the sessions of the Physical Society were Dean John T. Tate, President of the Society, Professor John Zeleny, Vice President, Professor Walker Bleakney, Dr. Karl K. Darrow, Dr. W. E. Forsythe and Dr. L. H. Germer. All regular sessions for the reading of contributed papers for both the Physical Society and the Optical Society were held on Friday and Saturday at Columbia University in the Pupin Physics Laboratories. Sessions of the Inter-Society Color Council were held on Thursday at 480 Lexington Avenue.

The joint session with the Optical Society of America and the Inter-Society Color Council was held on Saturday morning at ten o'clock in a studio of the National Broadcasting Company, RCA Building, 30 Rockefeller Plaza. This session was a symposium of invited papers on "Television." The President of the Physical Society, Dean Tate, presided. The invited papers were as follows: *Electron Optics as Applied in Television Systems* by V. K. Zworykin, RCA Manufacturing Company; *Application of Electron Multipliers to Voltage Amplifications* by P. T. Farnsworth, Farnsworth Television, Incorporated (this paper was not given on account of the illness of the author); and *Demonstrations in Television* by A. F. Van Dyck, Radio Corporation of America. The attendance at this symposium was about four hundred.

On Friday afternoon after the close of the regular program an informal meeting was held for the discussion of the splitting of uranium atoms, at which Professor Niels Bohr and Professor Enrico Fermi were the speakers.

On Friday evening the Society joined with the Optical Society and the Inter-Society Color Council for dinner at the Columbia University Faculty Club. This dinner was attended by one hundred and forty members and guests. Dean Tate, President of the Physical Society, presided and after introducing officers of the Physical Society, the Optical Society of America, representatives of the Inter-Society Color Council and Professor Niels Bohr, Honorary Member of the Physical Society, called upon Dr. Karl K. Darrow to speak on certain features of the City of New York.

Meeting of the Council

At its meeting on Friday, February 24, 1939 the Council transferred six candidates from membership to fellowship and elected thirty-one candidates to membership. *Transferred from membership to fellowship:* Paul L. Bayley, Enrico Fermi, Millard F. Manning, Karl W. Meissner, Gordon M. Shrum and Walter H. Zinn. *Elected to membership:* Tosia Amaki, Paul A. Anderson, David F. Bleil, Daniel Brandon, Karl Cohen, Clifford V. Franks, Otto R. Frisch, Thomas D. Hanscome, Goro Hayakawa, John T. Hayward, Lawrence R. Hill, Richard A. Johnson, Gilbert E. Klein, Tadao Miki, Shizuo Miyake, Goro Miyamoto, Elizabeth Monroe, Cal F. Muckenhoupt, Mokitiro Nogami, G. Otake, C. Dale Owens, Robert F. Plott, Richard B. Stambaugh, Dean W. Stebbins, D. Gordon Sharp, Eizo Tajima, Ryohei Toya, James L. Tuck, Jesse R. Watson, D. J. Zaffarano and Herbert I. Zagor.

The regular scientific program of the American Physical Society consisted of sixty-four contributed papers of which numbers 47, 56 and 63 were read by title. The abstracts of the contributed papers are given in the following pages. An author index will be found at the end.

W. L. Severinghaus
Secretary

Abstracts

1. Some Physical Properties of Liquid and Solid HD. F. G. Brickwedde and R. B. Scott, *National Bureau of Standards.*—About six liters of pure gaseous HD were separated from a mixture of H_2, HD and D_2 in a still having a refluxing column and operated in liquid hydrogen. Several properties of this sample of HD were measured with the following results: *Triple Point:* 16.60$_4$°K and 92.8$_8$ mm Hg. *Volume of Liquid* between triple point and 20.4°K: $V(\text{cm}^3\ \text{mol}^{-1}) = 24.886 - 0.30911T + 0.017177^2$. *Relation between Freezing Temperature and Pressure* to $P = 80$ kg cm^{-2}: $\log_{10}(328.4+P) = 1.85904 \log T + 0.24731$. *Latent Heat of Fusion* at triple point: 38.1 cal. mol^{-1}. *Latent Heat of Vaporization of Liquid* at 22.54°K: 257 cal. mol^{-1}. *Heat Capacity of the Solid:* varied regularly from 0.69 cal. mol^{-1} °K^{-1} at 12°K to 2.46 at the triple point. *Heat Capacity of the Liquid:* varied linearly from 4.48 cal. mol^{-1} °K^{-1} at the triple point to 6.29 at 22°K. The difference between the volumes of the liquid and solid phases at the triple point, calculated from the above data by means of the Clapeyron equation, is 2.66 cm^3 mol^{-1}. The following equations were found to represent the vapor pressure of HD[1] as a function of the temperature expressed on the scale[2] recently established at the National Bureau of Standards. *Solid* from 10.4°K to triple point, $\log_{10}P(\text{mm Hg}) = 4.70260 - (56.7154/T) + 0.04101T$. *Liquid* from triple point to 20.4°K, $\log_{10}P(\text{mm Hg}) = 5.04964 - (55.2495/T) + 0.01479T$. These properties of HD are compared with those of H_2 and D_2.

[1] R. B. Scott and F. G. Brickwedde, Phys. Rev. **48**, 483 (1935).
[2] H. J. Hoge and F. G. Brickwedde, Nat. Bur. Stand. J. Research **22**, March (1939).

2. Field Currents at High and Low Pressures. B. E. K. Alter and R. T. K. Murray, *Polytechnic Institute of Brooklyn.*—The fact that field currents can be obtained from metals immersed in gases at high pressure has been employed to study the field emission at high pressure and in a vacuum from the same cathode. The electrodes were steel spheres whose separation could be varied with a micrometer screw driven by an electric motor through reduction gears, the whole assembly being enclosed in a cylindrical steel container which could be evacuated or operated at pressures up to 130 atmospheres. Linear log current against reciprocal potential curves for constant distance, linear log current against distance curves for constant potential, and linear potential against distance curves for constant current were obtained. The measured fluctuations in the emission obtained in a vacuum were greater than those obtained at high pressure. Since under high pressure positive ion bombardment of the cathode is prevented, the observed fluctuations cannot be due to positive ion impact. This supports the theory that the emitting points are changed by local heating produced by the high current densities at the points. The increased fluctuations of the currents in a vacuum can be accounted for by positive ion impact on the cathode.

3. Field Measurements and Possible Correction of Aberrations for Magnetic Electron Lenses. L. Marton, *389 Park Ave., Collingswood, New Jersey.*—Experiments with two magnetic coils indicate that an improvement in the image quality can be obtained by opposing the currents in the coils and placing the object between the two field maxima. The position of the object with respect to the latter may be determined by measuring the field distribution ballistically with a field coil. Applying the same method for studying the fields in an actual electron microscope, the latter are found to have maximum values of the order of 7000 gauss. Some general relationships between lens design and image quality are discussed.

4. Optical and Magneto-optical Activity of Nickel Sulfate, α-Hexahydrate, in the Short Infra-Red Spectrum. L. R. Ingersoll, *University of Wisconsin;* Philip Rudnick and F. G. Slack, *Vanderbilt University.*—Previous measurements[1] of the optical activity of crystalline nickel sulfate, α-hexahydrate, in the visible and near ultraviolet regions have indicated active absorption bands in the infra-red region. Measurements of the natural rotatory power, the Verdet Constant, and of the transmission for this crystal have now been made through the spectral range from 0.60 mu to 2.0 mu. The method used in measuring the rotations is a modification of that previously described by Ingersoll.[2] The results show distinct anomalies in both the optical rotation and the magneto-optical rotation at approximately 0.69 mu and 1.16 mu, with corresponding absorption in these regions. Curves will be presented. The anomaly occurring at 1.16 mu in the optical rotatory curve is an exceptionally good example of anomalous rotatory dispersion and indicates a relatively very strong term of the Drude type in the rotatory dispersion equation. Preliminary calculations indicate that the single electron model of Condon, Altar and Eyring[3] will not account for this activity but that it may be accounted for on the basis of a pair of coupled linear oscillators on a model proposed by Kuhn.[4] Work on the analysis of the experimental results is being continued.

[1] F. G. Slack and Philip Rudnick, Phil. Mag., in press.
[2] L. R. Ingersoll, Phys. Rev. **9**, 257 (1917).
[3] E. U. Condon, William Altar and Henry Eyring, J. Chem. Phys. **5**, 753 (1937).
[4] E. U. Condon, Rev. Mod. Phys. **9**, 446 (1937).

5. Magnetic Susceptibilities in Weak Fields. L. G. Hector and Mahlon F. Peck, *The University of Buffalo.*—The Hughes induction balance method for measuring magnetic susceptibilities in weak fields first reported by Hector and Eckstein[1] has been improved in sensitivity to a point where diamagnetic liquids and some gases can be measured. The fields used vary from 5 to 35 oersteds. Carbon tetrachloride, benzene and toluene appear to have the same values of susceptibilities at these field strengths as are found when they are measured by classical methods in intense fields. On the other hand, present measurements indicate that water is approximately six percent more diamagnetic and oxygen approximately seven percent more paramagnetic in these weak fields than in the intense static fields ordinarily employed.

[1] L. G. Hector and G. R. Eckstein, Phys. Rev. **49**, 643 (1936).

6. Preparation of Single Crystals of Iron, Cobalt, Nickel and Their Alloys. P. P. CIOFFI AND O. L. BOOTHBY, *Bell Telephone Laboratories, Inc.*—The raw materials used were carbonyl iron, Katanga electrolytic cobalt and specially purified nickel. For all of the crystals except iron, the materials were further purified by heat treatment in pure moist hydrogen just below the melting point in a pure alumina crucible. The temperature was then raised until they melted together; subsequently, the temperature was lowered, in some cases automatically at the rate of 2°C/hour until solidification was complete. The alloys were homogenized by holding just below the melting point for 24 hours. Sometimes the resulting ingot was a single crystal weighing about 400 grams, more often it consisted of two or more crystals. A single crystal of cobalt weighing 300 grams was formed by this method in spite of the fact that it undergoes a phase transformation at 400°C. Smaller crystals (about five grams) of iron were made without melting by holding for a long time at 1480°C, then at 880°C in pure dry hydrogen. In the direction of the cubic axis the iron crystal was found to have a maximum permeability of 1,450,000 at $B=17{,}500$. The hysteresis loss and coercive force are considerably larger than have been expected for a crystal of this purity. The magnetic properties of the iron-nickel and nickel-copper crystals have been determined by Williams and Bozorth (see succeeding abstract).

7. The Magnetic Anisotropy of Iron-Nickel and Copper-Nickel Alloys. H. J. WILLIAMS AND R. M. BOZORTH, *Bell Telephone Laboratories, Inc.*—The magnetic anisotropy constant K_1 has been determined for nickel and a number of alloys of the Fe-Ni and Cu-Ni series. Specimens were cut from the large single crystals prepared by Cioffi and Boothby (see preceding abstract). The constants were determined either from torque measurements on single crystal disks in a magnetic field of high strength, or from the area between the magnetization curves for the [100] and [110] directions. For the latter method the specimens were cut in the form of hollow rectangles with each side parallel to a direction of the form <100> or <110>, as previously described.[1] For most of the crystals constants were determined at −196°C, 22°C and 200°C. For the two copper-nickel alloys (13 and 24 percent copper), K_1 was determined at a series of temperatures between −196 and 20°C and was found to obey the law: $K_1=K_{10}e^{-\alpha T^2}$, found to hold for nickel.[2] This relation permits extrapolation to 0°K. The constant so obtained (K_{10}) falls off rapidly with increasing copper content. In the iron-nickel series the composition for zero anisotropy is found to be near 70 percent nickel. Comparison is made with the data of others.[3]

[1] H. J. Williams, Phys. Rev. **52**, 747–51 (1937).
[2] N. L. Brukhatov and L. V. Kirensky, Physik. Zeits. Sowjetunion **12**, 602–9 (1937).
[3] J. D. Klein, Phys. Rev. **50**, 1178–81 (1936).

8. Theoretical Constitution of Metallic Beryllium. CONYERS HERRING* AND A. G. HILL, *Massachusetts Institute of Technology.*—Preliminary results have been obtained in a theoretical calculation of the binding energy of metallic beryllium by the method of Wigner and Seitz. Assuming that the Fermi energy of an electron with wave vector k is proportional to k^2, the calculated binding energy is about 65 kcal./g atom. This can be compared with the value of 75 kcal./g atom estimated by means of the Born cycle method.[1] The ratio of the Fermi energy in the metal to that for completely free electrons in this approximation is 0.62, calculated by the method of Bardeen.[2] Calculations of the energies of some of the electronic states near the top of the Fermi distribution show that the above assumption is not very good, and that the final computed value of the binding energy may be expected to be much larger than 65 kcal./g atom.

* National Research Fellow.
[1] Bichowsky and Rossini, *Thermochemistry of the Chemical Substances* (1936).
[2] J. Bardeen, J. Chem. Phys. **6**, 367 (1938).

9. On the Theory of Paramagnetic Relaxation. J. H. VAN VLECK, *Harvard University.*—The times of relaxation associated with the transfer of energy between spin and lattice are computed for a specific model, *viz.* a titanium or chromium ion surrounded by six water dipoles, which was previously used by the writer[1] in connection with static susceptibilities. An explanation is obtained of why titanium alum shows[2] no dispersion at radio frequencies at liquid-air temperatures. However, the calculated relaxation time for titanium at helium temperatures is considerably greater than the value computed by Kronig,[3] and far too large for agreement with experiment[4] unless the elevation of the lowest excited states is of the order 10^3 cm^{-1}, rather than 10^2 cm^{-1} as apparently indicated by magnetic theory.[1] The calculated relaxation times for chrome alum are also probably somewhat too high, but the discrepancy is not as great. The use of a definite model thus apparently does not alleviate all the difficulties encountered in previous rather schematic calculations.[5, 6]

[1] J. H. Van Vleck, J. Chem. Phys. **7**, 61, 72 (1939).
[2] Gorter, Teunissen and Dijkstra, Physica **5**, 1013 (1938).
[3] R. de L. Kronig, Physica **6**, 33 (1939).
[4] W. J. de Haas and F. K. du Pre, Physica **5**, 969 (1938).
[5] I. Waller, Zeits. f. Physik **79**, 370 (1932); W. Heitler and E. Teller, Proc. Roy. Soc. **155**, 629 (1936).

10. A Theory of Ferromagnetism. P. R. WEISS AND J. H. VAN VLECK, *Harvard University.*—An approach to the problem of ferromagnetism different from the well-known Heisenberg approximation can be obtained from Bethe's[1] method for calculating the critical constants of the ordering phenomena in alloys. The interaction between a central atom and its nearest neighbors is taken into account rigorously while the effect of the atoms outside this first shell, which is supposed to be exerted on the central atom only through the first shell, is approximated by a Weiss field which acts only on the first shell. The central atom is exposed only to the external applied field. The Weiss field is then determined as a function of the external field simply by equating the moments of the central atom and of an atom in the first shell calculated in their respective fields. The critical point is that temperature at which the ratio of the Weiss field to the external field becomes infinite. Several lattice types have been investigated and their results will be given. An expansion of the partition function

in powers of J/KT (J=the exchange integral) makes possible a comparison of the method with the rigorous theory as developed by Opechowski.[2]

[1] H. A. Bethe, Proc. Roy. Soc. **A150**, 552 (1935).
[2] W. Opechowski, Physica **4**, 181 (1937).

11. The Lack of "Sucking" Action by the Cathode Blast of Mercury Vapor in a Pool Rectifier. L. TONKS, *General Electric Company.*—Experiments of von Engel and Steenbeck[1] point to a "sucking" action by the blast of mercury vapor leaving the cathode pool of a rectifier which operates on the side arms to reduce the vapor in them to but a small fraction of its value in the condensing dome. This effect has been sought using ionization gauges on a side arm and at the top of the condensing dome and using thermocouples on the tube wall at the mercury condensation edge and at the top of the dome. The rectifier used had a dome capacity of 2.2 liters and a diameter of 7.7 cm at the side arms which were 5 cm in diameter. Both with free and anchored cathode spot *no trace of "sucking" action was found.* Theory gives a maximum decrease of pressure to $\frac{1}{2}$ the dome value, compared to the value $\frac{1}{15}$ found by von Engel and Steenbeck. The experiments showed that with the anchored spot the vapor pressures were only $\frac{1}{4}$ to $\frac{1}{3}$ what they were with the free spot but that the wall temperatures were higher. Both factors are explained by the evaporation of the spray thrown by the free spot onto the hot tube walls.

[1] M. Steenbeck, Wiss. Veröff. a. d. Siemens-Werken **15** (3), 42 (1936).

12. Ultracentrifuge for Liquids.* A. VICTOR MASKET, F. W. LINKE AND J. W. BEAMS, *University of Virginia.*—The air-driven vacuum type tubular centrifuge[1] has been adapted to the separation of mixtures and solutions. The chamber surrounding the tubular centrifuge was evacuated to less than a micron to avoid heating. Vacuum pump oil was circulated by a pump first through a thermostat and then the vacuum-tight oil glands, rapidly enough to maintain the hollow shafts at constant temperature. This temperature was the same as that of the spinning tube. Machines with the air turbines above as well as below the vacuum chamber were used. The liquid material to be centrifuged entered at one end of the spinning tube through a hollow shaft at a continuous rate and was separated when it reached the other end into a light fraction at the center and a heavy fraction at the periphery. These two fractions flowed out of the spinning tube through separate partitions in a hollow shaft and were separately collected. A solid rod mounted coaxially and inside the spinning tube increased the efficiency. Auxiliary Oilite or Bakelite bearings prevented the materials being centrifuged from coming in contact with oil leaking from the vacuum-tight oil glands. All surfaces with which the material being centrifuged came in contact were stainless steel or gold plated.

* Supported by a grant from the Research Corporation.
[1] J. W. Beams, Rev. Sci. Inst. **9**, 413 (1938).

13. Separation of Bromine Isotopes by Centrifugation. RICHARD F. HUMPHREYS, *Yale University.*—A Beams air-driven ultracentrifuge has been used to obtain a partial separation of the bromine isotopes. The technique employed was that of "evaporative centrifuging" first suggested by Mulliken.[1] A working interpretation for the separation factor has been developed, and the theory given by Mulliken for the molecular weight gradient produced has been altered to cover the case of nonequilibrium set up by removal of the vapor from the rotor. There results an expression for rate of removal in terms of coefficient of diffusion of the gas and the degree of nonequilibrium. Ethyl bromide was centrifuged in a field of 388,000 g and removed in fractions of one-tenth, all transport of the material both to and from the rotor being accomplished by vacuum distillation to reduce evaporation losses to a minimum. The enrichments obtained have been determined spectroscopically by means of relative intensity measurements of isotopic lines in the spectra of AgBr and $H\,Br^+$.

[1] R. Mulliken, J. Am. Chem. Soc. **44**, 1033 (1922).

14. Formation and Properties of Unsupported Flowing Liquid Films. BRIAN O'BRIEN, *University of Rochester.*—If a continuous film of liquid is projected from a long narrow slot, the film will, in general, collapse a short distance beyond the orifice due to surface tension. This can be prevented by a suitable component of velocity of the emerging liquid. Such films in the form of figures of revolution are useful as transparent gas tight enclosures about high intensity light sources, the liquid serving as a light filter. A 10-kw carbon arc has been operated for many hours within a water film in the form of a cylinder 8 cm diameter and 25 cm high without break in the flowing film. If broken such a film immediately reforms. Cylindrical films up to 30 cm diameter and 60 cm length have been produced in thickness of approximately $\frac{1}{3}$ mm. Their properties have been studied in some detail.

15. The Striated Luminous Glow of the Piezoelectric Quartz Resonator at Flexural Vibration Frequencies. J. R. HARRISON AND I. P. HOOPER, *Tufts College.*—Previous work has shown that the luminous glow due to the electrical discharge of a piezoelectric quartz resonator when vibrating in vacuum is sometimes striated in an unexpected way. This has been observed with X cut quartz rods vibrating at flexural vibration frequencies in the XY plane of the crystal. Double exposure photographs of this phenomenon are now shown which indicate the form and position of the striations on the quartz rod. The pressure of the residual gas and the applied voltage both have a marked effect on the position and number of the striations as is shown.

16. Nuclear Isomers in Radioactive Strontium. DAVID W. STEWART, *University of Michigan.* (*Introduced by J. M. Cork.*)—A further investigation has been made of the isomeric forms of Sr^{89} obtained in the bombardment of strontium with deuterons or neutrons. In agreement with earlier results,[1] the two periods of 3.0 hours and 55 days assigned to this isotope have been found to decay with the emission of negative electrons, producing stable Y^{89}. Accompanying the three-hour beta-activity is gamma-radiation, which is particularly interesting because it is complex and therefore of importance in interpreting the

nature of the isomerism. The energy of this radiation has now been determined by the measurement of recoil electrons ejected from a carbon radiator in a 12-inch cloud chamber. From a distribution of 475 tracks, at least two gamma-ray lines have been identified, with energies of 0.55 and 1.1 Mev, and relative intensities of at least 3 : 1. This intensity ratio may actually be much greater, and may approach 10 : 1. By combining these data with those on the upper limits of the two beta-spectra, a tentative energy-level diagram has been derived which indicates that the metastable state of Sr^{89} decays in the three-hour period with beta-particle emission followed by gamma-radiation. The ground state of Sr^{89} decays directly in the 55-day period.

[1] D. W. Stewart, J. M. Cork and J. L. Lawson, Phys. Rev. **52**, 901 (1937).

17. The Band Structure of Metallic Copper. MARVIN CHODOROW, *Massachusetts Institute of Technology.*—A general method of calculating wave functions and energies of electrons in crystals, due to Slater,[1] has been further developed and applied to Cu. In this method, the wave function inside the inscribed spheres of the atomic cells is expanded in a series of radial functions and spherical harmonics. Outside these spheres, where the potential is approximately constant, the wave function is expanded in a series of plane waves. The method is found to be feasible only for highly symmetrical points of the Brillouin zone, e.g., $k=2\pi/a(0,0,0)$, $2\pi/a(\frac{1}{2},\frac{1}{2},\frac{1}{2})$, $2\pi/a(0,0,1)$. For other values of k, the calculations become too cumbersome. In the application to Cu, the potential used was not a Hartree self-consistent field but a semi-empirical potential obtained from consideration of the solutions (for $l=2$) of the Fock equations for Cu^+. This potential partially takes into account the exchange interaction of a "d" electron with the other electrons of the atom. The width of the bands containing the "d" electrons is found to be appreciably narrower (about 1.7 ev) than those calculated by Krutter.[2] The conduction band is very similar to one containing free electrons, but is split into two sections by the perturbations of the other bands.

[1] J. C. Slater, Phys. Rev. **51**, 846 (1937).
[2] H. Krutter, Phys. Rev. **48**, 664 (1935).

18. Reducing the Reflection from Glass by Multilayer Films. C. HAWLEY CARTWRIGHT AND A. FRANCIS TURNER, *Massachusetts Institute of Technology.*—The reflecting power of a glass surface may be reduced to substantially zero by a film having an optical thickness of about 1250A and an index of refraction of 1.2 to 1.3. The Lorentz-Lorenz equation indicates that the index of refraction can be lowered by decreasing the density and indeed the index of any evaporated material can be decreased to the desired value by controlling the evaporating conditions. However, a decrease in density below normal is accompanied by a decrease in mechanical strength, seriously limiting the number of the materials suitable for rugged single films. Zero reflection by the use of a single film occurs when the two reflection vectors add to zero. This result can also be attained by the use of multilayer films so applied that the three or more reflection vectors add to zero. An abnormally low index of refraction is no longer required and a greater choice both of film materials and methods of application is possible. A rather rugged transparent film which practically eliminated reflection of visible light was made by evaporating sapphire and then quartz.

19. The Rossi Transition Curve for Small Angle Showers. W. M. NIELSEN, *Duke University.*—A study has been made of shower production in layers of iron over a range of thicknesses up to 320 g/cm². Simultaneous measurements of 7° showers and 28° showers were made with a counter arrangement similar to that recently employed.[1] With this arrangement a minimum of two particles from the producing material is necessary to discharge the four counters. The results differ somewhat from those of Schmeiser and Bothe[2] in showing no significant increase in the prominence of a second maximum at about 220 g/cm² on the 7° curve compared with the larger angle shower curves. We conclude that the processes which contribute to the showers which are observed at the possible second maximum are not necessarily restricted to small angles.

[1] Karl Z. Morgan and W. M. Nielsen, Phys. Rev. **52**, 564 (1937).
[2] Schmeiser and W. Bothe, Ann. d. Physik **32**, 161 (1938).

20. The Design and Construction of Reliable Geiger-Müller Counters. GORDON L. LOCHER, *Bartol Research Foundation of the Franklin Institute.*—Some general features of design and construction of Geiger-Müller counters which are stable over long periods of use are reviewed, and some criteria for discrimination between acceptable and unacceptable practices are discussed on the basis of experience with the production of more than 1500 tubes. Desirable practices in the construction of ordinary γ- and β-ray tubes include: (1) the exclusive use of clean (heated) bare tungsten wires, (2) shielding of welds to prevent breakdown at sharp points, (3) removal of moisture and grease from all internal surfaces, (4) removal of any material from the cylinder which may become transferred to the wire, in use, (5) treatment of all internal surfaces to eliminate free alkali metals, or materials that may generate them, in use, (6) elimination of photoelectric response of the cathode to any light that can penetrate the glass envelope, (7) establishment of very high surface resistance of all internal insulating surfaces, (8) use of a gas content whose pressure is not too low and whose constitution will not alter with use, (9) avoidance of dust inside the tubes, and (10) the treatment of the external surface of the glass envelope to make the surface resistance extremely high. The localized character of the discharge of a normal counter (especially the high current density at the wire) makes it imperative that excessive current shall not be allowed to pass through the tube, in operation. It is pointed out that the probability of production of a spurious discharge in a faulty counter is usually highest immediately after a previous discharge; hence such counters may seem to have "high sensitivity" to radiation, and a relatively low background rate, whereas they are unreliable, and worthless for measurements. Some experiments with gas mixtures are discussed.

21. Comparison of Counter and Electroscope Measurements in the Stratosphere. S. A. KORFF AND W. E. DANFORTH, *Bartol Research Foundation of the Franklin Institute.*

—Comparison of the several methods of measuring cosmic-ray intensities in the stratosphere is presented. It is shown that the results obtained by Millikan[1] using an electroscope and those found by Korff and Johnson[2] at about the same geomagnetic latitude using single Geiger counters are in good agreement. A geometrical factor is computed in order to take account of the different distributions of sensitive volume in the two cases. This comparison indicates that the correction to the electroscope observations due to the passage of simultaneous shower particles (or of single rays of great ionization) through it is less than ten percent. The observations of Korff, Curtiss and Astin[3] using low pressure counters are also found to agree with those of Millikan. It can be shown that such low pressure counters measure a quantity statistically proportional to the intensity observed with electroscopes. In so doing they take account of the passage through the counter of simultaneous shower rays and of rays of high specific ionization, while high pressure counters measure the number of ionizing events independently of the size of the event. The counter measurements made by Swann, Locher and Danforth[4] are found to be consistent with the electroscope measurements made by Millikan on the Settle-Fordney flight, but both give higher intensities at great altitudes than is found in the counter and electroscope flights made with small balloons. Hypotheses to explain this difference are discussed.

[1] I. S. Bowen, R. A. Millikan and H. V. Neher, Phys. Rev. **53**, 855 (1938).
[2] S. A. Korff and T. H. Johnson, Abs. Phys. Soc., Dec. 1938.
[3] S. A. Korff, L. F. Curtiss and A. V. Astin, Phys. Rev. **53**, 14 (1938).
[4] W. F. G. Swann, G. L. Locher and W. E. Danforth, J. Frank. Inst. **222**, 673 (1936).

22. The Origin of the Rays Which Produce the Bursts of Cosmic-Ray Ionization. C. G. MONTGOMERY AND D. D. MONTGOMERY, *Bartol Research Foundation of the Franklin Institute.*—The transmission through the atmosphere of the electrons and photons necessary to produce the observed size-frequency distribution of large bursts of cosmic-ray ionization is investigated. From the observations that the size-frequency distribution of bursts is independent of elevation, while the variation with elevation of the total number of bursts is not exponential, we conclude that the burst producing electrons are *not* transmitted through the atmosphere by the mechanisms of the cascade theory, but that in the lower atmosphere there must be a considerable number of electrons of high energy which are secondary to a penetrating component of the cosmic radiation. This conclusion is strengthened by observations of large showers from the air. It seems likely that these showers are also of secondary origin, since the spreading that a primary cascade would experience in traversing the atmosphere makes it unlikely that the observed high density of rays would occur by this process.

23. Electrophoretic Demonstration of Patent Pores of Human Skin. HAROLD A. ABRAMSON, *The Biological Laboratory, Cold Spring Harbor, and Mt. Sinai Hospital, New York.*—To investigate the paths by which the electrophoretic introduction of drugs into the intact human skin occurs, dyes of different charge like methylene blue and sodium prontosil were employed. Following electrophoresis of ½ percent methylene blue, the skin appears grossly to be uniformly dyed. The pattern of the patent pores which take a major part in the electrical transport of substances into the skin may then be developed by rubbing and washing vigorously to remove the most superficial layers of the skin. The developed pattern consists of many small uniformly stained, blue spots from about 0.07 mm to 0.5 mm in diameter. Practically all of the spots are at the site of the orifices of sweat glands (pores). Similar patterns are therefore obtainable in the palm of the hand. The patterns persist for several weeks. During this time, the uniformly dyed pores decolorize in the center with the formation of circular or elliptical blue rings, doughnut forms, which surround the pore orifices. The pore pattern with negatively charged prontosil corresponds to the methylene blue pattern but persists only a few days. These results confirm the liquid bridge theory of skin permeability of Abramson and Gorin for the electrical transport of ragweed protein into the skin.

24. Compact Pressure-Insulated Electrostatic X-Ray Generator for Cancer Therapy. J. G. TRUMP AND R. J. VAN DE GRAAFF, *Massachusetts Institute of Technology.*—A compact, pressure-insulated, electrostatic x-ray generator has been developed for use in cancer treatment and research. A further object of the work was the investigation, using a small and thus flexible machine, of the design factors involved in pressure-insulated electrostatic generators with a view to the subsequent development of higher voltages in compact apparatus. The generator is housed in a steel tank 34 in. in diameter and 100 in. high. At air pressures of 10 atmospheres gauge, 1250-kv x-rays are obtained with currents of one milliampere on the single 14-in. belt. A substantial increase in voltage can be obtained by the use of Freon gas. The dependence of voltage and current on pressure and on gas is discussed. The problem of belt charge is analyzed and a method is described for controlling the electrostatic fields within the column in order to realize the high charge densities possible at high pressure. The construction of a supporting column of high breakdown strength, of the x-ray tube, and other features of the design are described. At 1250 kv the x-ray intensity per milliampere of target current is 250 roentgens per minute at 50 cm from the target in the direction of the electron beam with two-mm lead and five-mm copper filtration. The present work follows the development of a 1000-kv, air-insulated, x-ray source* which has been in use for almost two years at the Huntington Memorial Hospital.

* J. G. Trump and R. J. Van de Graaff, J. App. Phys. **8**, 602 (1937).

25. A Measurement of Gamma-Radiation in Roentgens. T. N. WHITE, *National Cancer Institute;* L. MARINELLI AND G. FAILLA, *Memorial Hospital, New York.*—For the measurement of gamma-rays in roentgens, certain requirements must be fulfilled. Heretofore most measurements of this type have been made by "thimble chambers" of small size placed at a distance from the source. The necessary condi-

tions may be met also by a different geometrical arrangement of source and ionized volume, which offers certain advantages. With a small gamma-ray source at the center, measurements were made of the ionization in spherical air shells of thickness 0.04 to 3.5 cm and inner radii of 1 to 3.8 cm approximately. The air shells were defined by Lucite shells of suitable thickness. The gamma-ray output of radium in roentgens was obtained from these measurements by extrapolating to zero thickness of the air shell. By extending Lauritsen's analysis[1] of the influence of geometrical factors, a formula was derived which supplies a partial explanation of the variation of ionization in the air shells with respect to thickness.

[1] C. C. Lauritsen, Brit. J. Radiol. 11, 471 (1938).

26. A Portable Gamma-Ray Detector. L. MARINELLI, *Memorial Hospital, New York.*—The use of a commercial grid glow tube (KU 618) as a point counter will be described. The circuit requires essentially a 0.01-mf condenser, a resistance of five megohms and a source of potential of about 200 volts. The instrument provides a rather inexpensive means for the detection of gamma-ray sources and stray radiation as well as for demonstrations in radioactivity. An a.c. operated instrument, provided with a counting circuit and weighing seven pounds, will be shown. In its present form the natural counting rate of the device increases tenfold when exposed to the gamma-radiation of five mg of radium at a distance of five meters.

27. Some New Features in the Million-Volt X-Ray Installation at the Memorial Hospital. G. FAILLA, *Memorial Hospital, New York.*—The General Electric Company announced recently the completion of a million-volt x-ray generator to be installed in the new Memorial Hospital. For the accurate treatment of patients it is very desirable that the beam of radiation be adjustable in direction through 90° in a vertical plane. Since the generator weighs about two tons it is simpler to move a "collimator" with respect to the tube target. If the collimator is made of overlapping five-inch thick lead plates the device becomes too cumbersome. To provide a beam of x-rays which is adjustable both as to direction and cross section, the target is surrounded by a mercury tank into which is inserted at the appropriate angle a hollow "cell" of the proper shape and size. It is important to keep the patient under observation during the treatment. To accomplish this a window is provided in the thick concrete wall at one corner of the treatment room. A glass cell which fits into this window is filled with a transparent salt solution of sufficient absorptive power to protect the observer from scattered x-rays.

28. The Effect of Pressure on the Intensity of the Recombination Spectrum of Mercury. ROBERT C. GARTH, *Brooklyn College;* GEORGE E. MOORE, *Bell Telephone Laboratories;* AND HAROLD W. WEBB, *Columbia University.*—The effect of vapor pressure on the intensity of spectral lines in the recombination glow of mercury vapor was investigated. The pressure was varied from 0.1 mm to 1.7 mm and the concentration of ions maintained at approximately 2.5×10^{11} per cc as measured by the Langmuir probe method. The combined intensity of 5461 and 5770–90 was measured with a photometer, and photographic methods were used for measuring other lines in the visible and ultraviolet. It was found that the intensities in general increased with pressure, although the exact behavior of a line depended on its position in the spectral series. This result indicates that the rate of recombination is a function of the concentration of the neutral atoms as well as of the recombining ions and electrons, or that the metastable and other excited atoms influence recombination. The band spectrum of mercury was observed at pressures above 1.0 mm.

29. The Spectral Distribution of Energy in the Recombination Spectrum of Mercury. GEORGE E. MOORE, *Bell Telephone Laboratories;* ROBERT C. GARTH, *Brooklyn College;* AND HAROLD W. WEBB, *Columbia University.*—The distribution of energy in the recombination (afterglow) spectrum of Hg was measured in the spectral range from 2200A to 20,000A. The relative intensity of the strongest lines was found to vary in much the same way as in the arc. The intensity of the higher lines was relatively much stronger than in the arc so that the computed population of some of the higher energy levels was greater than for the lower levels in the same series. By determining the quanta due to radiative transitions into and out of various spectral levels, it was shown that most of the recombination occurred directly into the levels about 1.5 to 2.5 volts below the ionization potential. Continua were observed beyond the limits of eight different series, all being much less intense than the strong lines of the series. The dependence on the concentration of ions was studied and it was found that the intensity of the higher lines increased more than that of the lower. Recombination coefficients were calculated from the absolute intensities.

30. Spectra of SnH and PbH at High Pressure. W. W. WATSON AND R. SIMON, *Yale University.*—Although no band spectra are produced by Sn or Pb arcs in hydrogen at low pressure, a number of SnH and PbH band systems appear in a d.c. arc in hydrogen at four to five atmospheres pressure. A (0,0) $^2\Delta\rightarrow{}^2\Pi$ transition for SnH has first heads at 4054A and 4447A. The analysis gives $B=5.31$, $A=2182.7$ for $^2\Pi$, $B=4.91$, $A=-1.75$ for $^2\Delta$ and shows a sharp cutoff at $K'=17$. The apparently analogous transition for PbH occurs in the near ultraviolet, one principal head lying at 3810A. In the red and infra-red regions both molecules have spectra with unique intensity anomalies, such as a variation in the relative intensities of band branches with v, probably attributable to a near approach to case c conditions. The PbH red spectrum already described[1] has been extended to 9100A, revealing an additional electronic transition. The operation of the high pressure arc and its usefulness in the investigation of molecular spectra are discussed.

[1] W. W. Watson, Phys. Rev. 54, 1068 (1938).

31. Binding Energy of He^6 and Nuclear Forces. HENRY MARGENAU, *Yale University.*—The binding energy of He^6 is known from the experiments of Bjerge and Broström. In all probability, the ground state of this nucleus is a ^1S state, while the normal state of Li^6 is ^3S. The difference in the binding energies of these two nuclei which is due to the specific nuclear forces (after correction for the difference in the Coulomb energies) is known to be 3.7 ± 0.7 Mev. This value is nicely accounted for theoretically with the use of the customary nuclear parameters if the calculation is carried as far as the Feenberg-Wigner approximation.[1] The question arises as to the value of this difference when excited states are included in the perturbation calculation of the energies of the two nuclei. To answer it, a computation has been made for the ^1S state of the six-body problem similar to that for Li^6.[2] All doubly-excited states, but no others, were included. In zeroth order one obtains for the difference in the binding energies: $\Delta=2g(1-2u+5u^2)(\sigma u)^{1/2}(35.6)$ Mev, and this is equal to 3.7 Mev if the minimizing parameter σ has the same value as for Li^6 (1.4) and g, the ratio of Heisenberg to Majorana forces, is taken to be 0.23. However, with the inclusion of the doubly-excited states, the value of Δ drops to 1.26 Mev for $g=0.20$, to 1.53 Mev for $g=0.25$. Hence the agreement obtained in the Feenberg-Wigner approximation, which gives a very poor answer for the total binding energy of Li^6, is considerably disturbed when attention is given to excited states.

[1] E. Feenberg and E. Wigner, Phys. Rev. **51**, 95 (1937).
[2] H. Margenau and K. G. Carroll, Phys. Rev. **54**, 705 (1938).

32. The Theoretical Binding Energy of He^5. WARREN A. TYRRELL, JR., *Yale University.*—The binding energy of the unstable nucleus He^5 has been calculated both perturbationally and variationally. The functions employed are single particle Legendre functions. The zero-order approximation corresponds to an alpha-particle in the ground state and a p neutron. With values of the nuclear constants previously used,[1] H_{00} is -11.5 Mev. The second-order perturbation contributions of the doubly and quadruply excited functions lower this to -17.8 Mev. The convergence limit for functions of all degrees of excitation will be discussed. Variational calculations have been made with two variation parameters, one for four s particles forming an alpha-particle, and one for a p neutron. With the simplest symmetrized wave function, the plot of the energy E against the two variation parameters shows no minimum. For values of the alpha-particle parameter compatible with He^4 alone, the plot of E against the neutron parameter is almost horizontal for a certain range of the latter. This is in accord with expectation; moreover, the value of E in this region is in fair agreement with the experimentally determined instability.[2] A more refined variational calculation is in progress.

[1] H. Margenau and W. A. Tyrrell, Phys. Rev. **54**, 422 (1938).
[2] J. H. Williams, W. G. Shepherd and R. O. Haxby, Phys. Rev. **52**, 390 (1937).

33. Energy Levels of H^3, He^3 and He^4. KATHARINE WAY, *Bryn Mawr College.*—Wheeler's method of resonating groups was applied to the three-body nuclear problem. Particles 1 and 2 are considered the like particles. The wave function Ψ is then written:

$$\Psi=S_1F[(r_2+r_3)/2-r_1]\varphi(r_3-r_2)-S_2F[(r_1+r_3)/2-r_2]\varphi(r_3-r_2)$$

where the S's are appropriate spin functions and the φ's are deuteron wave functions which were found by numerical integrations of the deuteron wave equation. F is determined by the requirement that $E=\int\psi^*H\psi d\tau/\int\psi^*\psi d\tau$ be a minimum. V_{ij} was written $V_{ij}=-Ae^{-ar_{ij}^2}[(1-g-g_1-g_2)P_{ij}^M+gP_{ij}^H+g_1]+g_2P_{ij}^B]$ with $A=72\ mc^2$ and $1/a^2=2.25\times10^{-13}$ cm, and $g+g_2=0.22$. In the He problem the Coulomb term was added to V_{12}. For the state $S=\frac{1}{2}$, $L=0$, $g+g_2$ is the only important combination. The calculated energies of this state are -6.1 mMU for He^3 and -6.7 mMU for H^3. Experimental binding energies are 8.1 and 8.9 mMU, respectively. For the state $S=3/2$, $L=0$, $1-3g_1-3g_2$ is the decisive factor. Values of this combination which lead to bound states will be discussed. In the five-body problem when an approximate wave function $Ze^{-\beta R^2}$ (P state) was used for $F[(r_1+r_2+r_3+r_4)/4-r_5]=F(R)$ no virtual level of He^5 was found for any reasonable value of $1+g-5g_1-3g_2$.

34. A Study of Radioactive Be^7. J. E. HILL AND G. E. VALLEY, *University of Rochester.*—This isotope[1] (43 day) has been formed by bombardment of Lithium with protons of energies up to 6.5 Mev. The threshold for the reaction Li^7 (p, n) Be^7, determined by studying the 2.3-min. activity induced by the neutrons in silver plus paraffin, is 1.75 ± 0.05 Mev. This means that the mass of Be^7 exceeds that of Li^7 by 1.0 ± 0.05 Mev. The γ-ray spectrum of Be^7 is being closely examined both by cloud chamber and magnetic spectrograph to determine whether or not radiation other than the prominent 0.44 Mev line is present. In order that these results may not be inconclusive, the secondary electrons measured are recoils from aluminum 25 mg/cm^2 thick. If such radiation (e.g. annihilation) is present, its intensity is less than ten percent of the 0.44-Mev line. A Be^7 source less than one mg/cm^2 thick, and emitting about 10^4 quanta/sec., showed no definite evidence of positron emission, when examined in a cloud chamber filled with hydrogen at 110 cm Hg pressure. This is in agreement with previous results, and with the mass difference determined from the $p-n$ threshold.

[1] L. H. Rumbaugh, R. B. Roberts and L. R. Hafstad, Phys. Rev. **54**, 657 (1938).

35. On the Self-Energy of the Electron. VIKTOR WEISSKOPF, *The University of Rochester.*—The self-energy of the electron can be divided into two parts: the energy of the electrostatic field of the charge distribution and the energy of the interaction with the radiation field. It can be shown that in the quantum theory for a single electron the first part diverges linearly, as one expects for a charge with infinitely small radius. In the positron theory, however, this energy diverges logarithmically, which can be explained by the peculiar interaction between the electron and the vacuum. This effect is essentially connected with the exclusion principle. Any theory of particles with Bose

statistics leads to a quadratically divergent electrostatic self-energy. The energy of interaction with the radiation field is mainly due to the oscillations of the electron under the influence of the field fluctuations of the empty space. This energy diverges quadratically. In the positron theory, however, this term is canceled by another energy term, due to the current fluctuations of the vacuum. Here again the exclusion principle is essential. In Bose statistics the corresponding term has opposite sign, so that the total electrodynamic self-energy also diverges quadratically. Thus the "critical length" in the positron theory is about $l\sim(h/mc)e^{-137}$ whereas a theory with Bose statistics leads to $l\sim(h/mc)(137)^{-\frac{1}{2}}$.

36. Competition Between $p-n$ and $p-\gamma$ Reactions. CHARLES V. STRAIN, *The University of Rochester.*—When nickel is bombarded by high energy protons Cu^{61} (3.4 hr.), Cu^{62} (10.5 min.) and Cu^{64} (12.8 hr.) are formed. Each of the first two activities might be formed by either a $p-\gamma$ or a $p-n$ reaction; namely, (1) $Ni^{60}(p-\gamma)Cu^{61}$, (2) $Ni^{61}(p-n)Cu^{61}$ (threshold 2.9 Mev), (3) $Ni^{61}(p-\gamma)Cu^{62}$, (4) $Ni^{62}(p-n)Cu^{62}$ (threshold 4.6 Mev).

In a previous article[1] evidence was given that Cu^{62} was formed by (3) at proton energies below the threshold for reaction of (4). A cloud-chamber study of the positron spectra confirms this conclusion. With proton energies above the threshold of (2) (2.9 Mev) Ni^{61} can be transmuted by either a $p-\gamma$ or a $p-n$ reaction. From the excitation curves of the Cu^{61} and Cu^{62} activities the relative probabilities of the two reactions can be obtained in the energy range of 2.9 to 4.6 Mev. The ratio of the intensities of the $p-\gamma$ to the $p-n$ reaction of the nucleus Ni^{61} can be computed after correcting for the disturbing effect of the Ni^{60} $p-\gamma$ effect. This ratio falls sharply from a high value at three Mev to a value much smaller than $\frac{1}{4}$ at 4.5 Mev. This is a good illustration of the rapidly increasing probability of neutron emission with increasing velocity of the neutron.

[1] C. V. Strain, Phys. Rev. **54**, 1021 (1938).

37. Resonance Scattering of Protons by Lithium. EDWARD CREUTZ, *University of Wisconsin.* (*Introduced by G. Breit.*)—The scattering of protons from a thick lithium target has been studied in the energy region 260–600 kev at a scattering angle of 156°, using a ball counter. The number of counts per microcoulomb at 458 kev is 2.1 times the value at 408 kev and at 486 kev it has dropped to 1.41 times the value at 408 kev. The observed resonance peak is distorted by absorption of protons scattered deep in the target, but this effect is least for the low energy side, where the curve shows a maximum slope at the same proton energy as the lithium gamma-ray resonance within ±5 kev. Since the effect of absorption tends to move the maximum slope to lower energy, the lower limit of the scattering resonance maximum at 156° is 435 kev, assuming 440 kev as the resonance maximum for the 17-Mev gamma-radiation. The scattering from a thick Be target was found to increase smoothly with energy showing that the resonance effect is not a peculiarity of the counter. This scattering anomaly has been suggested by Professor Breit to indicate that the gamma-radiation obtained when Li^7 is bombarded with 440-kev protons arises from a virtual level of Be^8, and not from an excited alpha-particle, a previously tenable alternative hypothesis.

38. The Scattering of Neutrons by Hydrogen and Deuterium Molecules. MORTON HAMERMESH, *New York University,* AND JULIAN SCHWINGER, *Columbia University.*—The general method of treating the scattering of neutrons by molecules, taking account of the spin dependence of nuclear forces and the symmetry properties of molecules containing several identical particles, has been given by Schwinger and Teller, and applied by them to H_2. We have extended their calculations to a wider range of neutron energies and to several other transitions, and applied them to an analysis of the experimental data of Dunning *et al.* We find that their data can be fitted with a neutron-proton scattering cross section of $(20\pm2)\cdot10^{-24}$ cm², verifying the result obtained by direct measurement; but simultaneous agreement for both *ortho* and *para* H_2 can be obtained only by assuming a departure from thermal equilibrium in the form of a decreased number of neutrons in the region below ~0.01 ev and a possible high energy "tail." The larger value of the neutron-proton cross section increases the elastic scattering of *para* H_2, and makes it more susceptible of measurement. It has already been emphasized that such experiments would enable a determination of the range of the neutron-proton interaction in the triplet state. Calculations have been made for the scattering by *ortho* and *para* D_2, assuming various values of the scattering amplitudes for the doublet and quartet states. From such measurements, the values of these amplitudes may be deduced, thus affording an important source of information concerning nuclear forces.

39. The Scattering of D−D Neutrons. S. SEELY, W. H. ZINN AND V. W. COHEN, *Columbia University.*—Measurements of the total scattering cross sections of various elements for the 2.8-Mev neutrons from the D−D reaction previously reported by us[1] have been extended to a greater number of elements. The cross sections vary quite irregularly with atomic weight. Measurements of the cross sections of some elements for 2.4-Mev neutrons have also been made. Oxygen, in particular, showed a change in cross section with the change in energy of the incident neutrons. The neutron detection system consists of a small helium-filled ionization chamber two cm in diameter at a distance of 32 cm from the target. The ionization chamber is coupled to a linear amplifier, the associated scaling unit being so adjusted as to record only those pulses, as observed in an oscillograph, approximately twenty times the background.

[1] W. H. Zinn, S. Seely and V. W. Cohen, Phys. Rev. **53**, 921(A) (1938).

40. Elastic Scattering of Fast Neutrons. R. F. BACHER, *Cornell University.*—Experiments have been carried out to ascertain the albedo effect of fast neutron scattering by

Pb. The source of neutrons was a Be target located in a brass tube outside the cyclotron chamber proper, and bombarded with 5 to 10 μa of 1.5-mv deuterons. Fast neutrons were detected by a Cd-shielded Al detector which gave the 10-minute period of Mg^{27}. The activity of the detector which was placed four cm from the source was taken with and without Pb surrounding detector and source. When Pb was placed between source and detector, activity was reduced to 65 percent. When both source and detector were surrounded with Pb there was a slight increase in activity. The slight increase observed may well be due to the difficulty of repeating the irradiation. This result indicates that at least the greater part of the scattering is inelastic, with loss of energy by the neutrons sufficiently large so that they no longer activate the Al. This result is in agreement with the large energy losses observed for neutrons which have passed through Pb, but is in disagreement with various determinations* of the amount of elastic scattering which indicate from 60 to 90 percent.

* D. C. Grahame and G. T. Seaborg, Phys. Rev. 53, 795 (1938); E. Hudspeth and T. W. Bonner, Phys. Rev. 53, 928(A) (1938).

41. The Ionization Produced in Gases by Fast Neutron Irradiation. PAUL C. AEBERSOLD* AND GLADYS A. ANSLOW,** *University of California.*—A collimated beam of fast neutrons was directed along the axis of a cylindrical, brass ionization chamber of 100 cc volume and the ionization produced in fourteen gases at pressures from three mm of Hg to three atmospheres was investigated using an electrometer tube measuring device. The source was beryllium bombarded by deuterons accelerated to eight Mev in a cyclotron. The collimation was achieved by a channel through a water tank, the channel and the outside of the tank having thick walls of Pb to absorb gamma-rays produced in or scattered from the tank. To suppress gamma-rays from the source the beam was filtered through three cm of Pb. That the main ionization with such an arrangement is due to neutrons can be seen from the very different relative ionization in the various gases compared to that for gamma-rays alone. Moreover, calculations by two methods give small values for the percentage contribution by gamma-rays to the measured ionization. Subtracting this small contribution, the ionization due to neutrons alone is deduced and related to the values to be expected from the production of recoil nuclei in the gas by elastic scattering. The agreement with expectation using Dunning's cross sections is excellent except for N_2 and A for which disintegrations by neutron absorption are appreciable. The results show particularly that the relative ionization in various hydrogenous materials by fast neutrons can be closely approximated on the basis of elastic scattering of the neutrons.

* Fellow of the Finney-Howell Foundation.
** On sabbatical leave from Smith College.

42. On the Nuclear Moments of the Rubidium and Chlorine Isotopes. P. KUSCH AND S. MILLMAN, *Columbia University.*—A comparison of the ratios of the nuclear magnetic moments of two isotopes of the same element as obtained from an observation of hyperfine structure and as found by direct observation tests the validity of the assumption that magnetic interaction between the nuclear moment and the electronic structure is sufficient to explain observed h.f.s. splittings in atomic energy levels. We have applied the molecular beam resonance method to a measurement of the nuclear moments of Rb^{87} and Rb^{85}. Using Rb_2 molecules, the observed resonance minima and the known values of nuclear spins yield 2.730 and 1.340 as the moments of Rb^{87} and Rb^{85}, respectively, referred to the moment of Li^7, 3.250 nuclear magnetons. The observed ratio, $\mu_{Rb^{87}}/\mu_{Rb^{85}} = 2.037 \pm 0.5$ percent, is to be compared with the ratio 2.026 ± 0.2 percent found by Millman and Fox,[1] who measured the h.f.s. of the ground states of the rubidium isotopes by the atomic beam zero moment method. In view of the precision of the present result it is not certain that this difference represents a real physical effect. The nuclear g's of Cl^{35} and Cl^{37} have also been measured. The g values of these two nuclei are 0.546 ± 0.5 percent and 0.454 ± 0.5 percent, respectively. The spin of Cl^{35} is probably 5/2 from the measurements of Elliott[2] on the alternating intensities in band spectra. The moment of Cl^{35} is then 1.365 nuclear magnetons. No information on the spin of Cl^{37} is available.

[1] S. Millman and M. Fox, Phys. Rev. 50, 220 (1936).
[2] A. Elliott, Proc. Roy. Soc. 127A, 638 (1930).

43. The Electric Quadrupole Moment of In^{115}. DONALD R. HAMILTON AND NICHOLAS A. RENZETTI, *Columbia University.*—The h.f.s. $\cos^2$ interaction ascribed to a nuclear electric quadrupole moment, Q, has been investigated in the $^3P_{1/2}$ metastable state of In^{115} using the zero moment method of atomic beams.[1] Schüler's and Schmidt's spectroscopic determination of Q, using this state,[2] utilizes three h.f.s. separations; the present method takes advantage of 13 observables, i.e., the fields for zero moment peaks arising from certain of the 40 magnetic levels. These peaks are sensitive to Q; order is reversed and peak ratios, often measurable to $\frac{1}{4}$ percent, are sometimes changed by 30 percent. Their behavior is completely described in terms of the nuclear g factor,[3] the electronic g factor, and constants of the equation $\Delta\nu_F = (aC/2) + bC(C+1)$ giving the position of the levels in zero field. $(C = F(F+1) - I(I+1) - J(J+1).)$ The first term is the usual interaction. The second arises from Q; the constant b, involving atomic wave functions, is directly proportional to Q. Observed peak ratios determine b/a to one percent; a is obtained by field calibration in terms of the first peak of the Cs ground state and the $\Delta\nu$ of this state, 0.3067 ± 0.0004 cm^{-1}.[4,5] We find $a = (8.11 \pm 0.04) \times 10^{-3}$ cm^{-1} and $b = (0.0521 \pm 0.0007) \times 10^{-3}$ cm^{-1}. This gives an actual h.f.s. separation 0.1186 ± 0.0007 cm^{-1}, or 0.1217 ± 0.0006 cm^{-1} for $Q = 0$. Schüler and Schmidt give $a = 7.97$, $b = 0.048$, and total separation 0.120 cm^{-1}. Our b is eight percent higher than their 0.048, from which they deduce $Q = 0.8 \pm 0.2$.

[1] V. W. Cohen, Phys. Rev. 46, 713 (1934).
[2] H. Schüler and T. Schmidt, Zeits. f. Physik 104, 468 (1937).
[3] I. I. Rabi, S. Millman and J. R. Zacharias, Phys. Rev. 53, 384 (1938).
[4] L. P. Granath and R. K. Stranathan, Phys. Rev. 48, 725 (1935).
[5] S. Millman and M. Fox, Phys. Rev. 50, 220 (1936).

44. The Temperature in White Dwarf Stars. R. E. MARSHAK AND H. A. BETHE, *Cornell University.*—It is usually assumed that the temperature in a white dwarf is almost constant over the degenerate interior and changes appreciably only in the nondegenerate surface layer. For the temperature at the boundary of the two regions in Sirius B, values between $2\cdot10^7$ (Stromgren) and $6\cdot10^7$ degrees have been given. These values seem to be too high, due to the use of incorrect opacity laws. The actual opacity is 5 to 100 times less than the Kramers value, resulting in a boundary temperature of 0.8 to $1.0\cdot10^7$ degrees. In the interior the energy transport is mostly by conduction, conduction and radiation being about equally important at the boundary. There is an appreciable increase of temperature from the boundary to the center where $T\approx2.5\cdot10^7$ degrees. These high temperatures are only reconcilable with the observed small luminosity if the hydrogen content is very low. The transition region from nondegenerate to degenerate gas cannot be treated by the methods previously used in astrophysics which give much too low values for the density of free electrons. Instead, we propose to use the Thomas-Fermi equation with finite boundary conditions as for metals. This equation has been generalized to include the effect of finite temperature and a mixture of elements.

45. The Self-Energy of the Electron. H. A. BETHE, *Cornell University.*—It has never been decided whether the divergence of the self-energy of the electron is inherent in the fundamental equations of quantum electrodynamics or is due to the use of perturbation methods in their integration. We have found an almost exact method of integration for the particular case of the nonrelativistic Schrödinger theory. In this theory, only the A^2 term in the interaction between electron and (transverse) electromagnetic field need be considered but not the $A\cdot p$ term. In first approximation, the well-known result for the self-energy is obtained, viz.

$$W_1\approx\frac{hc}{r_0}\frac{e^2}{mc^2r_0}$$

where r_0 is the "cutting-off" radius. Successive approximations differ by a factor $\gamma=e^2/(mc^2r_0)$ and have alternating sign. For very large γ, perturbation theory is no longer valid; the radiation field will then in general contain many quanta. But just this fact can be used for the integration because the total energy of n quanta ($n\gg1$) will differ only slightly from its mean value of $2nhc/r_0$. Using this mean value instead of the actual energy, the rest of the integration can be carried out exactly and gives for the self-energy the value, $W\sim(hc/r_0)\gamma^1\sim r_0^{-1}$. This shows that the divergence is inherent in the fundamental equations and cannot be removed by improved methods of integration.

46. General Relativity Theory and Flat Space. N. ROSEN, *Massachusetts Institute of Technology.* (*Introduced by M. S. Vallarta.*)—At present it appears that gravitation is unimportant in the problem of the nucleus. It may be that it is actually of fundamental significance in determining nuclear forces but that existing theories have to be modified in order to show it. As a first step in the search for a suitable modification, the problem is considered of treating the general theory of relativity from the standpoint of an underlying flat space. In this way some properties of gravitational forces are obtained.

47. On Thermal and Stress Dependence of Elasticity in Solids. H. LUDLOFF, now at *Cornell University.* (*Introduced by H. A. Bethe.*)—Previously a method was devised by which the elastic constants are determined from the interference figures occurring in diffracting light from ultrasonics in solids. From the interference figures the directional dependence of thermal waves in an atomic lattice can also be directly obtained, so that in related thermodynamical investigations tedious calculations can be avoided. The original theoretical basis of the method can now be further generalized at two points: (1) The change in the interference figures, when the solid is transformed from the elastic to the plastic state, can now be quantitatively determined; and conversely from the observation of the changed interference figures the nonlinear relation between deformation and tension can be derived for any value of tensile stress. (2) Also the change of the interference patterns due to temperature dependence of the elastic constants can now be predicted from the more generalized derivation. Since for ultrasonics the change of the elastic behavior is very sensitive to temperature, the pattern behavior near the melting point should give, according to Brillouin, some information concerning the melting process.

48. Determination of the Nature of a Light Source from Wide-Angle Interference Experiments. O. HALPERN AND F. W. DOERMANN, *New York University.*—It has previously[1] been shown that wide-angle interference phenomena can be used to determine the nature of (electric and magnetic) multipoles which make up the light source. The interference pattern was found to depend in a characteristic matter on the geometrical arrangement, the optical properties of the mirrors used and the nature of the light source. Applying these considerations to a wide-angle interference experiment performed by Selenyi[2] the authors were able to determine the active centers in the fluorescence substance which served as source. The polarization properties of the pattern do not permit to decide whether the source consists of electric dipoles or magnetic quadropoles (which latter can, of course, be ruled out by other considerations). The dependence of the pattern on the angle of divergence of the two primary beams clearly shows that the source consists of electrical dipoles.

[1] O. Halpern and F. W. Doermann, Phys. Rev. **52**, 937 (1937); F. W. Doermann, Phys. Rev. **53**, 420 (1938).
[2] P. Selenyi, Zeits. f. Physik **108**, 401 (1938).

49. Measurement of X-Ray Production in the Range 0.8 to 2.0 Million Volts. L. C. VAN ATTA AND D. L. NORTHRUP, *Massachusetts Institute of Technology.*—Some preliminary focusing tests with an electron beam have been made in the accelerating tube of the Massachusetts Institute of Technology electrostatic generator in its new location in

Cambridge. In the course of these tests it has been possible to make some measurements on x-ray intensity as a function of angle, absorber and voltage in the range 0.8 to 2.0 mv. The x-ray intensity in the forward direction was found to increase approximately as the 5/2 power of the voltage while the concentration in the forward direction increased as would be expected. Absorption coefficients were measured for 1.0, 1.5 and 2.0 mv with lead thicknesses up to 2.5 cm. Intensity measurements were made with a Victoreen condenser type *r*-meter. The results are presented primarily because of their possible usefulness to those considering the installation of high voltage x-ray equipment.

50. The Uniqueness of an X-Ray Crystal Analysis. A. L. PATTERSON, *Bryn Mawr College.*—It has long been known that the essential problem of x-ray crystal analysis lies in the determination of the phases to be allotted to the quantities $F(hkl)$ whose absolute values can be obtained from x-ray intensity measurements. These quantities when given appropriate phases form the Fourier coefficients for the distribution of electron density in the crystal. A Fourier series whose coefficients are the measured quantities $|F(hkl)|^2$ has been used in x-ray analysis to give a direct determination of interatomic distances in crystals. Langmuir and Wrinch[1] have suggested that if the positions of the peaks in the F^2 series are known, the structure is uniquely determined. In the present paper it is shown that if the peaks in the F^2 series can be resolved, the structure determination can be made unique, except for the fundamental ambiguity of a center of symmetry. The proof depends on a knowledge of the atoms which compose the crystal and the demonstration that there is only one way in which a given set of atoms can produce a given F^2 series. A unique determination depends on the identification of the peaks of the F^2 series, and examples are presented which suggest that caution must be exercised in attempting to ascribe uniqueness to the interpretation of the structure of complex crystals.

[1] I. Langmuir and D. M. Wrinch, Nature **142**, 581 (1938).

51. A General Equation of State: Equations for Ammonia and Steam. J. L. FINCK, *New York, New York.*—In a published paper,* the writer has considered the possibility of enlarging the scope of thermodynamic systems by including metastable as well as the ordinary stable states. To do so, he has shown that it is necessary to consider p, v, T as three independent variables for a system in gaseous or liquid-vapor state. On this basis many phenomena can be explained very simply. In continuing this line of thought, the writer has been able to develop a general, explicit equation of state which may apply to a single gaseous phase, or a liquid-vapor system, where there is a single type of transformation. For the entropy η, and the three independent variables p, v, T, the equation is $\eta = a+bv+cp+dpv+(e+fv+gp+hpv)\ln T$. The latent heat of transformation is $\lambda_{P,T} = T(v_2-v_1)(\partial\eta/\partial v)_{P,T} = T(v_2-v_1)[b+dp+(f+hp)\ln T]$. Using the most recent ammonia and steam tables, the following values of the constants have been found. (η, p, v, T are in British units.)

	Ammonia		*Steam*	
	Liquid-vapor	Superheated	Liquid-vapor	Superheated
a	−6.3238	−31.4922	−6.1496	+0.8445
b	−0.6660	+ 0.12586	−0.4308	−0.005090
c	$+0.0_3$3982	− 0.07790	$+0.0_3$1059	$-0.0_3$1210
d	+0.03280	− 0.09284	+0.02659	$-0.0_4$4551
e	+1.0469	+ 6.6863	+0.9924	+0.12487
f	+0.11292	− 0.01886	+0.06808	$+0.0_3$8938
g	$-0.0_4$6312	+ 0.01118	$-0.0_4$1496	$+0.0_3$1446
h	−0.004761	+ 0.01046	−0.003639	$+0.0_4$9145

These equations check the experimental data over the entire saturation dome, in most cases, to much better than one percent. In the superheated regions the agreement is of the order of three to five percent over the entire pressure and temperature ranges given in the tables.

* J. L. Finck, J. Frank. Inst. **225**, 411–435 (1938).

52. Probability of *K* Ionization of Nickel by Cathode Rays. D. L. WEBSTER, *Stanford University;* L. T. POCKMAN, *Cornell University;* K. HARWORTH AND PAUL KIRKPATRICK, *Stanford University.*—The probability of K ionization of nickel by cathode-ray bombardment has been experimentally determined in arbitrary units as a function of cathode-ray energy in a range extending from two to twenty-two times the K ionization energy ($V_K = 8320$ volts) by measuring the dependence of the $K\alpha$ line intensity from thin nickel targets upon tube voltage. Only small theoretical corrections need be applied to the original data. The targets ranged in thickness from 10^{-6} cm to $2\cdot10^{-6}$ cm and were free except for a backing of cellulose acetate approximately 10^{-6} cm thick. A new technique has been developed for making and mounting thin films of large area (10 cm²). A comparison of these data with the corresponding data from helium and silver makes possible a direct qualitative estimate of both the influence of relativity and the influence of nonhydrogenic fields on the probability of K ionization. Although these data agree only roughly with nonrelativistic quantum mechanical theories, they agree within experimental error with the relativistic theory of Soden for $V/V_k > 4$ if theory and experiment are arbitrarily matched at $V/V_k = 22$. For $V/V_k < 4$, the theory falls below the experiment, in qualitative agreement with Soden's work on the limitation of the Born Approximation.

53. The Electronic Structure of Alloys. MILLARD F. MANNING, *University of Pittsburgh.*—Considerable progress has been made, particularly by Hume-Rothery, in the correlation and interpretation of the phonomena connected with solid solutions of metals. Except for the work of Jones, there have been few connections established between this work and the quantum-mechanical theory of metals. The case when the solvent is copper and the solute is one of the elements following it in the periodic table is the easiest to discuss. For this case the highest occupied levels around the copper atoms will be lower than highest levels corresponding to the solute atoms at the same atomic volume and crystal structure. This means that for dilute

solid solutions the solute atoms will have a positive charge and the copper atoms will have a negative charge. This negative charge around the copper atoms accounts for the expansion of the lattice and for the lowering of the freezing point. The negative charge on the solute atoms accounts for a number of properties. In particular, it offers an explanation for the fact that the coefficient of diffusion of copper in copper cannot be found by extrapolation of the observed coefficients of diffusion in copper of the elements following copper in the periodic table.[1]

[1] J. Steigman, W. Shockley and F. C. Nix, Washington Meeting, December, 1938.

54. Inertial Mass. PETER FIREMAN, *Magnetic Pigment Company, Monmouth Junction, New Jersey.*—The question is raised as to the reality of inertial mass as a specific attribute of matter: Is there in the inertial force of a mass anything apart or beyond the force of gravitation? In the author's opinion, inertia is always a manifestation of gravitational force, at times more obvious and at times less obvious. Obvious instance: a body resists external force owing to its weight. Less obvious instance: a highly polished steel sphere is resting on a perfectly smooth plane. A push starts it rolling; it keeps moving indefinitely. Why? Resting on a point, it was in a state of unstable equilibrium. The push disturbed its equilibrium, depressed its center of gravity in the direction of the motion due to the push. The disturbance is kept up, the depression continues and there is nothing to restore the original balance. Consequently the sphere keeps rolling on and on.

55. Difference in Scope of Theoretical Physics and Pure Mathematics. JOSEPH T. O'CALLAHAN, S.J., *College of The Holy Cross.*—With the ever increasing importance of mathematics in the study of physics, there has been manifest in recent years a tendency to regard theoretical physics merely as a branch of mathematics. To oppose this tendency it is necessary to insist upon the difference in the scope of the two sciences. Briefly the difference is this: theoretical physics incorporates in the problem some actual physical data, whereas no physical data are incorporated in any pure mathematical problem. This difference is elaborated to show that mathematics, as such, merely requires compatibility of elements forming the concepts; while the constructs of physics require a further compatibility with some actually existing reality. A short reference to experimental physics shows that there are three entirely different types of "law" involved, characteristic respectively of experimental physics, theoretical physics and pure mathematics. The example of the inverse square law of attraction is used to concretize the discussion.

56. A Re-evaluation of the Atomic Constants. FRANK G. DUNNINGTON, *Rutgers University.*—The experimental work on all significant determinations of the atomic constants e, m and h has been reexamined and the results recalculated with two changes: (1) all assumptions as to values of combinations of atomic constants have been eliminated so that the results given represent what the experiments actually yield and (2) a consistent set of auxiliary constants has been used throughout. A Birge-Bond diagram will be given to present the results graphically and illustrate clearly the discrepancy. A least squares solution of these results has been made *without* using the Rydberg formula. The results are:

$$e = (4.8025 \pm 0.0007) \times 10^{-10} \text{ e.s.u.},$$
$$m = (9.1073 \pm 0.0024) \times 10^{-28} \text{ g},$$
$$h = (6.6133 \pm 0.0034) \times 10^{-27} \text{ erg·sec.},$$
$$e/m_0 = (1.7590 \pm 0.0004) \times 10^{7} \text{ e.m.u.},$$
$$h/e = (1.3771 \pm 0.0007) \times 10^{-17} \text{ e.s.u.}$$

As to where the discrepancy originates, this solution together with an analysis of each type of measurement as to the fundamental laws involved indicates that either: (1) the existing body of experimental results is substantially correct and the Rydberg formula is in error, or (2) the Rydberg formula is correct and all the measurements of h/e and the radiation constants are in error, the error being in some cases presumably experimental, and in other cases in the theory involved.

57. Absorption Spectrum of Heavy Benzene at 2730–2250A. H. SPONER, *Duke University.*—The absorption spectrum of C_6D_6[1] at 2730–2250A was photographed in the first order of a three-m grating spectrograph. As in C_6H_6 the spectrum consists of a number of series with bands progressing in intervals of 878 cm^{-1} (totally symmetrical frequency in the upper state), each interval containing a progression with 140-cm^{-1} spacing. The whole system corresponds to a forbidden electronic transition $^1A_{1g} \rightarrow {}^1B_{2u}$ made allowed by the interacting twofold degenerate vibrations of symmetry $E_g{}^+$. In agreement with this the first bands of the two major series represent vibrational transitions 0→497 and 579→0, the 579 and 497 cm^{-1} being carbon frequencies of symmetry $E_g{}^+$ in the ground and excited states, respectively. This conclusion was drawn from the fact that the distance between the above-mentioned two bands is $38789 - 37713 = 1076 = 579 + 497$ and from the occurrence of other progressions displaced from the main series by 82 cm^{-1} toward long waves, thus indicating transitions $579 \rightarrow 2 \times 497$ and $2 \times 579 \rightarrow 497$. The frequency difference of 140 cm^{-1} is considered as an $n-n$ transition of the carbon $E_u{}^+$ vibration (in analogy to Kistiakowsky's and Solomon's explanation of the 160 cm^{-1} frequency difference in C_6H_6). Plausible interpretations can be given for other progressions. The analysis is in agreement with the one proposed for light benzene.[2]

[1] I am much obliged to Professor D. H. Andrews for lending me the heavy benzene.

[2] To be published shortly in cooperation with G. Nordheim, A. L. Sklar and E. Teller.

58. Further Studies on the Infra-Red Absorption Spectra of the Fatty Acids. R. C. HERMAN AND R. HOFSTADTER, *Princeton University.*—The monomer and dimer spectra of two more acetic acids, CD_3COOH and CD_3COOD, as well as light and heavy propionic acids, C_2H_5COOH and C_2H_5COOD, have been obtained with a rocksalt spectrometer. The wave numbers of the principal bands in the

monomer spectrum of CD_3COOH are: 3640, 2225, 1760, 1335, 1215, 1162, 1065, 925, 820, 796 cm^{-1}. Those in CD_3COOD are: 2660, 2270, 1760, 1280, 1160, 1060, 1000, 925, 812, 785 cm^{-1}. Although it has not been possible to make a complete assignment of bands, certain regularities have been observed in the monomers of the four acetic acids: CH_3COOH, CH_3COOD,[1] CD_3COOH, CD_3COOD. These will be discussed. The heat of association of heavy propionic acid has been found by using a method previously described.[1] The results of a single determination give a value of 6400 calories per bond per mole.

[1] R. C. Herman and R. Hofstadter, J. Chem. Phys. **6**, 534 (1938).

59. The Infra-Red Absorption Spectrum of Phenol Vapor. V. Williams, R. C. Herman and R. Hofstadter, *Princeton University.*—The absorption of the single molecules of phenol has been examined in the infra-red from 1μ to 13μ with a rocksalt spectrometer. The spectrum of the vapor was obtained at 93°C and 164°C at pressures of 14 mm and 19 mm, respectively. The regions from 2.3μ (4350 cm^{-1}) to 3.5μ (2860 cm^{-1}) and from 9μ (1111 cm^{-1}) to 12μ (850 cm^{-1}) were repeated at higher pressures (about 180 mm) in order to bring out weak bands. Our absorption curves do not show the association bands near 3μ (3333 cm^{-1}) found in solid and liquid phenol and in solutions of phenol in CCl_4,[1] but do show the free O—H band at 2.7μ (3705 cm^{-1}). This indicates that we have obtained the monomer spectrum. We find a sharp band at 8μ (1250 cm^{-1}) and a relatively broad band at 8.5μ (1176 cm^{-1}). The center of gravity of these two bands lies close to a band whose variations in position and intensity with temperature were studied by R. R. Brattain[2] with the same instrument. In this region of the spectrum of solid phenol, J. Lecomte[3] finds bands at about 8.4μ (1190 cm^{-1}) and 8.8μ (1137 cm^{-1}).

[1] J. J. Fox and A. E. Martin, Proc. Roy. Soc. London **162A**, 419 (1937).
[2] R. R. Brattain, J. Chem. Phys. **6**, 298 (1938).
[3] J. Lecomte, J. de phys. et rad. **8**, 489 (1937).

60. Accommodation Coefficient of Helium *vs.* Nickel. Barbara G. Raines, *Bryn Mawr College.*—The variation with temperature of the accommodation coefficient of helium against nickel was investigated in the range 90–369°K by measuring the heat losses of an "A" nickel wire at 90, 194, 273 and 369°K both in vacuum and in an atmosphere of spectroscopically pure helium which at equilibrium attained a pressure of the order of 10 dynes/cm^2. After flashing in vacuum, the nickel wire was allowed to come to equilibrium before the helium was introduced. The accommodation coefficient (a_0) for helium against gas-free nickel was determined by extrapolating the heat loss through the gas to zero time after its admission. Within the experimental error, a_0 was constant over the entire temperature range, the average of seven determinations being 0.067 ± 0.006. The mean values at the four temperatures do, however, show a slight increase with rising temperature, being 0.061, 0.066, 0.071 and 0.074 at 90, 194, 273 and 369°K, respectively. The equilibrium values (a_e) of the accommodation coefficient (attained after about four minutes) were found to be 0.51, 0.45, 0.36 and 0.33 at 90, 194, 273 and 369°K, respectively. The accommodation coefficients here reported have not been corrected for roughening of the surface of the wire due to heat treatment.

61. An Apparatus for Determining the Orientation of Crystals by X-Rays. F. E. Haworth, *Bell Telephone Laboratories, Inc.*—An apparatus has been developed in which orientations of single crystals, and the crystals in polycrystalline materials, can be studied with x-rays by rotating the specimen and moving a photographic film at the same time. The apparatus combines the best features of both the Weissenberg goniometer[1] and that of Dawson[2] by having the x-ray beam incident along the axis of a cylindrical film and thus recording a Debye-Scherrer circle instead of a layer line. The motion of the film and rotation of the specimen may be continuous or in steps. For motion in steps an automatic mechanism is used which exposes the film for a length of time controlled by an electric clock, and then moves the film and rotates the specimen an amount controlled by a revolution counter geared to the motor. When the cylindrical film is flattened the Debye-Scherrer circles become straight lines and a transparent net with rectangular coordinates is used to measure the angles. The data are then easily plotted in stereographic projection.

[1] K. Weissenberg, Zeits. f. Physik **23**, 229 (1924).
[2] W. E. Dawson, Phil. Mag. **5**, 756 (1928).

62. An Investigation into the Gettering Powers of Various Metals for the Gases Hydrogen, Oxygen, Nitrogen, CO_2 and Air. Louis F. Ehrke and Charles M. Slack, *Westinghouse Electric & Manufacturing Company.*—Measurements of the "gettering" or clean-up ability of aluminum, magnesium, thorium, uranium, misch metal, zirconium and barium for the common gases were made. In most cases the measurements were quantitative and represent gettering powers unassisted by an electric discharge or other source of ions. The effect of temperature conditions on the gettering and keeping properties of several of the getters is given. The superior gettering powers of the diffuse layers produced by vaporizing the getters in the presence of a gas, as compared to those of the bright getter deposits produced in a high vacuum, were confirmed. Barium and misch metal were found to be the most active of the materials tried, and the convenient forms in which barium is now commercially obtainable would seem to make it first choice for most work, though it is not effective in the presence of Hg vapor. Magnesium and aluminum showed little activity without the presence of a discharge. Thorium and uranium showed considerable activity for H_2 and O_2, but the high temperatures needed for flashing make them rather inconvenient to use.

63. Thermal Conductance of Metallic Contacts. C. Starr and R. B. Jacobs, *Massachusetts Institute of Technology.*—In cryogenic apparatus, the thermal conductance between two clean metallic surfaces, in contact in a vacuum, is sometimes of importance. Such contacts may be employed

for thermal switching purposes, and must be free of grease in order to operate at low temperatures. The properties of clean gold, silver and copper contacts, operating in vacuum, were studied at room and liquid nitrogen temperatures as a function of contact pressure up to three kg/cm². The thermal conductance of the contacts was found to increase with increasing contact pressure; the relationship was linear for copper only. The flatter the contact surfaces, the better was the conductance. At room temperatures, gold and silver were both equally better than copper, but at liquid nitrogen temperatures the order of merit was silver, gold, copper. Copper and gold grow progressively worse with time at low temperatures, perhaps due to adsorption phenomena. Silver did not exhibit this behavior, and as its contact conductance is least affected by temperature, it is the logical choice as a thermal contact material for low temperature work.

64. Determination of the Radon Content of the Spring Waters of Fairmount Park. J. LLOYD BOHN AND FRANCIS H. NADIG, *Temple University.*—Fairmount Park has an area of over 3000 acres within the city limits of Philadelphia, and has numerous springs which are the subject of this investigation. Of 12 springs already determined the values run from 2×10^{-10} to 35×10^{-10} curies per liter of water. Some of these values are rather high for springs in the United States and Canada[1] except those near known radium deposits. The more active springs issue from an early Cambrian formation while the less active ones issue from a Precambrian formation known as Wissahickon gneiss. Data on the radon content of tap and river waters and on the radium content of some of these waters will be included.

[1] Bulletin of the National Research Council on Radioactivity, Number 51, by A. F. Kovarik and L. W. McKeehan.

AUTHOR INDEX TO ABSTRACTS OF THE NEW YORK MEETING

Abramson, Harold A.—No. 23
Aebersold, Paul C. and Gladys A. Anslow—No. 41
Alter, B. E. K. and R. T. K. Murray—No. 2
Anslow, Gladys A.—see Aebersold, Paul C.

Bacher, R. F.—No. 40
Beams, J. W.—see Masket, A. V.
Bethe, H. A.—No. 45
—— see Marshak, R. E.
Bohn, J. Lloyd and Francis H. Nadig—No. 64
Boothby, O. L.—see Cioffi, P. P.
Bozorth, R. M.—see Williams, H. J.
Brickwedde, F. G. and R. B. Scott—No. 1

Cartwright, C. Hawley and A. Francis Turner—No. 18
Chodorow, Marvin—No. 17
Cioffi, P. P. and O. L. Boothby—No. 6
Cohen, V. W.—see Seely, S.
Creutz, Edward—No. 37

Danforth, W. E.—see Korff, S. A.
Doermann, F. W.—see Halpern, O.
Dunnington, Frank G.—No. 56

Ehrke, Louis F. and Charles M. Slack—No. 62

Failla, G.—No. 27
—— see White, T. N.
Finck, J. L.—No. 51
Fireman, Peter—No. 54

Garth, R. C., G. E. Moore and H. W. Webb—No. 28
—— see Moore, G. E.

Halpern, O. and F. W. Doermann—No. 48
Hamermesh, Morton and Julian Schwinger—No. 38
Hamilton, Donald R. and Nicholas A. Renzetti—No. 43
Harrison, J. R. and I. P. Hooper—No. 15
Harworth, K.—see Webster, D. L.
Haworth, F. E.—No. 61
Hector, L. G. and Mahlon F. Peck—No. 5
Herman, R. C. and R. Hofstadter—No. 58
—— see Williams, V.
Herring, Conyers and A. G. Hill—No. 8
Hill, J. E. and G. E. Valley—No. 34
Hill, A. G.—see Herring, Conyers
Hofstadter, R.—see Herman, R. C.
—— see Williams, V.
Hooper, I. P.—see Harrison, J. R.
Humphreys, Richard F.—No. 13

Ingersoll, L. R., P. Rudnik and F. G. Slack—No. 4

Jacobs, R. B.—see Starr, C.

Kirkpatrick, P.—see Webster, D. L.
Korff, S. A. and W. E. Danforth—No. 21
Kusch, P. and S. Millman—No. 42

Linke, F. W.—see Masket, A. V.
Locher, Gordon L.—No. 20
Ludloff, H.—No. 47

Manning, Millard F.—No. 53
Margenau, Henry—No. 31
Marinelli, L.—No. 26
—— see White, T. N.

Marshak, R. E. and H. A. Bethe—No. 44
Marton, L.—No. 3
Masket, A. V., F. W. Linke and J. W. Beams—No. 12
Millman, S.—see Kusch, P.
Montgomery, C. G. and D. D. Montgomery—No. 22
Montgomery, D. D.—see Montgomery, C. G.
Moore, G. E., R. C. Garth and H. W. Webb—No. 29
—— see Garth, R. C.
Murray, R. T. K.—see Alter, B. E. K.

Nadig, Francis H.—see Bohn, J. Lloyd
Nielsen, W. M.—No. 19
Northrup, D. L.—see Van Atta, L. C.

O'Brien, Brian—No. 14
O'Callahan, Joseph T., S.J.—No. 55

Patterson, A. L.—No. 50
Peck, Mahlon F.—see Hector, L. G.
Pockman, L. T.—see Webster, D. L.

Raines, Barbara G.—No. 60
Renzetti, Nicholas A.—see Hamilton, Donald R.
Rosen, N.—No. 46
Rudnik, P.—see Ingersoll, L. R.

Schwinger, Julian—see Hamermesh, Morton
Scott, R. B.—see Brickwedde, F. G.
Seely, S., W. H. Zinn and V. W. Cohen—No. 39
Simon, R.—see Watson, W. W.
Slack, Charles M.—see Ehrke, Louis F.
Slack, F. G.—see Ingersoll, L. R.
Sponer, H.—No. 57
Starr, C. and R. B. Jacobs—No. 63
Stewart, David W.—No. 16
Strain, Charles V.—No. 36

Tonks, L.—No. 11
Trump, J. G. and R. J. Van de Graaff—No. 24
Turner, A. Francis—see Cartwright, C. Hawley
Tyrrell, Warren A., Jr.—No. 32

Valley, G. E.—see Hill, J. E.
Van Atta, L. C. and D. L. Northrup—No. 49
Van de Graaff, R. J.—see Trump, J. G.
Van Vleck, J. H.—No. 9
—— see Weiss, P. R.

Watson, W. W. and R. Simon—No. 30
Way, Katharine—No. 33
Webb, H. W.—see Garth, R. C.
—— see Moore, G. E.
Webster, D. L., L. T. Pockman, K. Harworth and P. Kirkpatrick—No. 52
Weiss, P. R. and J. H. Van Vleck—No. 10
Weisskopf, Viktor—No. 35
White, T. N., L. Marinelli and G. Failla—No. 25
Williams, H. J. and R. M. Bozorth—No. 7
Williams, V., R. C. Herman and R. Hofstadter—No. 59

Zinn, W. H.—see Seely, S.